# Biosynthesis Pathway & Transport of Endotoxin - Promising Antibacterial Drug Targets in the *Burkholderia cepacia* Complex (BCC)

*Karin Bodewits*

Doctor of Philosophy

University of Edinburgh

2010

# Declaration

I declare that this thesis was composed by myself and that the work contained therein is my own, except where explicitly stated otherwise in the text.

(*Karin Bodewits*)

*To my parents*

# Acknowledgements

I want to thank Dr. Dominic Campopiano for giving me the chance to do a PhD in his research group. I am grateful to Prof. John Govan who has always been actively involved in my project, gave a lot of support throughout the PhD, and very useful advice regarding this thesis. Also, my funding bodies, the Derek Stewart Charitable Trust and the School of Chemistry, are thanked.

I would like to thank all the past and present PhD students, Post-Docs and staff of the CF lab and lab 229 as each member helped me at some point. Special thanks is going out to Scott, Cathy, Dervla, Alan, Josefin, Thomas, Sam and my project student Christopher for all their help.

Outside of the two labs I worked in, I would like to thank Prof. Christian Raetz (Duke University, USA) for his help and collaboration on the CHIR-090 project; Prof. Miguel Valvano (University of Western Ontario, Canada) for help on the D-cycloserine project and technical advice on genetic manipulation of *Burkholderia*; Andrew Cronshaw and Liz Blackburn for their help with the MALDI and the LptA project.

Special thanks is going out to all the people working in the old library for their help with LaTeX and the espresso supply. Also many thanks to all the members of the Leigh group who always welcomed me for lunch.

A great thanks to all the people who made my time in Edinburgh enjoyable either in the lab or outside the lab. Two persons are especially thanked in this regard, Anne Caniard and Dean Wood. Without Anne the first two years of my PhD could not have been as good as they were, I truly missed her during my last year. Many thanks for making me cry of laughter at least once a day and giving me a special memory with the Beatles song "Good morning." I wish you all the best in the future. Dean, thanks a lot for always being there for me, helping to spread

plates on Sundays, repairing my bike and all the other things. Though there is always a random bone broken of your skeleton, I do wish you all the health and all the best.

Philipp, thank you very much for your help and support regarding the writing of this thesis and the preparation for the *viva voce* examination. I could say "I could not have done it without you," but this would be British politeness quatsch. However, it was lovely and very funny with you. I guess it makes sense to thank the Creationists, Scientologists, Jehova's Witnesses, Mormons, Baptists, Christian Union, and the Destiny Church in the same paragraph. Following this line, I also thank the Kings Arms, the Royal Oak, Gilmore, and the Germans in general.

I would like to thank my sisters. Joke, thanks for making all my visits to Amsterdam a memorable experience over and over again. These were the days I realised what I was missing out on by living on the other side of the North Sea. Afke, thanks for taking care of the cutest cat on the planet. I wish both of my sisters some very fruitful years. Special thanks is going out to my grandparents as well.

I dedicated this thesis to my parents. They raised me with love, they supported me in all decisions I made, and were always there for me.

| | |
|---|---|
| ACP | Acyl carrier protein |
| AMP | Antimicrobial peptide |
| ADP | Adenosine diphosphate |
| ATP | Adenosine triphosphate |
| Bcc | *Burkholderia cepacia* complex |
| $\beta$CDA | $\beta$-chloro-D-alanine |
| bcesm | *Burkholderia cepacia* epidemic strain marker |
| BLAST | Basic Local Alignments Search Tool |
| CAMP | Cationic antimicrobial peptide |
| CF | Cystic fibrosis |
| CFTR | Cystic fibrosis transmembrane conductance regulator |
| cfu | Colony forming units |
| CHIR-090 | N-aroyl-L-threonine |
| CS | Cycloserine |
| cv | Column volumes |
| DCS | D-cycloserine (or Seromycin) |
| DLS | Dynamic light scattering |
| DMSO | Dimethyl sulfoxide |
| DNA | Desoxyribonucleic acid |
| EDTA | Ethylenediaminetetraacetic acid |
| Endotoxin | Lipid A |
| EPS | Exopolysaccharide |
| His6 | Six consecutive histidine residues |
| IM | Inner membrane |
| IMAC | Immobilized metal affinity chromatography |
| IPTG | Isopropyl $\beta$-D-1-thiogalactopyranoside |
| ISA | Isosensitest agar |
| ISB | Isosensitest broth |
| kb | Kilo base |

| | |
|---|---|
| kDa | Kilo dalton |
| $k_{cat}$ | Turnover number |
| Kdo | 3-deoxy-D-manno-octulosonic acid |
| $K_M$ | Enzyme-substrate binding constant |
| Ko | D-*glycero*-D-*talo*-oct-2-ulopyranosylic acid (Ko) |
| L-Ara4N | 4-amino-4-deoxy-L-arabinose |
| LB | Luria Bertani |
| LCS | L-cycloserine |
| LDH | Lactate dehydrogenase |
| Lipid $IV_A$ | Lipid A precursor |
| Lipid A | Endotoxin |
| Lipid X | 2,3-diacylglucosamine 1-phosphate |
| L-PPG | L-proparagyglycine |
| LPS | Lipopolysaccharide |
| MALDI-TOF | Matrix-Assisted Laser Desorption/Ionisation Time-Of-Flight |
| Mb | Mega base |
| MBC | Minimal bactericidal concentration |
| MIC | Minimal inhibitory concentration |
| MW | Molecular weight |
| NA | Nutrient agar |
| $NAD^+$/ NADH | Nicotinamide adenine dinucleotide |
| NB | Nutrient broth |
| NMR | Nuclear Magnetic Resonance |
| NTA | Nitrilotriacetic acid |
| OM | Outer membrane |
| ORF | Open reading frame |
| PBS | Phosphate buffered saline |
| PCR | Polymerase chain reaction |
| PDB | Protein Data Bank |

| | |
|---|---|
| PK | Pyruvate kinase |
| PLP | Pyridoxal 5'-phosphate |
| PMP | Pyridoxamine 5'-phosphate |
| PMSF | Phenylmethylsulfonyl fluoride |
| PmxB | Polymyxin B |
| RFLP | Restriction fragment length polymorphism |
| rRNA | Ribosomal ribonucleic acid |
| RT | Reverse transcriptase |
| SDS-PAGE | Sodium dodecyl sulfate polyacrylamide gel elecrophoresis |
| SOC | Super optimal broth with catabolite repression |
| TFA | Trifluoroacetic acid |
| TPCK | Tosyl phenylalanyl chloromethyl ketone |
| TNF | Tumor necrosis factor |
| TLC | Thin layer chromatography |
| TLR4 | Toll-like receptor |
| UDP-GlcNac | UDP-*N*-acetylglucosamine |
| UDP-monoacyl-GlcNac | UDP-(3-*O*-(*R*-3-hydroxyacyl))-*N*-acetylglucosamine |
| UDP | Uridine diphospate |
| UDP-Ara4O | UDP-4-ketopentose |
| UMP | Uridine monophospate |
| UV | Ultra-violet |

# Abstract

*Burkholderia cepacia* complex (Bcc) species are opportunistic pathogens in patients with cystic fibrosis (CF), which are able to cause lethal infections. The Bcc are inherently resistant to most classes of antibiotics, which makes successful treatment problematic. Lipid A (also known as endotoxin), the hydrophobic anchor of lipopolysaccaride (LPS), is the bio-active component of LPS. One of several unique characteristics of the lipid A of the Bcc, is the permanent attachment of 4-amino-4-deoxy-L-arabinose (L-Ara4N) to the lipid A molecule. Also, the genes involved in L-Ara4N biosynthesis are necessary for viability in *B. cenocepacia*. Here we present research on lipid A biosynthesis, modification, and transport in the Bcc and highlight promising antimicrobial targets.

The synthetic antibiotic CHIR-090 is an inhibitor of LpxC, an enzyme involved in the lipid A biosynthetic pathway. I investigated the activity of CHIR-090 against the Bcc and found that sensitivity to this antibiotic was both species- and strain-specific. CHIR-090 displayed MICs between 0.1 and 12.5 $\mu$g/ml against a panel of *B. multivorans*, the most prevalent *Burkholderia* species in CF. The species- and strain-specific sensitivity towards CHIR-090 was further explored and a strong correlation was found between the presence of a unique open reading frame, named $LpxC_2$, in resistant species.

To address the problem of multiple drug-resistance of the Bcc, we investigated the activity of the pyridoxal 5′-phosphate (PLP)-dependent enzyme inhibitor cycloserine (CS) against the Bcc. CS is used as a second line of defense against

*M. tuberculosis*. The activity of the D-enantiomer of CS (DCS) against the Bcc was tested and displayed MICs between 2 and 128 $\mu$g/ml and acted bactericidal towards the Bcc. Additionally, DCS inhibition of recombinant ArnB from *B. cenocepacia* J2315, a PLP-dependent enzyme necessary for viability in the Bcc, was studied. ArnB was inhibited reversibly by DCS. ArnB was further explored as a promising drug-target in the Bcc, but only CS has been identified as an inhibitor so far.

In this thesis it was attempted to find the reason why is L-Ara4N modification of lipid A necessary for viability in *B. cenocepacia*. Therefore, two proteins were characterised, which are involved in lipid A transport: LptA, the periplasmic lipid A binding protein, and LptB, the cytoplasmic ATP-ase. LptA was found to be able to bind both modified and unmodified lipid A *in vitro* and therefore is not L-Ara4N specific. Furthermore, LptA could bind deep-rough-, rough-, and smooth- LPS, similar to that described for *Escherichia coli* LptA. The kinetic parameters of LptB were determined *in vitro* ($k_{cat} = 5.71$ min$^{-1}$ and $K_M = 0.88$ mM), and were comparable to *E. coli* LptB. The ATP-ase activity of LptB was not influenced by the presence of any forms of LPS (modified or non-modified). Therefore, we concluded that both *B. cenocepacia* J2315 LptA and LptB are not L-Ara4N specific.

# Contents

# Chapter 1

# Introduction

## 1.1 Cystic fibrosis and microbiology

Since medieval times an association between young children with a salty skin and early death has been observed. We now know these children were most likely suffering from the most common (1 in 2,500) inherited condition in Caucasians, cystic fibrosis (CF).

> **Wehe dem Kind, das beim Kuss auf die Stirn salzig schmeckt, es ist verhext und muss bald sterben.** *Alemannic proverb from the 17$^{th}$ century*
>
> (Woe is the child that tastes salty when kissed on the forehead, it is bewitched and must die soon.)

CF was firstly recognized as a disease in 1938 by Dr. Dorothy H. Anderson, who linked pancreatic changes with steatorrhoea (increased fat in the faeces) and pneumonia (inflammation of the lung tissue), and hypothesized that the CF condition was the result of a recessive genetic defect [1]. In the fifties, Paul di Dant'Agnese and coworkers found proof for increased concentrations ($\geq$ 60 mEq/L) of sodium

and chloride in the sweat of CF patients [2, 3], a feature that could be used to accurately diagnose this condition. The CF diagnosis test, suggested by Shwachman et al., was performed by placing a patient's body in a plastic bag for 30 minutes to over 2 hours to arouse sweating [4]. Gibson and Cooke recognized the obvious risks associated with this procedure, which they could replace by a simpler and safer test, in which pilocarpine is introduced into the skin by iontrophoresis, thereby stimulating localized sweating [5].

At the end of the 1990s the 'CF gene' was identified on the long arm of chromosome 7. This 250 kB gene, encoding a predicted protein of 1,480 amino acids of, at that time, unknown function. Sequence analysis revealed that it consists of two similar motifs, both having a membrane association and an adenosine triphosphate (ATP) domain (an ABC transporter homologue). In 1989, the research groups of Francis Collins, Lap-Chee Tsui and John Riordan, simultaneously published a description of "the identification of the CF gene" in the same issue of Science [6, 7, 8]. Knowing which gene is responsible for CF made a more refined diagnosis of the disease possible. Additionally, the ability to detect mutations in the 'CF gene' at the DNA level showed that around 70% of the CF patients have a specific deletion of 3 base pairs in the gene, encoding a phenylalanine residue. This was described as mutation "$\Delta$508." The remaining 30% of patients have different and often multiple mutations in the gene [6], and today over 1,600 mutations have been reported [9].

The observation that CF patients seem to have a chloride permeability defect suggested that the 'CF gene' either encodes for a $Cl^-$ channel itself or encodes a $Cl^-$ channel regulator. Hence, the protein was named "cystic fibrosis transmembrane conductance regulator" (CFTR). In 1992, three years after the discovery of the CF gene, John Riordan and co-workers published the purification of recombinant CFTR and showed that upon incorporation of the protein into proteoliposomes, regulated $Cl^-$ channel activity could be detected [10]. At present, it is known

that CFTR is an ATP-driven ion channel that transports $Cl^-$ across the plasma membrane and is needed for optimal water flow in epithelial cells. Malfunction or absence of CFTR leads to dehydrated mucus accumulation in all organs containing exocrine epithelia, such as the lungs, intestines, pancreatic ducts, testes ducts, and sweat gland ducts [11, 12].

A striking characteristic of CF is the higher susceptibility to bacterial infections of the respiratory tract [12, 13]. This is due either to the accumulation of dehydrated mucous that obstructs the cilia and other pulmonary clearance mechanisms, or to the absence of the hypotonic salt gradient caused by lowered $Cl^-$ transport over the membrane [14]. In either case, without intensive antibiotic therapy to delay or treat early lung infections, chronic microbial infection of the lungs leads to acute exacerbations and pulmonary failure, the principal causes of morbidity and mortality in individuals with CF.

> **In wine there is truth, in beer there is strength, in water there is bacteria** *German proverb*

Historically, the major pathogens recovered from the sputum of CF patients were considered to be *Staphylococcus aureus*, *Haemophilus influenza* and *Pseudomonas aeruginosa*. However, recently the role of anaerobes and other potential pathogens has been questioned [15]. In the last two decades, species of the *Burkholderia cepacia* complex (Bcc), have increasingly been isolated from the CF lung [12, 16, 17] and since 2002, a rising number of *Burkholderia pseudomallei* infections have been reported [18, 19, 20, 21, 22, 23]. *B. pseudomallei* is well known as the highly virulent agent of melioidosis, a life-threatening disease endemic in southeast Asia and northern Australia [24].

Though the risk of Bcc infection is relatively low in healthy humans, it is of great concern for CF patients. In most organ transplant centres, isolation of Bcc is a contraindication for life-saving surgery. Furthermore, infection by Bcc

leads, in approximately one third of infected individuals, to a septic shock, the so-called 'Cepacia syndrome.' This life-threatening syndrome is characterised by necrotizing pneumonia which culminates in a rapid decline of lung function and can ultimately lead to the death of the patient [25]. Furthermore, Bcc infections are transmissible from one patient to another [12], leading to epidemic outbreaks [26, 27], and cannot be treated due to the resistance of Bcc to most antibiotics. Taking all of this into account, it is widely accepted that Bcc infection requires the segregation of infected individuals from the rest of the CF population, a draconian form of infection control which has a major impact on both the psychological well-being of the patient and the (re-) organization of clinics [28].

Though quality of life and life expectancy has greatly increased for CF patients in the $20^{th}$ century (from a short and painful life to an average life time of 30-40 years), due to the wide use of antibiotics and refinement of conventional care [29], the management of lung infections remains challenging. In particular, treatment of Bcc infections is severely limited by the innate broad-spectrum resistance of these bacteria. As evidence, only four cases of successful antibiotic treatment of Cepacia syndrome have been reported, and in all cases required a combination of at least four antibiotics [30]. Clearly, there is an obvious and urgent need for new antimicrobial agents that are effective against Bcc infections.

Although CF clinics have been confronted with Bcc for over two decades, including several major intercontinental epidemic outbreaks, it is still not understood why Bcc, in contrast to other species, can trigger such a rapid pulmonary deterioration. Further research is needed on virulence factors of Bcc and on the differences in these factors when compared to other CF pathogens. This research is fundamental to gain knowledge and discover Bcc's Achille's heel that could be targeted by new antimicrobial agents.

## 1.2 *Burkholderia cepacia* complex and virulence factors

The Bcc comprises an expanding group of closely-related Gram-negative bacteria with a complex taxonomy. Initially recognized by Walter Burkholder as the causative agent of onion rot, and originally known as *Pseudomonas cepacia* [31], these organisms were first recovered from the CF lung in the late 1970's. In 1992, several *Pseudomonas* species, including *P. cepacia*, were reclassified (based on rRNA sequences) to the new genus *Burkholderia* and *P. cepacia* was renamed *Burkholderia cepacia* [32]. Around the same period, recognition of the genomic diversity in *B. cepacia* isolates from CF patients led to the introduction of the term Bcc to describe organisms comprising of at least five different species [33, 34, 35, 36]. At present, the Bcc consists of 17 species (Table 1.1) the majority of which have been recovered from CF patients [37]. As an aid to Bcc studies, two panels of Bcc reference isolates have been assembled representing the first nine species recognised [35, 38]; these include both environmental and clinical isolated strains.

Table 1.1: The *Burkholderia cepacia* complex (Bcc)

| **genomovar** | **species name** | **genomovar** | **species name** |
|---|---|---|---|
| I | *B. cepacia* | X | *B. ubonensis* |
| II | *B. multivorans* | XI | *B. latens* |
| III | *B. cenocepacia* | XII | *B. diffusa* |
| IV | *B. stabilis* | XIII | *B. arboris* |
| V | *B. vietnamiensis* | XIV | *B. seminalis* |
| VI | *B. dolosa* | XV | *B. metallica* |
| VII | *B. ambifaria* | XVI | *B. contaminans* |
| VIII | *B. anthina* | XVII | *B. lata* |
| IX | *B. pyrrocinia* | | |

Bcc are non-spore forming bacteria that are naturally found in water, soil, and are particularly associated with the rhizosphere of plants [39]. In addition to their non-phytopathogenic role, Bcc can cause opportunistic infections in CF patients and life-threatening pneumonia in patients with chronic granulomatous disease. Therefore, the Bcc is one of the rare examples of a pathogen that is shared by both plants and humans [40]. It has been shown by several research groups that Bcc, like some other bacterial species, can enter mammalian cells, survive, and depending on the cell-line used, replicate intracellularly [41, 42, 43]. Bcc species can survive in activated macrophages and respiratory epithelial cells, features that might add to their pathogenicity in CF patients [44, 45]. Some Bcc strains produce a brown melanin-like pigment (studies on *B. cenocepacia* suggest a pyomelanin), that can protect the cells from intracellular oxidative stress [46].

Species of the Bcc are extremely metabolically versatile [47, 48], capable of degrading a wide variety of compounds, including some man-made pollutants (such as trichloroethylene and polychlorinated biphenyls) [49]. This is exemplified in the case of *B. multivorans* as its name means "the eater of everything." In addition, Bcc are capable of long-term survival under minimal nutritional conditions [12]. They are found in pharmaceutical solutions, shampoo, hospital equipment, "sterile solutions" [35, 50], and are the main contaminant in water supplies of space shuttles [51]. At the end of 2009, Bcc made it into the UK news, by contaminating Vicks Sinex nasal spray (Proctor & Gamble), leading to the recall of 120,000 bottles. As mentioned above, the main difficulty with handling Bcc is that they are extra-ordinarily resistant to antimicrobial agents. This is exemplified by their ability to use penicillin G as a sole carbon source [52].

Ironically, in contrast to their pathogenic and contaminating role, members of the Bcc can be highly beneficial in the natural environment. Some species are able to fix nitrogen within the rhizospheres of crops and thereby promote plant growth. Due to their metabolic versatility Bcc has considerable potential for

bioremediation purposes [16]. They can produce anti-fungal compounds (cepacin, altercidins, cepacidines, siderophores, and pyrrolnitrin) that prevent molding of fruit and root rot of seedlings (ironically, anti-fungal compounds excreted by Bcc may inhibit colonization of *Candida* and other fungal species in the CF lung) [12, 16, 53].

Several studies have focused on the capability of Bcc strains to compete with other bacterial species. Forty percent of Bcc species show antibiotic activity against other Bcc species and other Gram-negative bacteria. *B. ambifaria* shows the greatest antimicrobial potential among the Bcc strains tested. One of the interesting antimicrobial compounds, recently isolated from *B. ambifaria*, has been identified as the known natural product enacyloxin [54]. Future research might lead to the identification of other novel compounds produced by Bcc strains that can be used to treat infections.

The biotechnological potential of the Bcc as biopesticides and bioremediation agents to reduce global pollution stands in contrast to their pathogenicity and has led to an intense debate between agricultural- and medical microbiologists [17, 55, 56]. On the one hand, the agricultural microbiologists argue that not all Bcc strains might be pathogenic for humans and thus could be released in the environment [17]. On the other hand, medical microbiologists argue that Bcc infections are likely to be directly acquired from the environment [57] and that there is not enough evidence for lack of virulence of any of the species [55, 56]. As a result of this ongoing debate, the U.S. Environmental Protection Agency presently restricts the use of Bcc species for biotechnological applications.

### Bacterial systematics and the Bcc

In bacterial systematics, typically the 16s rRNA gene sequences are used to identify new species or distinguish between them. However, between the different Bcc strains there is limited sequence variation (98-100% identity) in this gene. In

contrast, the *recA* gene (encoding a protein essential for repair and recombination of DNA) shows sufficient variation between Bcc species and can be used for identification. The *recA* gene is first amplified, using Bcc specific primers, followed by a restriction fragment length polymorphism (RFLP) analysis [38]. Different species can be distinguished based on their RFLP profile. This method has been proven to be accurate to identify species directly from sputum of CF patients and after selective culturing [38, 58]. As yet, RFLP profiles have not been published for all Bcc species.

### 1.2.1 Clinical relevance & epidemic strains

In the absence of epidemic outbreaks, Bcc is recovered from 5-10% of the adult CF population and, in 80% of the Bcc infections, the isolates are identified as *B. cenocepacia* or *B. multivorans* [16, 59]. These infections are either obtained from patient-to-patient transmission or acquired from the environment with some geographical variation in prevalence of the different Bcc species. After infection, the clinical outcomes differ greatly from patient to patient even when the same strain is involved. In some patients there is little increase in morbidity, whereas other patients have a rapid decline of lung function and die soon after infection.

Before the introduction of strict patient segregation, some Bcc isolates were transmitted readily from one CF patient to another, resulting in serious epidemic outbreaks [26, 27]. *B. cenocepacia* is the most virulent species and accounts for most epidemics in the CF population. However, *B. multivorans* was responsible for a dramatic epidemic outbreak in 1992 amongst CF children in Glasgow [60]. The most prevalent epidemic *B. cenocepacia* strains in the UK [26] and Canada [61] belong to the particularly virulent, clonal, ET-12 lineage [62] and are highly transmissible. The main strains used in this thesis are *B. cenocepacia* strain J2315, responsible for an epidemic outbreak in Edinburgh in 1989 [26], and *B. cenocepacia* strain K56-2 [63], clinically isolated in Canada, both are members of the

ET-12 lineage.

*B. cenocepacia* consists of four different subgroups based on *recA* sequencing and RFLP analysis: IIIA, IIIB, IIIC, and IIID [64]. The clinical significance of the different subgroups is unclear but all the members of the ET-12 lineage belong to subgroup IIIA. The genome of *B. cenocepacia* J2315 and nine other Bcc strains have been sequenced and are available on www.burkholderia.com. J2315 has a total genome size of 8,056 Mb and a 66.9% GC content. The genome is divided into three large chromosomes and a small 92-kb plasmid. The inherent resistance of members of the Bcc has been linked to the relatively large ( 8-9 Mbp) genomes of these bacteria which contain multiple antibiotic resistance genes [65].

### 1.2.2 Virulence factors

Most Bcc species produce a wide variety of putative virulence factors that might cause Cepacia syndrome, but none of these factors has been established as the main causative agent. Bcc can produce proteases, siderophores, hemolysin, cytotoxins, catalases [12] and an exopolysaccharide (EPS), called Cepacian. Cepacian is capable of interfering with antimicrobial peptides (AMPs) and therefore inhibits peptide-based immune defenses [66]. Production of Cepacian is induced by growth on certain carbohydrates, in particular mannitol [67].

Members of the ET-12 lineage have shown to have cable pili and possess the epidemic strain marker (bcesm). Cable pili are able to bind to the cytokeratin 13 receptor that is overexpressed in CF lung epithelial cells and therefore is likely to induce cytokine production. Bcesm is a DNA fragment, found in some epidemic strains but not in non-epidemic CF strains, that contains a number of virulence determinants [68, 69]. Furthermore, Bcc have shown the ability to form biofilms in vitro, with both *P. aeruginosa* and other Bcc. This feature may increase resistance to antibiotics and host-defense mediators. However, it has been reported recently that *in vitro* biofilm formation of Bcc has no effect on the susceptibility

to the six most commonly used antibiotics [70].

Like for many other Gram-negative bacteria, lipopolysaccharide (LPS), the main component of the outer membrane, is a virulence factor in Bcc. LPS, also referred to as endotoxin, is a bioactive molecule that can activate the immune system by forming a Toll-like receptor (TLR4)-MD2-LPS complex (the structure of this complex has been solved recently [71]), thereby inducing pro-inflammatory cytokines [72]. Before 1997 and the expansion of Bcc taxonomy, LPS from '*B. cepacia*' was shown to be highly pro-inflammatory, and elicited a nine-fold higher release of tumor necrosis factor alpha (TNF-$\alpha$) from monocytes compared to the LPS from *P. aeruginosa* [73]. In the same "pre-Bcc period," the interaction of '*B. cepacia*,' *E. coli* and *P. aeruginosa* LPS with neutrophils was investigated. It was shown that both *E. coli* and '*B. cepacia*' LPS increased CD11b (involved in phagocytosis) and complement receptor 3 (CR3, involved in transmigration) expression on neutrophils. Moreover, their LPSs are potent priming agents for a respiratory burst response. However, *P. aeruginosa* LPS had little to no effect on CD11b and CR3 expression and primed neutrophils to a low degree [74]. TNF-$\alpha$ production by human monocytes, stimulated by '*B. cepacia*' LPS, was four-fold greater than for *P. aeruginosa* LPS. Levels of monocyte cytokine production, stimulated by whole '*B. cepacia*' cells were found to be similar to extracted LPS, suggesting that this virulence factor plays a prominent role in inflammation [75]. Subsequently, the proinflammatory activity of the first five Bcc species was compared. It was shown that there is a difference in TNF-$\alpha$ induction between species and strains within the same species. Interestingly, amongst the Bcc, *B. cenocepacia* isolates cause the greatest cytokine induction [76].

## 1.3 Lipopolysaccharides

In 1676, the Dutch scientist Antonie van Leeuwenhoek first discovered the "existence of bacteria" by using a single-lens microscope that he designed himself. About 200 years later, in 1884, Christian Gram developed a staining method to visualize bacteria, that turned out to be capable of distinguishing between Gram-positive and Gram-negative bacteria. However, it was not until the development of the electron microscope that the distinctive cell envelope of Gram-negative bacteria was discovered [77].

> **There is no doubt that the discovery of regular arrays of morphological units in the surface layers of some bacteria is one of the exciting achievements of electron microscopy and raises many interesting questions, both in microbiology and in the wider fields of cell and molecular biology.** *Glauert & Thornley 1969*

The cell envelope of Gram-positive bacteria consists of two layers, the cytoplasmic or inner membrane (IM), surrounded by a thick peptidoglycan layer. The cell envelope of Gram-negative bacteria (Figure 1.1) on the contrary consists of three layers, the IM, a thinner peptidoglycan layer, and the outer membrane (OM). The IM consists of a phospholipid bilayer and proteins. The peptidoglycan layer or periplasm, mainly consists of peptidoglycan, teichoic acids and soluble proteins. The OM encapsulates the peptidoglycan and is composed of an asymmetrical bi-layer and proteins. The inner leaflet of the bi-layer is formed from phospholipids and the outer leaflet primarily from LPS [78]. LPS is stabilized by associated cations (e.g. $Mg^{2+}$) which form salt bridges between the electrostatically repulsive LPS molecules. LPS on the outer surface of bacteria improves the barrier function, making Gram-negative bacteria resistant to antibiotics that can be successfully used to treat Gram-positive infections [79].

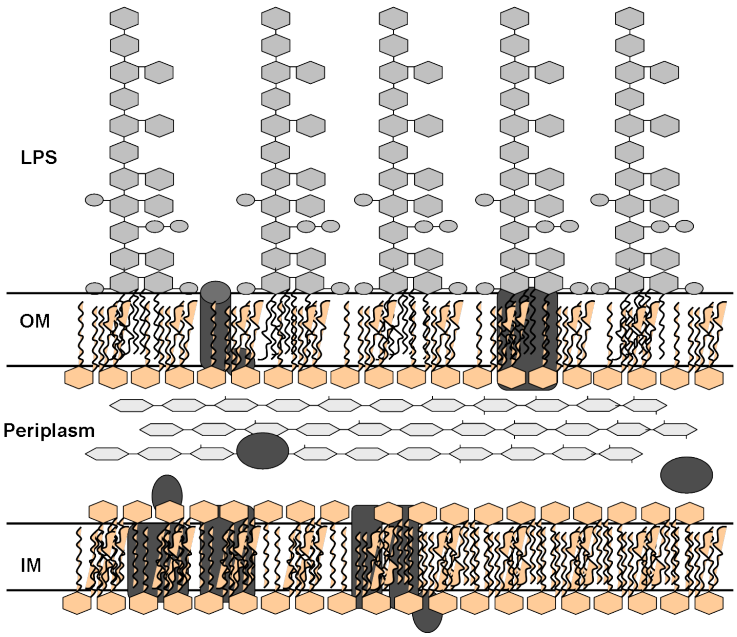


Figure 1.1: Schematic representation of the cell envelop of Gram-negative bacteria. Adapted from [80].

LPS consists of three structural domains, the conserved lipid A domain, the polysaccharide core, which can be divided into the inner core and the outer core, and the highly variable extended polysaccharide region, called the O-antigen [81] (Figure 1.2). All three domains are not consistently present. Strains containing all three domains, are referred to as "smooth". If the envelope lacks the O-antigen region, it is called "rough". If it lacks the O-antigen and outer core, it is called "deep-rough." Deep-rough LPS seems to be the minimal requirement for viability in most Gram-negative bacteria [82] in their natural environment. However, strains have been modified, so that only the lipid A domain is expressed, and they are viable when grown under laboratory conditions [83]. Lipid A is the hydrophobic anchor moiety of LPS that builds the outer monolayer of the OM and is the bioactive component of LPS that can activate the immune system. For Bcc species it has been shown that the level of cytokine induction is the same for both smooth- and rough- LPS-containing strains [76]. For the purpose of this thesis, only the lipid A and inner core domains are discussed.

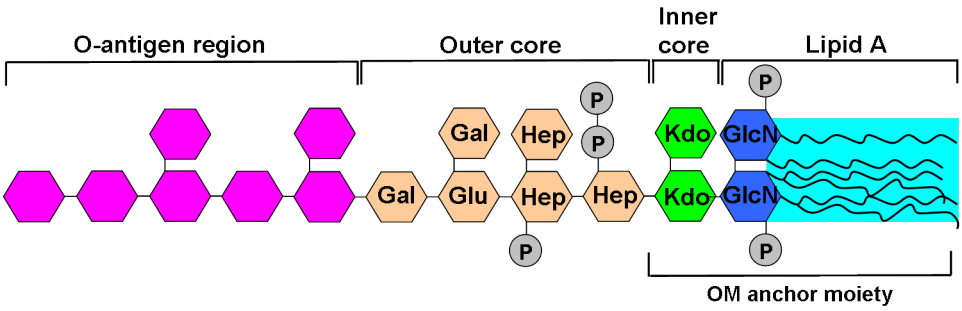


Figure 1.2: Schematic representation of the three structural domains of LPS. Adapted from [80].

### 1.3.1 Lipid A and inner core structures

The lipid A backbone is relatively conserved among Gram-negative bacteria. It consists of a typical $\beta(1' \text{-}6)$-linked disaccharide of glucosamine, which is tetra-, penta-, or hexa- acylated. The glucosamine is glycosylated in most species with one, two, or three 3-deoxy-D-manno-octulosonic acid (Kdo) sugars at position $6'$, as shown in Figure 1.3.

> **Studies of LPS not only showed us the impressive diversity of LPS structures in the bacterial kingdom but also led to the realization that the LPS structure may be modified in response to the conditions prevailing the environment.** *Hiroshi Nikaido, 2003 [79]*

Lipid A is considered as the most conserved component of LPS, but the diversity in structure is still broad. The lipid A of every bacterial species (or genus) identified so far seems to be unique in the length and number of incorporated fatty acids and the presence or absence of certain lipid A modifications (Figure 1.3). Lipid A modifications may help Gram-negative bacteria to adapt and resist environmental stress and are mediated by changes in the local environment, such as changes in calcium-concentration, pH, temperature, and the presence of AMPs. Several species add or remove fatty acids, which can lead to resistance to certain

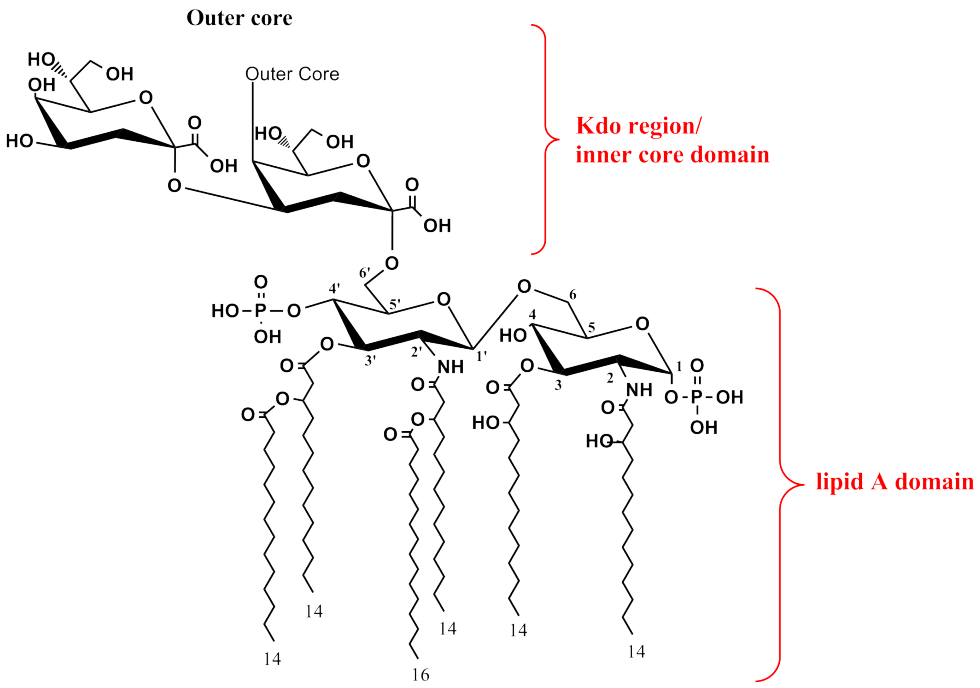


(a)

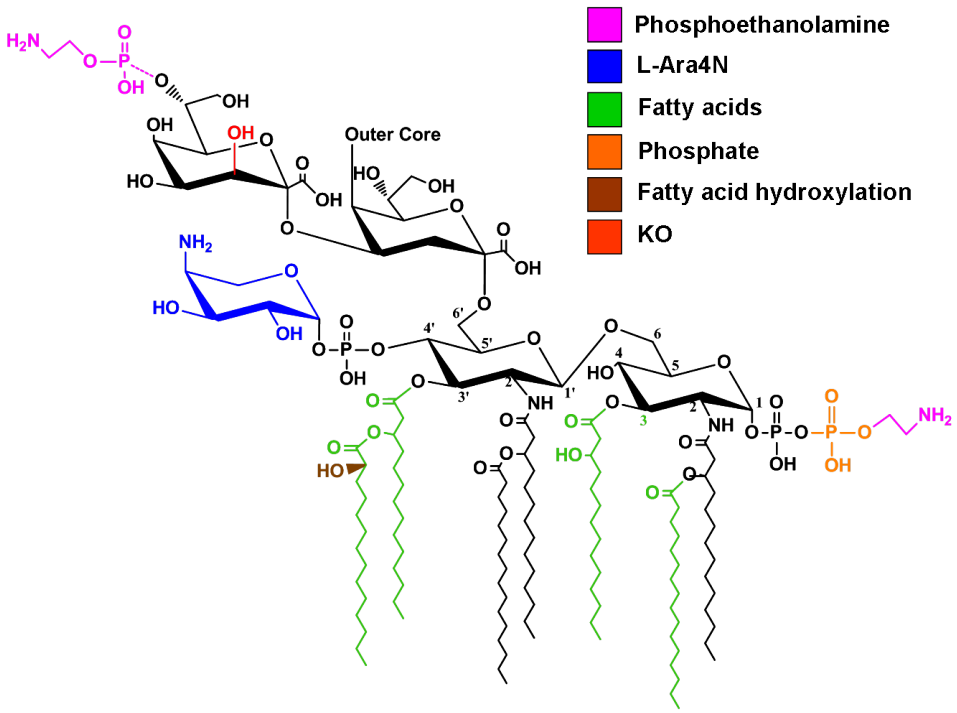


(b)

Figure 1.3: A) $Kdo_2$-lipid A of *E. coli*. B) Common lipid A modifications of Gram-negative bacteria. Pink= incorporation of phosphoethanolamine; blue= incorporation of L-Ara4N; green= addition or removal of fatty acids; orange= addition of a phosphate group; brown =addition of a hydroxyl group on a fatty acid; red= addition of hydroxyl group in one of the Kdo residues. Adapted from [81, 84, 85].

AMPs, and can change the immuno-stimulation potential of lipid A [86, 84, 87]. Unsaturated fatty acids can be incorporated when the bacteria are grown at lower temperatures to adjust the OM fluidity [88].

The attachment of 4-amino-4-deoxy-L-arabinose (L-Ara4N) and/ or phosphoethanolamine, at the phosphate groups at 1 and 4′, or to the outer Kdo residue are common modification strategies of Gram-negative species. Such modifications lead to resistance to polycationic compounds, such as polymyxin B (PmxB) [81, 89, 90], that enter the cell via a self-promoted uptake mechanism, by binding to LPS. When PmxB binds to LPS it displaces $Mg^{2+}$, thereby disrupting the $Mg^{2+}$ cross bridges between anionic LPS molecules and destabilizing the OM [91, 92]. L-Ara4N reduces the net negative charge of lipid A, resulting in a reduced binding affinity of PmxB [79]. Instead of L-Ara4N, various species incorporate galactosamine or galacturonic acid residues in the lipid A.

In addition, some lipid A structures lack the phosphate group at the 1 or 4′ position, or have a diphosphate at those positions. In a few species, the hydrogen group on the anomeric carbon atom at position 1 is oxidized to a lactone after removal of the phosphate group [87]. In a small number of species, including *Burkholderia* species, an additional hydroxyl group is incorporated at C3 of one of the Kdo residues to form D-*glycero*-D-*talo*-oct-2-ulopyranosylic acid (Ko) in the inner core. Most enzymes involved in the lipid A modifications, found up to now, have been identified [87].

### Lipid A structure of the Bcc

Bcc are highly resistant to the majority of antibiotics, including PmxB. This resistance, together with the fact that no detectable amounts of Kdo sugars could be found in the cell digest of '*B. cepacia*,' suggested that this bacterium has a unique lipid A structure. In 1991, Cox and Wilkinson were the first to report that the lipid A of '*B. cepacia*' contains a single Kdo sugar. They con-

cluded that PmxB resistance is most likely the consequence of the low number of carboxylate and phosphate groups as well as the presence of L-Ara4N [93]. Later in 1998, a characteristic Ko-Kdo disaccharide in the inner core region of *B. cepacia* ATCC 25416 was identified. The Ko residue of the disaccharide was non-stoichiometrically substituted with L-Ara4N at position 8 [94]. The lipid A structure of *B. cepacia* ATCC 25416 was further characterised and showed to have a bisphosphorylated glucosamine backbone with L-Ara4N residues attached on both phosphates [95]. More recently, lipid A structures, with or without inner core, have been described for a number of Bcc species, including *B. cenocepacia* J2315 [96], *B. cepacia* BTS7 [97], *B. cepacia* ATCC 25416, *B. multivorans*, *B. vietnamiensis*, and *B. pyrrocinia* [28]. The different structures show many common features (Figure 1.4).

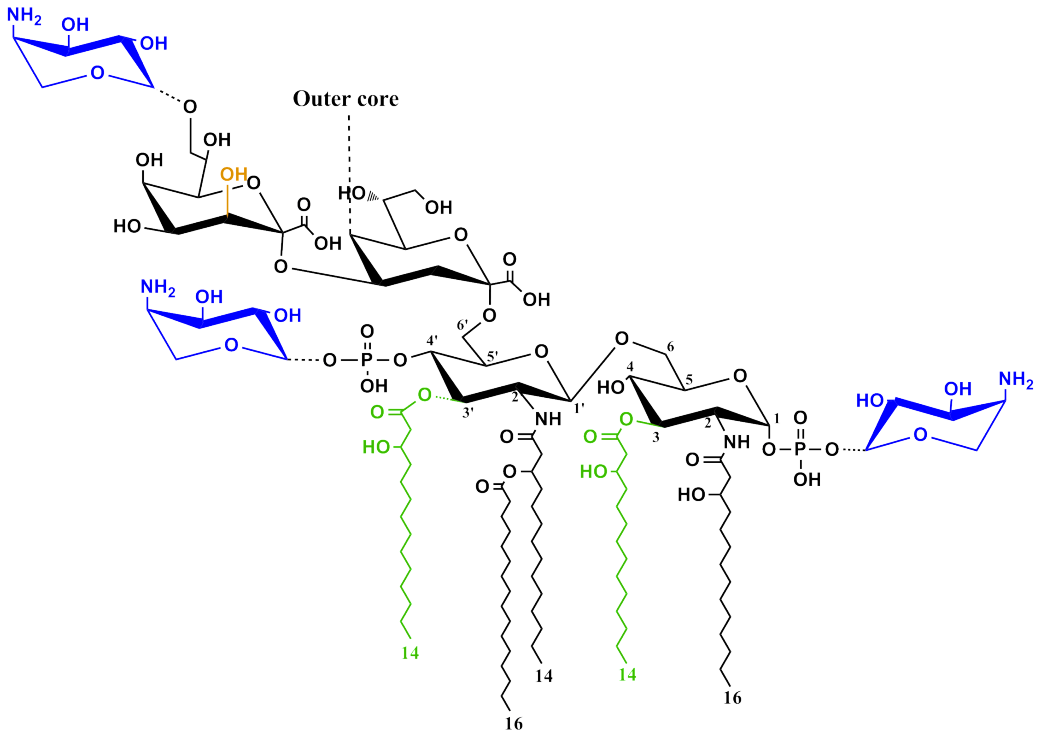


Figure 1.4: Lipid A structure found in Bcc species, showing the lipid A backbone (black), non-stoichiometrical substitution of L-Ara4N (blue), the OH group of the Ko residue (red), and the diversity in number of fatty acids (green). Adapted from [28].

The lipid A contains a $\beta(1'\text{-}6)$-linked disaccharide of glucosamine that is phospho-

rylated at the 1- and 4′- positions, derivatized C16:0 (3-OH) and C14:0 (3-OH) as primary fatty acids and C14:0 as a secondary fatty acid. The inner core structures all contain a Ko-Kdo disaccharide, in which L-Ara4N can be attached to the Ko residue. L-Ara4N can also be attached to both phosphate groups. Hence, the lipid A of Bcc has the potential to be biosynthesized with three L-Ara4N residues. Recently, the Campopiano group, in collaboration with researchers at the Centre of Infectious diseases (Edinburgh University) and the Infectious Diseases Research Group of the University of Western Ontario, showed that the putative genes involved in L-Ara4N biosynthesis (discussed in section 1.5) are, unlike in other Gram-negative bacteria, necessary for viability in *B. cenocepacia* [98]. This finding, together with the available lipid A structures, suggests that L-Ara4N is always present in Bcc LPS.

To date, isolated lipid A species have been shown to be penta- or tetra-acylated: hexa-acylated structures have not been identified in Bcc. It is interesting to note that from research on lipid A from other species, the general consensus is that lipid A molecules with less than six fatty acids are less immuno-stimulatory, and might even act as an LPS antagonist. However, Bcc lipid A always contains fewer fatty acids and is still capable of inducing a high immune-response compared to other species [28, 96, 97, 99].

Knowledge of the inner core region of Bcc LPS is vital in discussing the physicochemical and biological properties of the OM [28]. The presence of Ko is considered as a factor that stabilizes the linkage of Kdo to the glucosamine backbone. This specific feature prevents hydrolysis of the inner core from lipid A. The role that Ko might play in the immunostimulatory activity and other biological properties of LPS remains to be clarified.

Ko residues have also been found in the inner core of *Acinetobacter* species [100, 101], *Yersinia pestis* [102], *Serratia marcescens* [103], and *B. caryophylli* [104]. In *Acinetobacter* species the lipid A and inner core are attached by a Ko-(2→6)GlcN

linkage instead of a Kdo-(2→6)GlcN linkage found in lipid A of the Bcc, *Y. pestis*, and *B. caryophylli*. Unique to Bcc species, is that the Ko residue is always present (e.g. L-Ara4N), whereas in the other species for a fraction of LPS the Kdo residue is substituted with another Kdo. Therefore, it might be that the introduction of a Ko residue is a modification strategy in non-Bcc Gram-negative bacteria. This feature, as for L-Ara4N [98], suggests that the enzymes involved in Ko biosynthesis and incorporation are constitutively expressed in Bcc. Hence, Ko biosynthesis enzymes might be potential targets for the future development of drugs against Bcc.

For the purpose of these studies, the remainder of the introduction will focus on lipid A biosynthesis, transport and L-Ara4N modifications.

## 1.4 Lipid A and inner core biosynthesis

Since 1972, it has been known that LPS is synthesized at the inner surface of the cytoplasmic membrane [105]. Later work on the LPS biosynthetic pathway suggested that rough LPS (lipid A and core) and the O-antigen are synthesized and transported independently over the IM, and are ligated at the periplasmic site of the IM [106].

The first steps towards the elucidation of the lipid A biosynthetic pathway were the isolation and characterisation of two lipid A precursors, in 1977 lipid $IV_A$ of *Salmonella typhimurium* by P. Rick [107], and lipid X (2,3-diacylglucosamine 1-phosphate) of *E. coli* in 1981 by Masahiro Nishijima [108]. Since then, the lipid A pathway has been elucidated and excellent reviews are available [81, 84, 87, 109].

The lipid A pathway, also called the Raetz pathway, has been mainly characterised by Christian Raetz and collaborators, using *E. coli* and *S. typhimurium* as model organisms. The biosynthesis appears to be highly conserved among

Gram-negative bacteria and nine constitutive enzymes are involved (Figure 1.5). Of the nine enzymes in *E. coli*, LpxA, LpxC, and LpxD are soluble proteins, LpxB and LpxH are peripheral membrane proteins, and LpxK, KdtA, LpxL, and LpxM are inner membrane proteins. The active sites of all (structurally characterised) proteins have been found to be facing the cytoplasmic surface of the inner membrane [85].

UDP-*N*-acetylglucosamine (UDP-GlcNac) is, as for peptidoglycan biosynthesis, the first precursor of the pathway. It is reversibly acylated at position 3 by LpxA. LpxA requires the thioester *R*-3-hydroxyacyl-acyl carrier protein (ACP) as the obligate fatty acyl chain donor [110]. The length of the incorporated fatty acyl chain differs between species and varies between C10 and C14 [111, 112] Though it was published as the "first committed step of the pathway" [110], the reaction has an unfavorable equilibrium constant (Keq= $\sim$0.01) [113].

The second step is catalysed by LpxC, which deacetylates UDP-(3-*O*-(*R*-3-hydroxyacyl))-*N*-acetylglucosamine (UDP-monoacyl-GlcNac) at position 2 and is the actual first "committed" or irreversible step of the pathway. UDP-monoacyl-GlcN, which allows addition of a second fatty acyl chain, and free acetate are the products of this reaction [114].

LpxD adds an *N*-linked fatty acid to the free amino group, generated by LpxC, and forms UDP-2,3-diacyl-GlcN. Like LpxA, LpxD also requires an acyl-ACP donor [115].

Thereafter the synthesis splits in two. The pyrophosphate linkage of part of the UDP-diacyl-GlcN intermediates is cleaved by LpxH, yielding 2,3-diacylglucosamine 1-phosphate (lipid X) and UMP [116]. The other part remains uncleaved.

LpxB, brings the two pathways back together, and is responsible for the condensation of one lipid X molecule with one UDP-diacyl-GlcN molecule which forms the typical acylated $\beta$-1′-6 linked disaccharide of glucosamine [117].

LpxK phosphorylates the 4′-position of the disaccharide, using ATP as a cofactor [118], forming the precursor lipid $IV_A$.

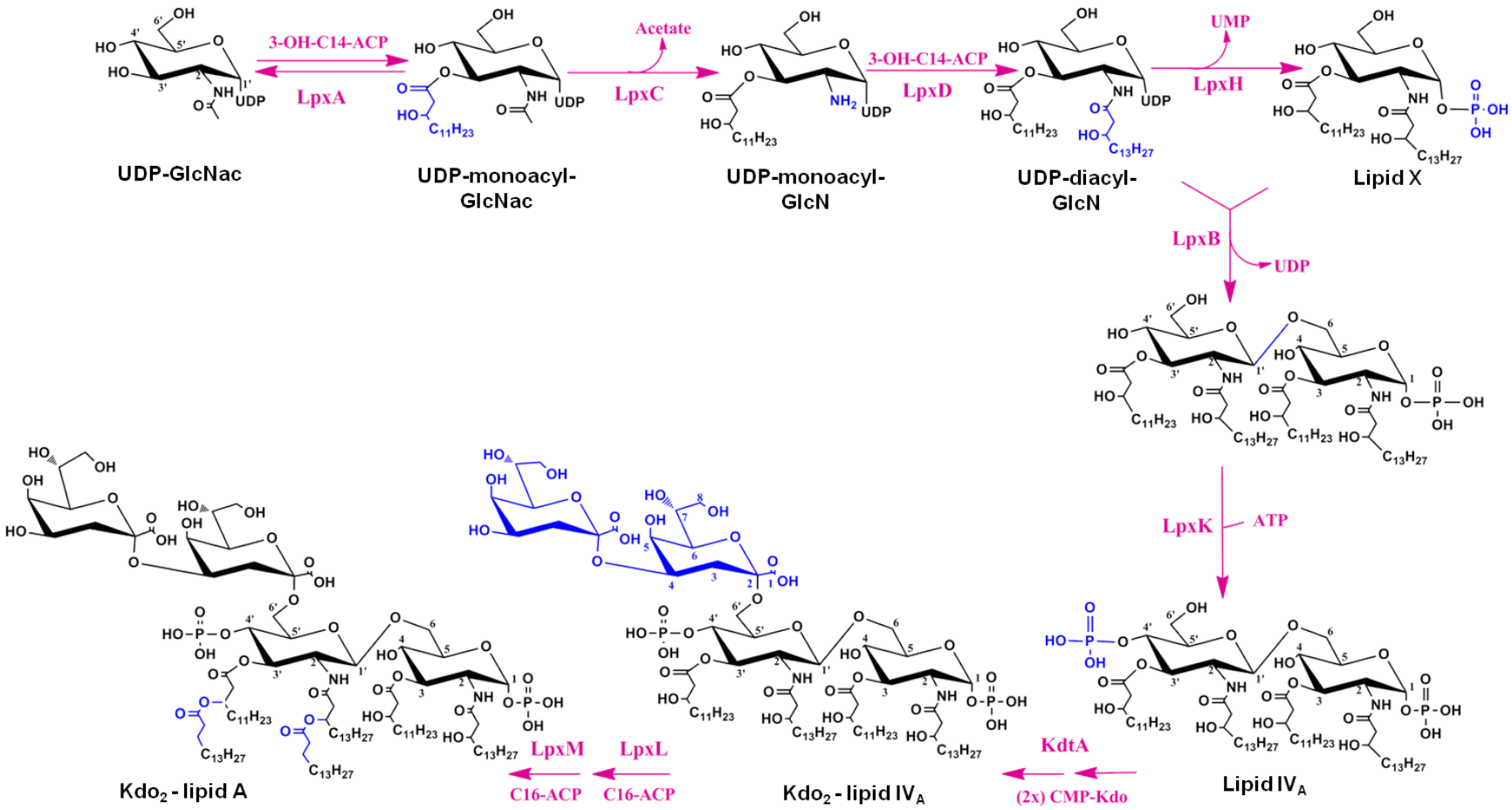


Figure 1.5: $Kdo_2$-lipid A biosynthetic pathway (The Raetz pathway) in *E. coli*. Adapted from [85].

The last three steps of the lipid A biosynthesis are catalyzed by KdtA, LpxL and LpxM. KdtA is a 3-deoxy-D-manno-octulosonic acid (Kdo) transferase [119, 120]. KdtA is an enzyme whose activity differs between species. It can be monofunctional, adding one Kdo residue to lipid $IV_A$, as reported for *Haemophilus influenza* [121], bifunctional, e.g. in *E. coli* [119], *Acinetobacter haemolyticus* [122], and *B. cepacia* [95], trifunctional, as in *Chlamidia trachomatis* [123], or even tetrafunctional, as in *Chlamidia psittaci* [124]. However, the addition of two Kdo sugars seems to be most common. The Kdo residues form the inner core of LPS and the outer core/ heptose region is connected to position 7 of the first Kdo residue.

LpxL and LpxM complete the lipid A biosynthesis by the addition of two secondary fatty acyl chains at the $2'$ and $3'$ positions. Like LpxA and LpxD, they use acyl-ACP thioesters as substrate donors. Unlike LpxA and LpxD, ACP can be replaced with coenzyme A thioesters [125, 126]. Depending on the bacterial species, LpxL and LpxM require prior attachment of the Kdo residues to the lipid substrate, or can take place when the Kdo residues are not present [127].

As mentioned earlier, and in contrast to *E. coli*, in the lipid A of Bcc species and several other species, one Kdo residue is replaced by a Ko residue in the inner core. It remains unclear how Ko is synthesized and incorporated into the lipid A. There are two possible ways: 1) the Kdo transferase adds two Kdo residues of which one is hydroxylated afterwards at position 3 by an unknown monooxygenase; 2) Ko is synthesized in the cytoplasm and transferred in an independent manner. However, previous studies of the Kdo transferases, of the Ko containing species, *B. cepacia* ATCC 25416 [95], *A. haemolyticus* and *A. baumannii*, [122] has shown these enzymes to be bifunctional. This evidence, together with the finding that the inner core of *Acinetobacter* is linked to lipid A through Ko, supports the hypothesis that a hydroxyl group is introduced after the addition of two Kdo residues to lipid A.

### 1.4.1 LpxC (UDP-3-O-acyl-GlcNac deacetylase)

The LPS biosynthesis pathway provides a promising target for the development of new antibiotics against multi-drug resistant Gram-negative pathogens [128]. In recent years one specific target that has attracted interest is LpxC. The reasons for this attention include 1) LpxC catalyses the first committed step in the lipid A biosynthesis pathway and is necessary for viability; 2) LpxC is a metalloenzyme and can, like $Zn^{2+}$- dependent hydrolases, be effectively inhibited by hydroxamate-containing compounds; and 3) LpxC has no eukaryotic homologs, thus reducing the hazards of human toxicity of LpxC-specific drugs.

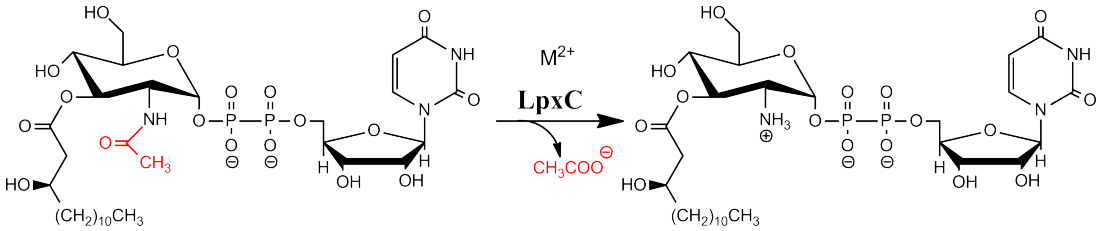


Figure 1.6: Enzymatic reaction catalyzed by LpxC. Adapted from [114].

LpxC removes the acetyl moiety from the substrate UDP-3-O-acyl-GlcNac, generating a free acetate and UDP-3-O-acyl-GlcN (Figure 1.6). LpxC requires a single $Zn^{2+}$ ion in the active site for enzyme activity [129]. From sequence analysis it has not been possible to identify common $Zn^{2+}$ binding motifs (e.g. HXXE, HXXEH or HEXXH) in any LpxC enzyme of different species, therefore single amino acid substitutions in *E. coli* of 10 conserved residues found in 11 species were made to identify groups that coordinate $Zn^{2+}$. Four residues that could coordinate $Zn^{2+}$ were identified during this study, His79, His238, Asp242, and His265 [130]. Recently, another study by Hernick and colleagues has suggested that LpxC has been misclassified as a $Zn^{2+}$-dependent enzyme due to enzymatic assays and crystallography being carried out under aerobic conditions. It is six- to nine- fold more active with the redox-sensitive metal ion $Fe^{2+}$ bound under anaerobic conditions [131]. As previously found for $Zn^{2+}$ [129], up to 1 M $Fe^{2+}$/

1 M enzyme activates LpxC, whereas a further increase of [$Fe^{2+}$] inhibits activity [131].

In 2003, the structure of *Aquifex aeolicus* LpxC was elucidated by nuclear magnetic resonance (NMR) and x-ray crystallography (Figure 1.7) [132]. In addition to the structure of the enzyme alone, there are also structures available of the enzyme in complex with myristic acid [132, 133], UDP [133, 134], and with several enzyme inhibitors [135, 136]. Furthermore, the crystal structure of *P. aeruginosa* LpxC complexed with an inhibitor has been elucidated [137].

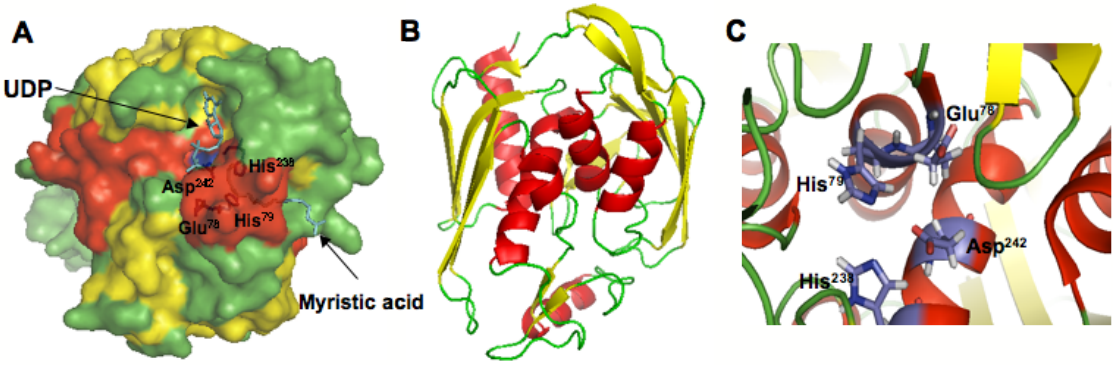


Figure 1.7: Crystal structure of *A. aeolicus* LpxC. A) LpxC space fill (red= $\alpha$-helices, yellow= $\beta$-sheets) with UDP and myristic acid bound. UDP is bound close to the active site. Myristic acid is located in the hydrophobic passage of the protein. The active site residues, His79, His238, Asp242, and Glu78 are highlighted. B) LpxC cartoon, with $\alpha$-helices and $\beta$-sheets. C) The active site/ metal binding site of LpxC. The structures were made using PyMoL and PDB file 2IER was taken from http://www.rcsb.org [132, 133].

*A. aeolicus* LpxC belongs to the $\alpha+\beta$ class of proteins and consists of two topologically similar domains linked by 16 residues. Both domains contain a five-stranded $\beta$-sheet and two $\alpha$-helices. The active site cleft is sandwiched between the two domains and is flanked by the two small subdomains, a $\beta\alpha\beta$ and a $\beta\beta\beta$ domain. A $\sim$15-$\AA$-long hydrophobic tunnel leading out of the active site is present where the aliphatic tail of the fatty acid of the substrate binds and stabilizes the $\beta\alpha\beta$ subdomain conformation. The crystal structure of LpxC with $Zn^{2+}$ bound showed that the metal, located in the active site, is coordinated by His79, His238, Asp242, and

a water molecule [132]. Glu78 probably serves as a general base in the deacetylase reaction. It abstracts a proton from the $Zn^{2+}$-bound water molecule, generating a hydroxide ion which is capable of a nucleophilic attack on the carbonyl group of the substrate by the hydroxide ion (Figure 1.8). A tetrahedral intermediate is then formed and the amino group accepts a proton from Glu78, thereby cleaving the amide bond, producing acetate and UDP-3-*O*-acyl-GlcN [132, 138]. There are different hypotheses whether Glu78 is the only amino acid serving as both the base and acid or whether His265 and Glu78 act in an acid base pair mechanism [139, 140].

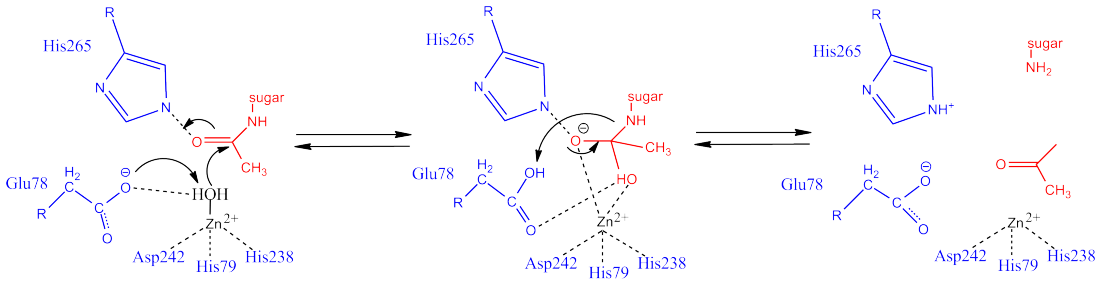


Figure 1.8: Proposed catalytic mechanism of LpxC. Adapted from [132, 138].

### LpxC as a drug target

Theoretically, an antibiotic that is functional against LpxC enzymes from a wide range of Gram-negative bacteria should interact with the conserved features among the LpxCs of different organisms. To identify these conserved features, the *A. aeolicus* LpxC sequence was aligned with thirty LpxCs from different species. *A. aeolicus* is a thermophilic bacterium (growing at 95 $^{o}$C), considered as one of the earliest diverging eubacteria on the evolutionary tree. With the help of the high resolution structures of this enzyme, several compounds (Figure 1.9 have been designed and found to inhibit *E. coli* LpxC, *P. aeruginosa* LpxC, and/ or *A. aeolicus* LpxC [128, 141, 142].

The first LpxC inhibitors designed were hydroxamate containing compounds, such as L-161,240 and BB-78485. These compounds are active against *E. coli* LpxC,

but have little effect on *P. aeruginosa* [128, 141, 143]. Later, the hydroxamate containing substrate analogue, TU-514, reported to be a potent inhibitor of *E. coli* LpxC *in vitro*. However, TU-514 did not show antibacterial activity due to its incapability to penetrate the cell wall of Gram-negative bacteria [142].

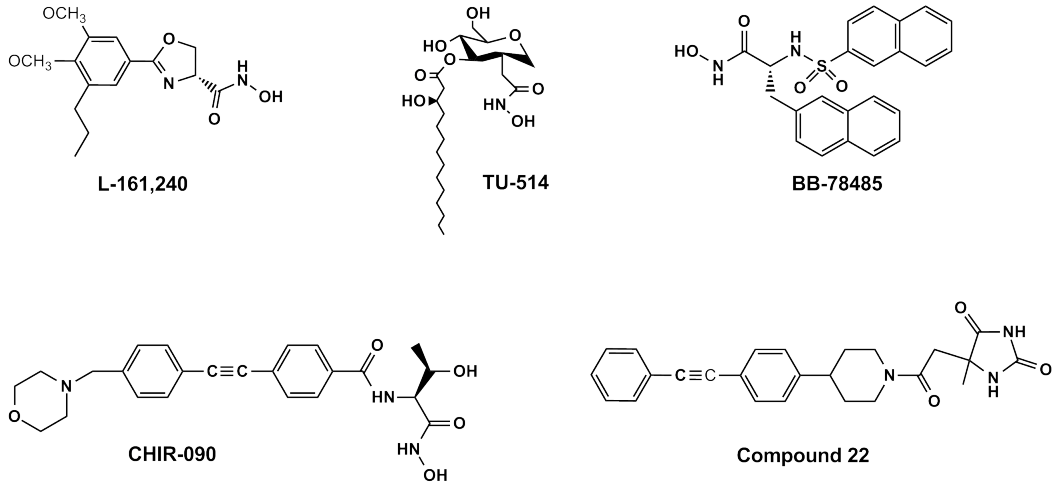


Figure 1.9: Five potent LpxC inhibitors. Adapted from [128, 141, 142, 144, 145].

Recently, the novel LpxC inhibitor CHIR-090 (N-aroyl-L-threonine), shown in Figure 1.9, was designed [144]. CHIR-090 has slow, tight-binding characteristics that act in a time-dependent manner on LpxC [144, 146]. The crystal structure of the *A. aeolicus* LpxC-CHIR-090 complex (Figure 1.10) shows that the hydroxamate moiety coordinates the catalytic $Zn^{2+}$ ion and binding is further strengthened through interactions with conserved residues in the active site. The biphenyl acetylene moiety of CHIR-090 inserts into the hydrophobic passage and the morpholine unit can be found in the distal end of the hydrophobic passage [135].

CHIR-090 is capable of penetrating the cell membrane of Gram-negative bacteria and displays promising antibacterial activity against *E. coli*, *P. aeruginosa*, *A. aeolicus*, and several other Gram-negative bacteria [144, 146]. So far it seems that, of all hydroxamate containing LpxC inhibitors designed, CHIR-090 is the most potent inhibitor and might have clinical utility.

Hydroxamate is a functional group that acts as a very good zinc chelator. How-

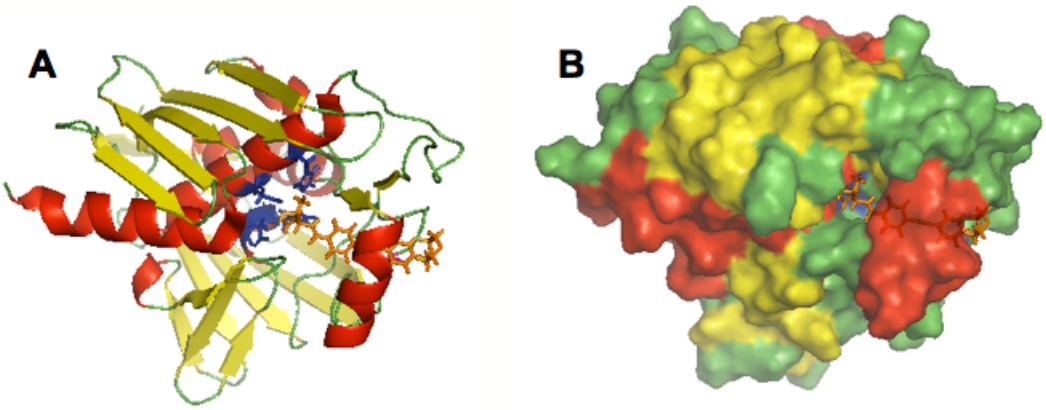


Figure 1.10: Crystal structure of *A. aeolicus* LpxC with the inhibitor CHIR-090 bound. A) LpxC-CHIR-090 complex cartoon. The active site residues are indicatied in blue and CHIR-090 in orange. The hydroxamate moiety of CHIR-090 is facing the active site residues. B) LpxC-CHIR-090 sphere. The biphenyl acetylene moiety of CHIR-090 is located in the hydrophobic passage of the enzyme. PDB file 2JTC was taken from http://www.rcsb.org [135].

ever, due to its activity against many metalloenzymes, compounds containing a hydroxamate group might display a lack of specificity. Non-specific binding of an inhibitor to enzymes other than its primarily target, could lead to unwanted side-effects. Therefore, a new class of LpxC inhibitors is now being explored and has been patented, in which the hydroxamate group is replaced by a hydantoin. Compound 22, shown in Figure 1.9, is an example of this new class of inhibitors and has shown, both *in vitro* and *in vivo*, activity against *P. aeruginosa* [145].

## 1.5 Aminoarabinose biosynthesis

The mechanism of L-Ara4N modifications and biosynthesis of L-Ara4N has been extensively studied in *E. coli* and *Salmonella* by Christian Raetz and co-workers. Eight enzymes are involved in the L-Ara4N biosynthesis, transport, and attachment to lipid A (Figure 1.11).

In *E. coli* the first step is carried out by Ugd, an UDP-glucose dehydrogenase, that oxidises UDP-glucose to UDP-glucuronic acid [147]. Recently, it has been found

that *P. aeruginosa* and *B. cenocepacia* both contain two genes that encode for proteins with Ugd activity [148, 149]. The second step is the oxidative decarboxylation of UDP-glucoronic acid by the C-terminal domain of ArnA, yielding UDP-4-ketopentose (UDP-Ara4O) [147]. The pyridoxal 5′-phosphate (PLP)-dependent enzyme, ArnB, then transaminates UDP-Ara4O, yielding UDP-$\beta$-L-Ara4N [150]. The equilibrium of this transamination is on the side of the ketone, but is shifted to the amine by a consecutive following reaction, carried out by the N-terminal domain of ArnA. This domain of the enzyme formylates the freshly formed UDP-$\beta$-L-Ara4N, yielding UDP-L-Ara4-formyl-N (UDP-L-Ara4FN). ArnC, the fourth enzyme of the pathway, transfers UDP-L-Ara4FN to undecaprenyl phosphate, releasing UDP [151]. Undecaprenyl phosphate-$\alpha$-L-Ara4FN is deformylated by ArnD, and undecaprenyl phosphate-$\alpha$-L-Ara4N is ready to be flipped over the membrane [151]. Two proteins are involved in the flipping process, ArnE and ArnF [152], which form a heterodimer. After arriving at the outer layer of the IM, L-Ara4N is attached to lipid A at the 4′-phosphate by ArnT [153].

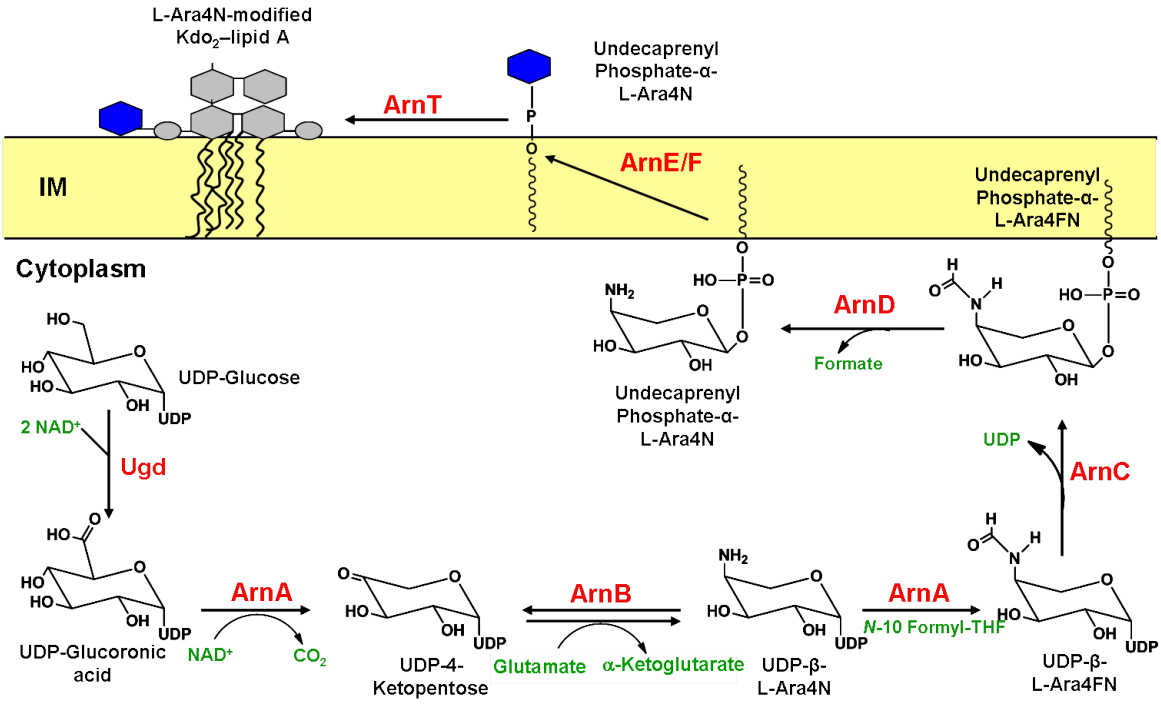


Figure 1.11: *E. coli* L-Ara4N biosynthesis, transport, and attachment to lipid A. Adapted from [152].

In *E. coli* and *Salmonella*, and unlike the genes involved in lipid A biosynthesis, the genes involved in L-Ara4N, except for Ugd, are located in an operon, called the *arn* operon (Figure 1.12) [147, 154]. Originally, the *arn* gene operon was called the *pmr* locus, due its direct link to PmxB resistance. The operon is not continuously expressed in *E. coli* and *Salmonella*, but is induced in response to the local environment (e.g. presence of AMPs, limiting $Mg^{2+}$ conditions), through the activation of the two-component regulatory system PmrA-PmrB. In these two species, gene knock-outs or deletions of any of the genes in the *arn* operon does not effect viability but leads to loss of PmxB resistance [154, 152].

The putative *arn* gene homologues were recently identified in *B. cenocepacia* J2315. Though the organization is different than in *E. coli* and *Salmonella*, the putative homologues of the arn genes of *B. cenocepacia* J2315 are also located together in an operon (Figure 1.12) [98]. To date, the activity of any of the putative genes in the operon has not been proven; however, analysis of the operon suggests several differences in the enzymes involved in the pathway between *B. cenocepacia* and other well studied species. ArnA is a bifunctional enzyme in *E. coli* and *Salmonella*, where the C-terminus of the enzymes catalyzes the second step of the pathway and the N-terminus catalyzes the fourth step of the pathway. In contrast, in *B. cenocepacia*, both reactions appear to be carried out by two proteins encoded by separate genes, *ArnA1* and *ArnA2*. Furthermore, the genes encoding the heterodimer flippase *ArnE* and *ArnF*, could not be identified in *B. cenocepacia*. By low sequence homology to ArnE/ ArnF it is thought that the *ArnG* gene in the *B. cenocepacia arn* operon encodes a putative flippase.

In contrast to *E. coli* and *Salmonella*, the putative *arn* genes are necessary for viability in *B. cenocepacia* [98] and therefore the enzymes involved in L-Ara4N biosynthesis are potential targets for the development of anti-Bcc drugs.

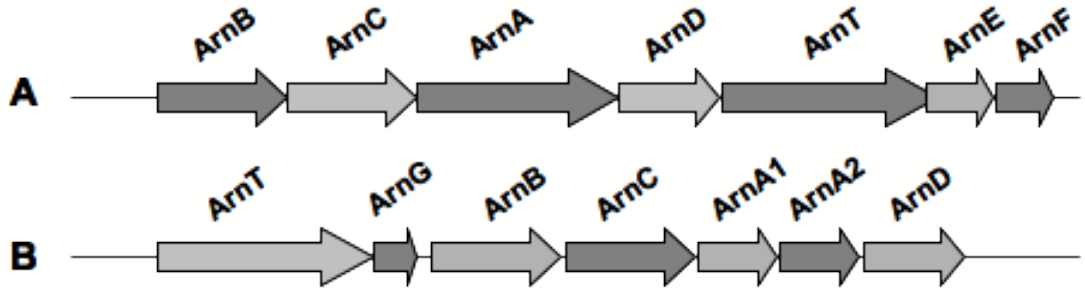


Figure 1.12: Genetic organization of the Arn operon found in: **(A)** *E. coli* and *Salmonella* [152]; and **B** the putative Arn operon of *B. cenocepacia* J2315 [98].

### 1.5.1 ArnB (UDP-Ara4O aminotransferase)

ArnB is an aminotransferase that converts UDP-Ara4O into UDP-Ara4N, using PLP as a co-factor. Like most enzymes that use PLP as a co-factor [155], ArnB acts on amino acids, preferably L-glutamate [150]. The crystal structure of *S. typhimurium* ArnB has been published, and together with biochemical analysis of the protein, the full reaction mechanism of the enzyme (Figure 1.13) was proposed [156]. The crystal structure of the holo-form of the homodimeric ArnB shows that the co-factor PLP is covalently attached to the amino group of a conserved Lys188 residue via a Schiff base. This holo-form of the protein is also known as the internal aldimine (E-PLP). The reaction consists of two half reactions.

In the first half an external aldimine is formed by the displacement of the lysine-PLP aldimine bond by the L-glutamate-PLP aldimine bond. Then formation of the quinonoid intermediate takes place by deprotonation in the $\alpha$-position of L-glutamate, followed by the reprotonation of the quinonoid species to generate ketimine 1. The ketimine is hydrolyzed, giving the reduced cofactor pyridocamine-5′-phosphate form (E-PMP) and free $\alpha$-ketoglutarate.

The second half of the reaction starts with the binding of UDP-Ara4O to E-PMP, generating ketimine 2. Next, ketimine 2 is deprotonated in the $\alpha$-position from

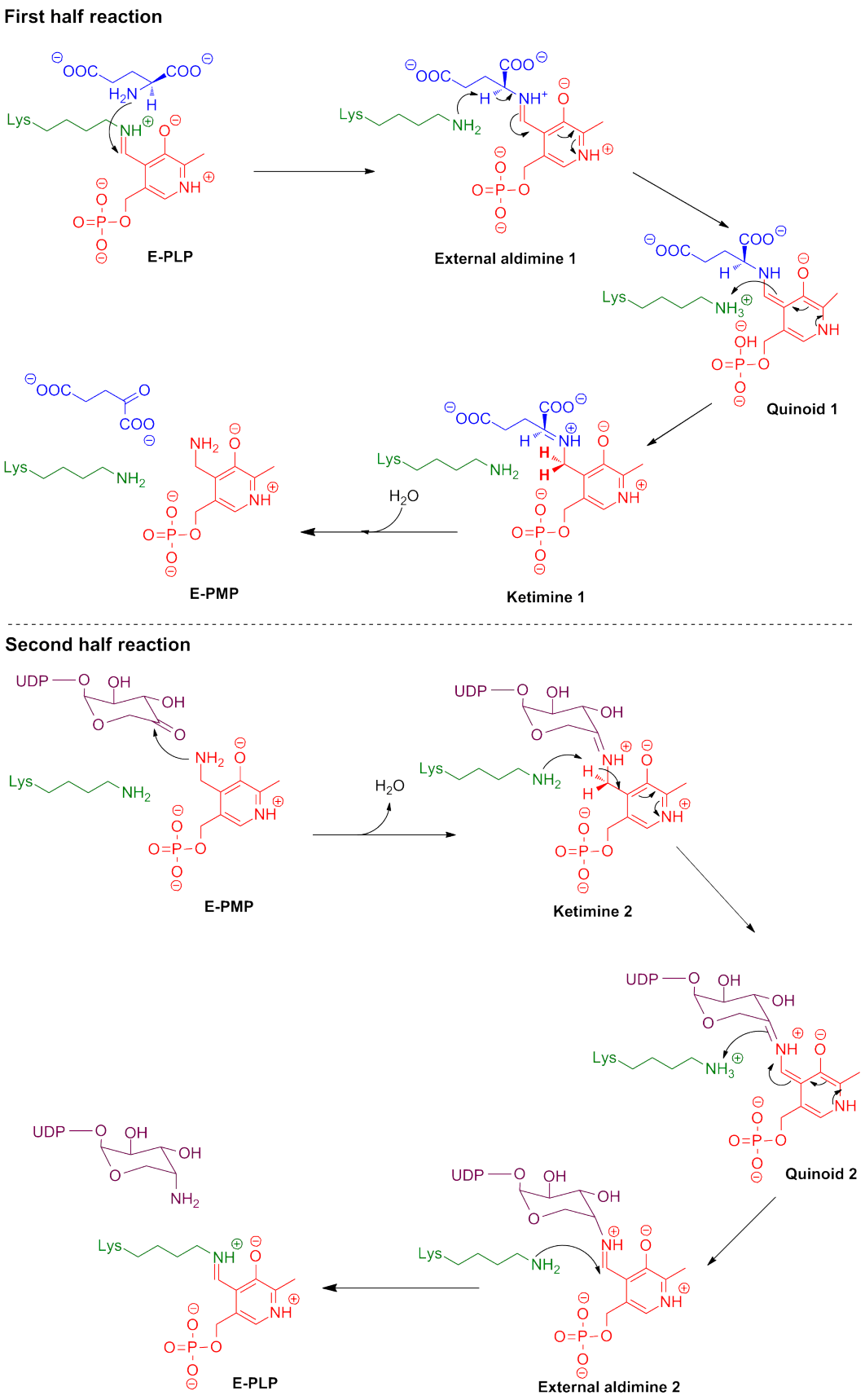


Figure 1.13: Catalytic mechanism of *Salmonella* ArnB. The first- and second-half reaction are shown. Adapted from [156].

UDP-Ara4O, forming quinonoid 2. This intermediate is reprotonated to the external aldimine 2, which is then hydrolyzed, regenerating the E-PLP form and UDP-L-Ara4N.

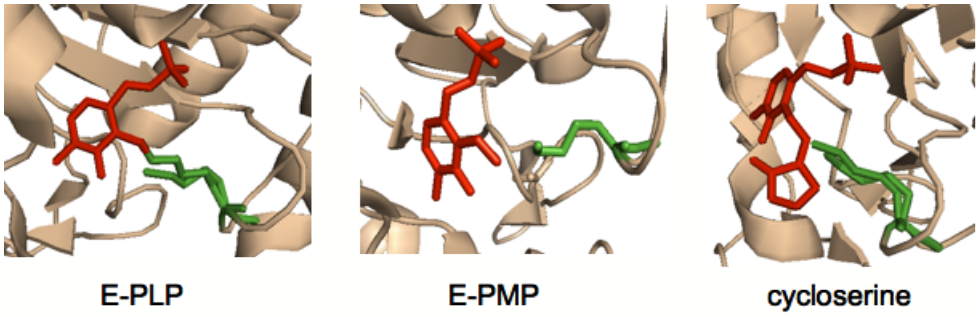


Figure 1.14: The active site of *S. typhimurium* ArnB. Shown are the E-PLP state, the E-PMP state, and with cycloserine bound in the active site. PDB file 1MDZ was taken from http://www.rcsb.org [156]

Interestingly, the ArnB enzyme of *S. typhimurium* can be inhibited by L-cycloserine (LCS, 4-amino-3-isoxazolidone). The crystal structure of ArnB with LCS in the active site (Figure 1.14) shows that LCS binds to the co-factor by replacing the PLP-lysine aldimine bond by a LCS-PLP amine bond [156].

Cycloserine (CS) is a cyclic amino acid mimic and two enanthiomers exist, D-cycloserine (DCS, also known as Seromycin) and L-cycloserine (LCS). DCS is a well known but now little used antibiotic known to inhibit a wide range of PLP-dependent enzymes. Today, it is primarily used as a second line of defence to treat multiple drug-resistant *Mycobacterium tuberculosis* infections, as well as some neurological disorders. In *M. tuberculosis* the primary targets of DCS are the PLP-dependent enzymes D-alanyl-D-alanine ligase and D-alanine racemase, both involved in peptidoglycan synthesis.

## 1.6 Lipid A transport

All three structural domains of LPS, the O-antigen region, the core, and lipid A are synthesized at the cytoplasmic site of the IM. The O-antigen and lipid A

are transported independently to the periplasmic site of the IM, where the two domains are ligated by an enzyme called WaaL [81]. The outer core and O-antigen sugars are transported over the IM by the O-unit transporter Wzx [157, 158]. Polymerization of the sugar units takes place in the periplasm by Wzx polymerase, before ligation to lipid A [81]. Though the lipid A biosynthesis pathway has been very well studied, the mechanism by which lipid A or LPS in its full length (lipid A plus the core and O-antigen domain) is transported to the OM is less well understood [159, 160].

The first step in the movement of lipid A to the OM is the translocation from the site of synthesis, the inner leaflet of the IM, to the outer leaflet of the IM. It is generally believed that this process is mediated by the ABC transporter MsbA. This transporter belongs to the ATP-binding cassette superfamily, and is essential for viability. *E. coli* conditional MsbA mutants accumulate lipid A and phospholipids in the IM [161], and lipid A is capable of modulating MsbA activity [162]. *E. coli* late acyl-transferase (LpxL) mutants accumulate tetra-acylated lipid A in the cytoplasm and are greatly impaired in cell division. Overexpression of MsbA in those mutants restores normal growth [163]. It has never been proven that MsbA can transport lipid A, but recently it has been shown to transport phospholipids and other lipid species across the IM [164].

In the last few years, seven other lipopolysaccharide transport (Lpt) proteins essential for the transport of lipid A have been identified. A schematic presentation of the location of those seven proteins is shown in Figure 1.15. After lipid A is flipped across the IM by MsbA, it has to be extracted from the phospholipid bilayer, a process that requires energy. The lack of an obvious energy source in the periplasm makes the mechanism of trafficking hard to understand. Four proteins, LptB [165], LptC [166], LptF, and LptG [167] form a complex in the IM [168] and are most likely involved in the extraction [106]. LptB is located at the cytoplasmic site of the IM and exhibits ATP hydrolytic activity [168, 169].

LptF and LptG are both IM proteins that most likely form the transmembrane components of the ABC transporter co-operating with LptB. LptC is found at the outer leaflet of the IM and encodes one membrane spanning domain [166]. The structure of LptC has been solved very recently and LptC can bind lipid A *in vitro* [170]. However, the exact function of the complex remains to be clarified. The trafficking of lipid A through the periplasm to the OM is most likely mediated by LptA [165]. LptA is a soluble periplasmic protein [165] that has been shown to bind lipid A in vitro [171]. Furthermore, LptA can displace lipopolysaccharide from LptC *in vitro* [170].

Two other proteins are involved, LptD [172, 173] and LptE [174]. Both proteins are located in the OM and form a 1:1 complex [175]. There are two classes of proteins in the OM, $\beta$-barrel proteins and lipoproteins [78]. LptD is a $\beta$-barrel protein and LptE is a lipoprotein. LptE has been shown to bind LPS *in vitro* [175]. As for the other Lpt proteins, the mechanism of operation of the LptD/LptE complex is unknown.

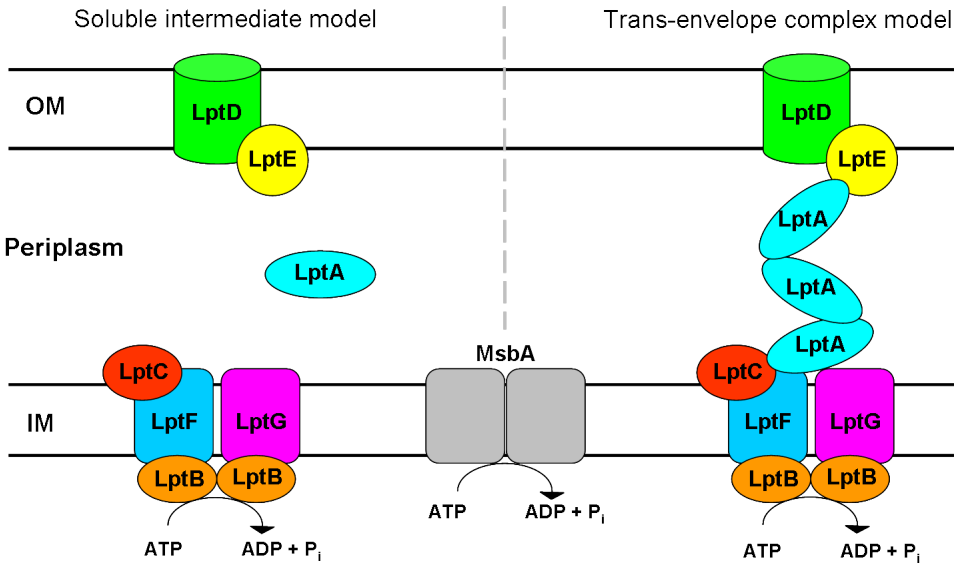


Figure 1.15: Schematic representation of the proteins involved in lipid A trafficking from the cytoplasm to the OM in *E. coli* and two models of lipid A transport across the membrane. Adapted from [106].

Two models exist for lipid A trafficking and the proteins involved, the soluble intermediate model and the the trans-envelope complex model (Figure 1.15). In the first model, LptA is a soluble protein that acts as a chaperone, and transports lipid A from the LptBFGC IM complex to the OM LptDE complex [106]. This model looks fairly similar to lipoprotein transport over the IM to the OM. Lipoproteins are transported by the Lol system, where a complex formed of LolCDE forms the IM ABC transporter. LolA has the periplasmic chaperone function, which mediates trafficking through the periplasm and binds to the LolB receptor at the OM [176].

In the trans-envelope complex model, multiple LptA proteins bridge the periplasm, connecting the IM LptBFGC complex to the OM LptDE complex [160, 106]. The first proof of this model was published in 2005, before the LptA protein was identified. It was shown that, in contrast to lipoproteins, newly synthesized LPS could not be released from spheroplasts upon addition of periplasmic extracts [177]. In 2008, the crystal structure of LptA was published, and though the protein is identified as a monomer by size-exclusion chromatography, it crystallizes as a fibre in the presence of LPS [178]. Recently, it has been shown that all seven Lpt proteins can be co-purified as a complex suggesting they interact directly, a finding that supports the trans-envelope complex model [175].

### LptA (Lipopolysaccharide transport protein A)

LptA, the soluble periplasmic protein shown to bind lipid A of *E. coli*, is a 185 aa protein, with a putative signal peptide of 27 aa that enables transport of the protein to the periplasm [165].

As mentioned above, the structure of *E. coli* LptA, has been solved (Figure 1.16). LptA consists, like the human LPS binding protein MD-2, mainly of $\beta$-sheets. LptA has eleven anti-parallel $\beta$-sheets that twist $90^o$ over the length of the protein, forming a hydrophobic cleft. The crystal structures that have up to now been

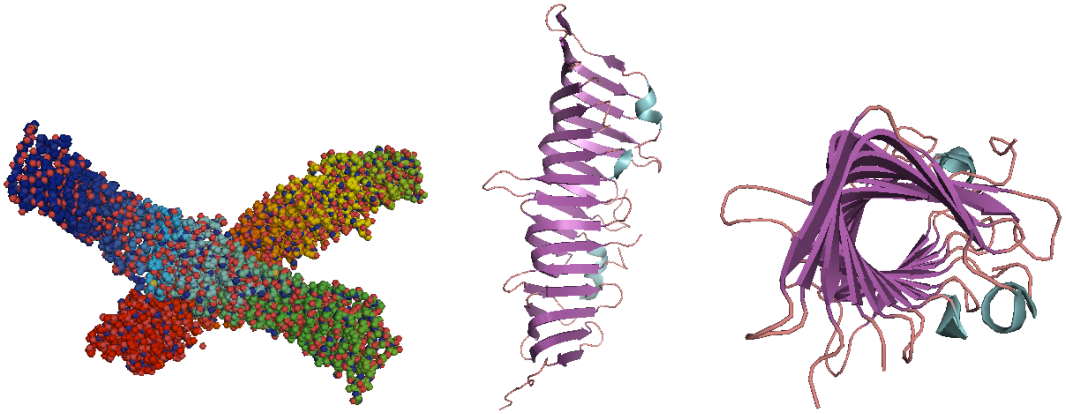

(a) (b) (c)

Figure 1.16: Crystal structures of *E. coli* LptA. A) Spheric image of fibres consisting of LptA proteins crystallized together. B) Cartoon of two LptA proteins, side view. C) Cartoon of two LptA protein, top view. PDB files 2R19 and 2R1A were taken from http://www.rcsb.org [178].

solved for *E. coli* LptA do not contain LPS [178]. The structure of MD-2 on the other hand, has been solved recently with LPS bound and shows that the fatty acids of LPS bind to the MD-2 hydrophobic $\beta$-sheet pocket [71]. It might be that, as for MD-2, only the fatty acids bind in the hydrophobic cleft of LptA, a hypothesis supported by the work of Tran et al. [171], who showed that LptA is capable of binding smooth-LPS, $Kdo_2$-lipid A and lipid $IV_A$. Figure 1.16 A shows eight LptA proteins forming a fiber. Interestingly, this co-crystallization only occurred when induced with either smooth- or rough- LPS. When not triggered by LPS, only two proteins co-crystallized, as illustrated in Figure 1.16 (b and c).

### LptB (Lipopolysaccharide transport protein B)

LptB belongs to the superfamily of ABC-transporters, and in *E. coli*, the *LptB* gene is located immediately downstream of *LptA*. In a general study on protein complexes of the *E. coli* IM and OM, LptB was initially described to be associated to the IM [179]. Later, purified LptB was found to form a complex with LptF and LptG [168, 169]. ATP-hydrolysis by LptB could be observed after purification.

Though some ATP-ases can be activated or inhibited by their substrate, LptB activity is not affected by the presence of smooth-LPS or $Kdo_2$-lipid A [168]. *E. coli* LptB is capable of hydrolyzing ATP, UTP, GTP and CTP, but showed a clear substrate preference for ATP [169].

LptB recently has received renewed interest as a target for new antimicrobial agents. As an aid in these studies, a high-throughput assay for activity was recently developed [169]. Two commercially available kinase inhibitor libraries (244 compounds) have been tested against *E. coli* LptB and two potent inhibitors have been highlighted (Figure 1.17). Furthermore, in a previous study [168], the well known ATP-ase inhibitor, orthovanadate, was shown to be inhibitory against *E. coli* LptB. Although, all three compounds inhibit LptB *in vitro*, *in vivo*, killing assays have not been succesful to date [169].

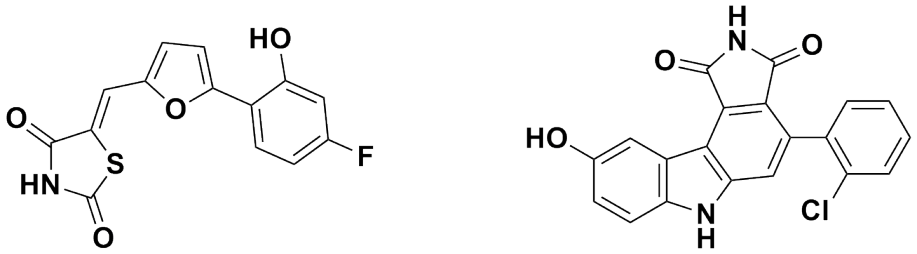


1 2

Figure 1.17: Two published *E. coli* LptB inhibitors. Adapted from [169].

## 1.7 Aims

Species belonging to the Bcc are not harmful to healthy individuals, but can cause life-threatening lung infections in people suffering from CF. The Bcc are amongst the most antimicrobial-resistant pathogens encountered in human infections, making successful treatment of the infection virtually impossible. Once the CF lung gets infected by the Bcc, it can cause the lethal "Cepacia syndrome." In this thesis, I focused my research on one of the virulence factors, lipid A, which

might cause "Cepacia syndrome," and antimicrobial drugs that target lipid A biosynthesis.

This thesis is divided into three sections:

1. CHIR-090 activity against the Bcc;
2. D-cycloserine activity against the Bcc;
3. L-Ara4N specificity of lipid A transport.

The aim of the first section (CHIR-090 activity against the Bcc) was to study the effects of specific inhibitors of the enzymes involved in lipid A biosynthesis against the Bcc. To study this, I used the most potent LpxC inhibitor published to date, CHIR-090. A second aim was to investigate the species- and strain-specific susceptibility towards CHIR-090.

The aim of the second section (D-cycloserine activity against the Bcc) was to study the potential use of the PLP-dependent enzyme inhibitors D-cycloserine and L-cycloserine in the treatment of Bcc infections. An additional aim was to study *B. cenocepacia* ArnB as a drug target, since this enzyme is necessary for viability.

The aim of the last section (L-Ara4N specificity of lipid A transport) was to improve the understanding of why L-Ara4N is necessary for viability in *B. cenocepacia* but not in other Gram-negative bacteria. To do so, I decided to study two proteins involved in lipid A transport, LptA and LptB.

The work presented here constitutes one of the first research projects on the Bcc enzymes involved in lipid A biosynthesis and transport. Since lipid A is an important virulence factor and enzymes involved in biosynthesis and transport of this molecule are necessary for viability, it offers an important target for research.

# Chapter 2

# The activity of the Lipid A Biosynthesis Inhibitor CHIR-090 against the Bcc

**Part of this chapter was published:**

Bodewits K., Raetz C. R., Govan J. R., Campopiano D. J. Antimicrobial activity of CHIR-090, an inhibitor of lipopolysaccharide biosynthesis, against the Burkholderia cepacia complex. *Antimicrobial Agents and Chemotherapy* **(2010)**, 54, 3531-3533.

The discovery and introduction of antimicrobial drugs around the 1930s, led to an era in which millions of people were saved from the fatal effects of bacterial infections. Before the availability of antimicrobial agents, hospitals were filled with patients with tuberculosis, pneumonia, rheumatic fever, and many other diseases caused by pathogenic bacteria. However, from the 1930s onwards the wards were mainly filled with patients with diseases that are not caused by bacteria, such as cancer, diabetes and heart problems [180]. In the 1980s, many researchers, clinicians, and pharmaceutical companies thought that after nearly

half a century of increasing control of microbial diseases, the problem of bacterial infections has been overcome, and research tended to focus on controlling fungi- and viral- infections [181, 182]. However, in the 1990s, people were confronted with a world-wide re-emerge of bacterial infections which could not be treated successfully or not as easily as before. The most important reason for this phenomenon is the acquisition of antibiotic-resistance genes by pathogenic bacteria, which coincides with a reduction in the discovery of new antibiotics with novel activity. The rapidity of the acquisition of the antibiotic-resistance genes by pathogenic bacteria increased after the 1980s due to increased air travel, the higher frequency of invasive surgery, a higher number of immunocompromised individuals in the population, and the increased survival of patients with chronic debilitating diseases, such as CF [182]. Hence, for the last ∼30 years, the options for treatment of bacterial diseases is have reduced and there is now an urgent need for new agents with novel antimicrobial activity against both existing and emerging bacterial pathogens.

### The LpxC inhibitor CHIR-090

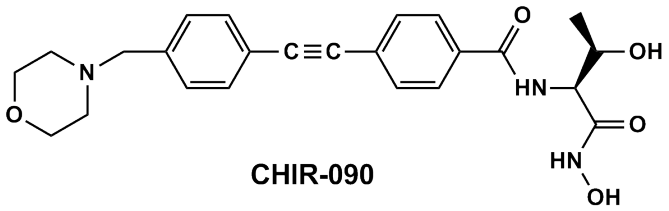

CHIR-090

Figure 2.1: The LpxC inhibitor CHIR-090 (N-aroyl-L-threonine). Adapted from [144].

The lipid A biosynthesis pathway has been recognized as an attractive target for new agents design to treat infections caused by Gram-negative bacteria [128, 181]. The most potent inhibitor of this pathway found so far is the synthetic antibiotic CHIR-090 (Figure 2.1). This antibiotic has been shown to be a slow, tight-binding inhibitor of the purified LpxCs from different species [135, 144, 146]

and displayes good antimicrobial activity against several Gram-negative bacteria, including *E. coli* and *P. aeruginosa* [146]. In this chapter, the potential of antibiotics targeting lipid A biosynthesis to treat Bcc infections is explored, using CHIR-090 as a model antibiotic (kindly provided by Professor C. R. H. Raetz, Duke University, USA).

## 2.1 CHIR-090 against the Bcc

To assess the antibacterial activity of CHIR-090 against *B. cenocepacia* and *B. multivorans*, the main Bcc species recovered from CF sputum, a disc diffusion test was carried out. This is a commonly-used assay, where an agar plate is inoculated uniformly with the bacteria of interest. Then, a filter paper disk impregnated with the antibiotic is placed onto the plate so that the antibiotic can diffuse through the agar. When grown overnight, the bacteria will grow confluently on top of the plates, with or without zones of bacterial growth inhibition around the antibiotic disk. The diameter of the inhibition zone depends on the susceptibility of the bacteria, the concentration of antibiotic, and the speed of diffusion of the antibiotic.

A panel of six strains was assembled, including two positive control strains. The control strains *E. coli* K-12 (MG1655) and *P. aeruginosa* (PAO1) were used based on previously published work in which CHIR-090 was shown to be active against those strains [146]. One *B. multivorans* strain (C5393) and three *B. cenocepacia* strains (J2315, K56-2, and SAL-1) were included. The three *B. cenocepacia* strains belong to the clonally-related ET12 lineage and were chosen for their difference in LPS profile and their relevance in epidemic outbreaks. *B. cenocepacia* J2315, the strain responsible for an epidemic outbreak in Edinburgh [26], produces rough LPS. *B. cenocepacia* K56-2, a Canadian CF isolate [63], produces smooth LPS. *B. cenocepacia* SAL-1 is a genetically manipulated strain derived from *B. cenocepacia* K56-2, and produces deep-rough LPS [183]. Previously, it

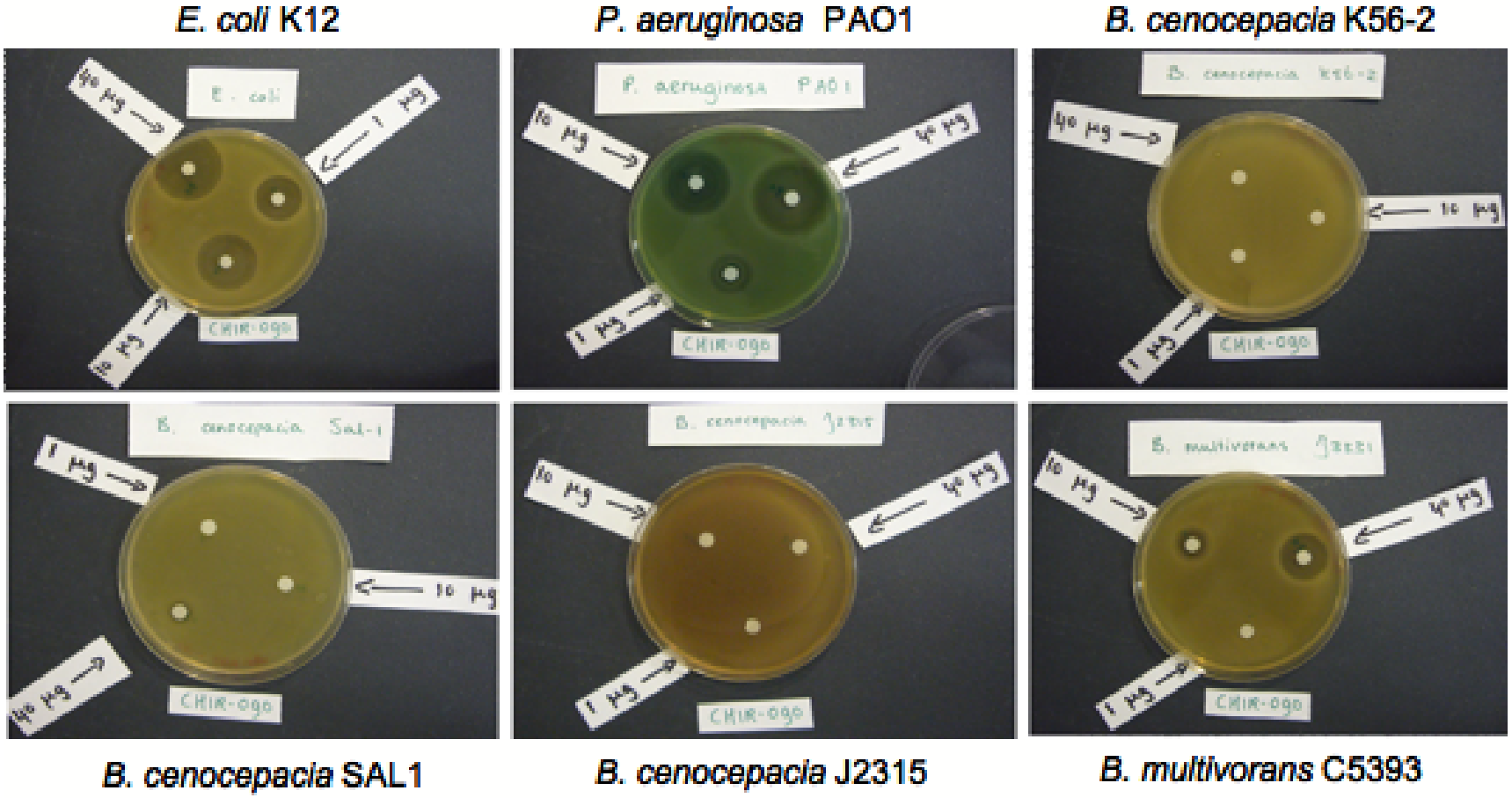


Figure 2.2: Antibacterial disc diffusion assay of CHIR-090 against four Bcc strains, *E. coli* and *P. aeruginosa*. Each disk contained 40 $\mu$g, 10 $\mu$g or 1 $\mu$g CHIR-090.

has been shown that clear zones of inhibition of CHIR-090 against *P. aeruginosa* could be obtained using 10 $\mu$g/disc [146]. Therefore it was decided to carry out a disc diffusion assay with discs containing CHIR-090 concentrations in the same range (e.g. 0, 1, 5, 10, 20, and 40 $\mu$g/disc). The results for 1, 10, and 40 $\mu$g against the six strains are shown in Figure 2.2.

The growth of *E. coli* and *P. aeruginosa* was clearly inhibited by the lowest amount of CHIR-090 (1 $\mu$g), whereas *B. multivorans* was inhibited by 10 $\mu$g containing discs. In contrast, growth of all three *B. cenocepacia* strains was not inhibited with discs containing 40 $\mu$g CHIR-090. In further tests, these strains displayed resistance even when discs containing 100 $\mu$g were used (data not shown).

Analysis of my data suggests that there is no correlation between CHIR-090 growth inhibitory activity and the LPS profile of individual strains. By using the three *B. cenocepacia* strains K56-2 (smooth LPS), J2315 (rough LPS), and SAL-1 (deep-rough LPS), I can conclude that the presence of an O-antigen or complete core region does not affect the susceptibility to CHIR-090.

Despite the fact that species of the Bcc are genetically closely related, growth of *B. multivorans* could be inhibited, whereas growth of *B. cenocepacia* could not. This unexpected result lead us to subsequently test CHIR-090 activity against more Bcc species.

I used the disc diffusion assay to determine the sensitivity to CHIR-090 of the Bcc reference panels [35, 38], consisting of 45 Bcc strains[1] representing the first nine reported Bcc species (Table 2.1).

Prior to the assay, DNA of all 45 Bcc strains was isolated and a *recA*/RFLP analysis was performed to confirm the identity of the strains (Appendix A.1). Further studies were only carried out with the *recA* positive strains.

A concentration of 40 $\mu$g CHIR-090 was used throughout the study. The results

[1]The *B. cenocepacia* K56 derivative SAL-1 was also included in this study, but does not belong to the Bcc reference panel

Table 2.1: CHIR-090 sensitivity of the Bcc reference panel and the presence of the $LpxC_2$ gene. L2 = presence of $LpxC_2$; S = sensitivity to CHIR-090; IZ = diameter of inhibition zone (mm).

| Strain | L2 | S | (IZ) | Strain | L2 | S | (IZ) |
|---|---|---|---|---|---|---|---|
| ***B. cepacia*** **(I)** | | | | ***B. dolosa*** **(VI)** | | | |
| ATCC25416 | + | - | - | AU0645 | - | + | 18 |
| ATCC17759 | + | - | - | CEP021 | - | + | 24 |
| CEP509 | + | - | - | E12 | - | + | 23 |
| LMG17991 | | | | STM1441 | - | + | 21 |
| ***B. multivorans*** **(II)** | | | | ***B. ambifaria*** **(VII)** | | | |
| C5393 | - | + | 20 | AMMD | - | + | 23 |
| LMG13010 | - | + | 14 | ATCC53266 | - | + | 24 |
| C1575 | - | + | 15 | CEP0996 | - | + | 22 |
| CF-A1-1 | - | + | 22 | | | | |
| JTC | - | + | 23 | | | | |
| C1962 | - | + | 24 | | | | |
| ATCC17616 | - | + | 17 | | | | |
| 249-2 | - | + | 26 | | | | |
| ***B. cenocepacia*** **(III)** | | | | ***B. anthina*** **(VIII)** | | | |
| J2315 | + | - | - | W92 | - | - | - |
| BC7 | + | - | - | C1765 | - | + | 13 |
| K56-2 | + | - | - | J2552 | - | - | - |
| C5424 | - | + | 19 | AU1293 | - | + | 10 |
| C6433 | + | - | - | | | | |
| C1394 | | | | | | | |
| PC184 | - | + | 18 | | | | |
| CEP511 | + | - | - | | | | |
| J415 | - | + | 21 | | | | |
| ATCC17765 | + | - | - | | | | |
| SAL-1 | + | - | - | | | | |
| ***B. stabilis*** **(IV)** | | | | ***B. pyrrocinia*** **(IX)** | | | |
| LMG14292 | + | - | - | ATCC15958 | - | + | 20 |
| C7322 | + | + | 14 | ATCC39277 | - | + | 22 |
| LMG14086 | + | - | - | BC011 | - | + | 23 |
| LMG18888 | + | - | - | C1469 | + | - | - |
| ***B. vietnamiensis*** **(V)** | | | | | | | |
| PC259 | - | + | 26 | | | | |
| LMG16232 | - | + | 23 | | | | |
| FC441 | - | + | 9 | | | | |
| LMG10929 | - | + | 23 | | | | |

of the disc assay against the whole panel are summarised in Table 2.1[2]; clearly-observed zones are reported as (+) and no growth inhibition as (-). For the (+) strains, the diameter of the inhibition zones are given. It was clear at this stage that despite the close taxonomic relationship of all Bcc species, individual isolates displayed remarkable differences in their susceptibility to CHIR-090 even within a single species. For example, of the eight *B. cenocepacia* (III) strains, two (C5424 and PC184) were sensitive and six resistant. Moreover, three of the highly transmissible ET12 lineage (J2315, K56-2 and BC-7) were resistant, and C5424 was sensitive. All representative strains of *B. multivorans*, *B. vietnamiensis*, *B. dolosa* and *B. ambifaria* showed sensitivity to CHIR-090.

### 2.1.1 CHIR-090 against *B. multivorans*

*B. multivorans*, one of the most prevalent Bcc species recovered from the CF lung [59], could be inhibited by CHIR-090. Encouraged by this finding, the MICs were determined for all *B. multivorans* strains of the panel (Table 2.2). In the absence of published guidelines to determine MICs for the Bcc, the decision was made to use the internationally-accepted BSAC methodology [184] for other Gram-negative pathogens. As described in the BSAC guidelines, the quality control strains *P. aeruginosa* ATCC27853, *P. aeruginosa* ATCC10145, and *E. coli* ATCC25922 were used. Due to a lack of a suitable antibiotic active against all members of the Bcc, PmxB was used as a control for activity against *P. aeruginosa* and *E. coli*. PmxB was used as a positive control for the uniquely-high resistance of *B. multivorans* (and all other members of the Bcc).

The CHIR-090 MICs for *B. multivorans* were strain-dependent, and ranged from 0.1 to >100 $\mu$g/ml. CHIR-090 was particularly active against *B. multivorans* 249-2, previously noted for its resistance to beta-lactams (including the ability to use penicillin G as a sole nutrient) [52], whereas it was not active against the

[2]Table 2.1 also presents results which will be discussed in the next section of this chapter

Table 2.2: MIC values ($\mu$g/ml) of CHIR-090 and polymyxin B (PmxB) against, *E. coli*, *P. aeruginosa*, and *B. multivorans* a panel of strains (antibiotic concentration ranged from 0 to 100 ($\mu$g/ml).

| Strain | Source/reference | CHIR-090 | PmxB |
|---|---|---|---|
| ***E. coli*** | | | |
| ATCC25922 | ATCC | 0.05 | 0.78 |
| ***P. aeruginosa*** | | | |
| ATCC27853 | ATCC | 0.78 | 3.13 |
| ATCC10145 | ATCC | 0.78 | 3.13 |
| ***B. multivorans*** | | | |
| C5393 | Vancouver CF clinic [185] | 3.13 | >100 |
| LMG13010 | Belgium CF clinic [186] | >100 | >100 |
| C1575 | Glasgow Epidemic [60] | 12.5 | >100 |
| CF-A1-1 | Cardiff CF clinic [187] | 1.56 | >100 |
| JTC | CGD patient [188] | 1.56 | >100 |
| C1962 | Brain abscess [189] | 3.13 | >100 |
| ATCC17616 | Environmental strain [47] | 6.25 | 50 |
| 249-2 | Derived from ATCC17616 | 0.10 | >100 |

*B. multivorans* type strain isolated from a Belgian clinic [36]. The low MICs for most *B. multivorans* highlights the potential of CHIR-090 against *B. multivorans*.

## 2.2 Species and isolate specific susceptibility or resistance

To explore the species and strain-specific susceptibility to CHIR-090, a BLAST search was carried out for putative LpxC genes present in the available *Burkholderia* genomes (Figure 2.3, www.burkholderia.com). Sequence analysis revealed that the annotated LpxC genes are highly conserved and display high sequence homology to LpxCs from organisms such as *P. aeruginosa* and *E. coli*; thus, the resistance of most *B. cenocepacia* strains against CHIR-090 in contrast to the susceptibility of *B. multivorans* could not be explained by differences in the se-

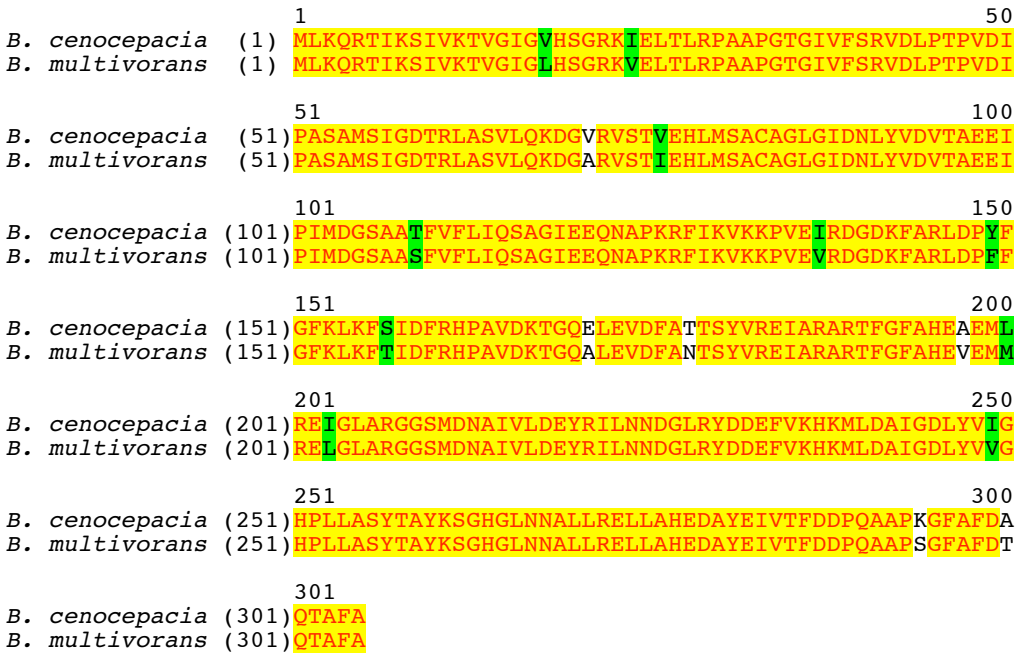


Figure 2.3: Sequence alignment of the translated *LpxC* genes of *B. cenocepacia* J2315 (BCAL3455) and *B. multivorans* ATCC17617 (Bmul2829).

quence differences between the putative *LpxC* genes in the genome. To illustrate the high sequence homology between the putative Bcc *LpxC* genes, an alignment of the translated genes of *B. cenocepacia* J2315 and *B. multivorans* ATCC17617 is shown in Figure 2.3. The two *LpxC* genes are 95% identical and 98% similar to each other.

During the *Burkholderia* genome analysis, I discovered LpxC orthologs in many species with low amino acid sequence similarity to the well-characterised LpxC from *E. coli*. Also, the second putative ORF was annotated in the genomes as *LpxC*. For example, in *B. cenocepacia* J2315, there are two putative ORFs annotated as LpxC; BCAL3455 that shows 71% similarity to *E. coli* LpxC, and BCAL3219 that shows 44% similarity to *E. coli* LpxC. In the genome of *B. multivorans* ATCC17617, only one putative ORF is annotated as *LpxC*, namely Bmul2829, which is 71% similar to *E. coli* LpxC. I could hypothesise that this unique LpxC ortholog, found in *B. cenocepacia* J2315, but not *B. multivorans* ATCC17617, might be responsible for resistance to CHIR-090.

### 2.2.1 A LpxC ortholog possibly responsible for resistance

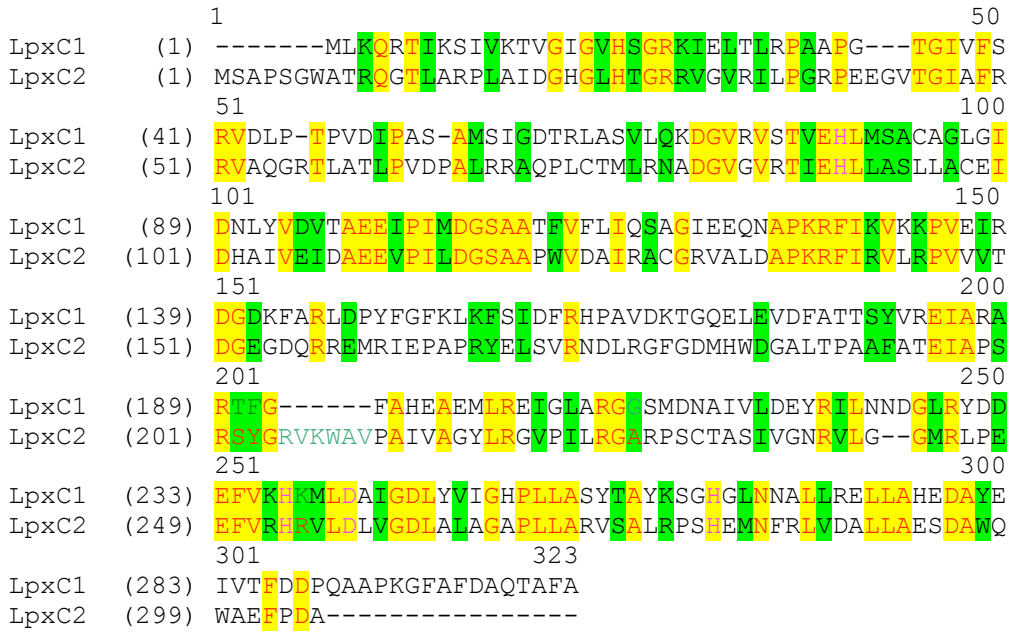


Figure 2.4: Amino acid sequence comparison of $LpxC_1$ (BCAL3455) and $LpxC_2$ (BCAL3219) of *B. cenocepacia* J2315. Grey-Pink aa, putative active site residues; blue-green, CHIR-090 binding residues (identified in *A. aeolicus*) in $LpxC_1$; blue-red, CHIR-090 binding residues in $LpxC_2$.

Amino acid alignment of the two putative open reading frames (ORFs) found in *B. cenocepacia* J2315, BCAL3455 and BCAL3219, also referred to as *LpxC*$_1$ and *LpxC*$_2$ respectively, is shown in Figure 2.4. $LpxC_1$ and $LpxC_2$ show 47% similarity and 29% identity. A Blast analysis was performed, using all microbe genomes available on the NCBI website (http://www.ncbi.nlm.nih.gov), and it was found that the presence of *LpxC*$_2$ is unique to *Burkholderia* species, but is not present in all *Burkholderia* species. Of the *Burkholderia* species sequenced so far, *B. cenocepacia*, *Burkholderia* sp383, *B. pseudomallei*, and *B. mallei* have a *LpxC*$_2$ homolog, whereas *B. multivorans*, *B. thailandensis*, *B. ambifaria*, and *B. vietnamiensis* lack the second putative LpxC.[3]

From sequence analysis of the different LpxC enzymes of different species (Ap-

[3] *Burkholderia* sp383, *B. pseudomallei*, *B. mallei*, and *B. thailandensis* do not belong to the Bcc.

pendix A.2) and the $LpxC_1$ and $LpxC_2$ alignment (Figure 2.4), it would not be surprising if $LpxC_2$ of *B. cenocepacia* shows UDP-3-*O*-acyl-GlcNac deacetylase activity and at the same time is not inhibited by CHIR-090.

Jackman et al [130] suggested that only 33 amino acids of the LpxCs of 11 diverse Gram-negative bacteria were conserved within the species. Out of these 33 amino acids, 27 are present in $LpxC_2$ as well. Furthermore, the four $Zn^{2+}$ binding motif/ active site residues, typical for LpxCs and known to be essential for catalysis, are present in $LpxC_2$. Barb et al [135] described the structure of the *A. aeolicus*

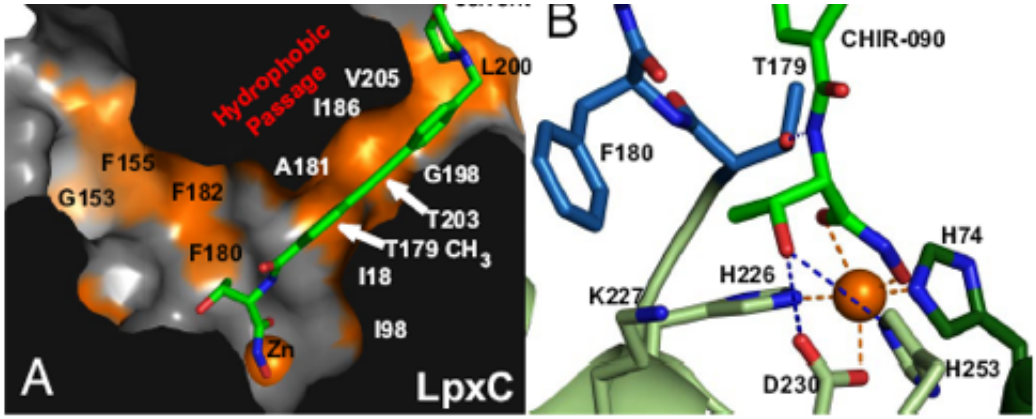


Figure 2.5: CHIR-090 bound into the active site of *A. aeolicus* LpxC. Taken from [135].

LpxC-CHIR-090 complex and indicated the amino acids involved in CHIR-090 binding (Figure 2.5). Having had a closer look at these essential amino acids, I concluded that it is not likely that CHIR-090 would inhibit $LpxC_2$. *A. aeolicus* T179, with which the CHIR-090 threonyl group forms a hydrogen bond, is replaced by serine in $LpxC_2$, thereby predominantly changing the geometry. A mutation of this threonine in LpxC of *A. aeolicus* has already proved to lead to much less inhibitory activity of CHIR-090 on LpxC [135]. Residue F180 of *A. aeolicus* LpxC, with which the methyl group of threonyl of CHIR-090 is in van der Waals contact is replaced by a tyrosine in $LpxC_2$. The two residues, H253 and D230, that are both essential for catalysis and might form hydrogen bonds with the threonyl hydroxyl oxygen of CHIR-090 are both present in $LpxC_2$.

K227, which is the third potential amino acid to form a hydrogen bond with the hydroxyl oxygen of CHIR-090, is replaced by an arginine in $LpxC_2$, changing the hydrogen bonding pattern. Many residues identified as important for the biphenyl acetylene moiety and morpholine unit insertion in the hydrophobic passage by forming hydrophobic interactions, are mutated in $LpxC_2$ to either charged residues or other hydrophobic residues.
Moreover, an arginine residue in $LpxC_2$ replaces G198 of *A. aeolicus*. A mutation in this glycine to an hydrophilic residue (serine) is found in the CHIR-090 insensitive LpxC of *R. leguminosorum* as well. For *R. leguminosorum* LpxC it was suggested as one of the differences in amino acid sequence that might be responsible for the decrease in affinity for CHIR-090 by blocking the hydrophobic passage [135]. Additionally, the putative $LpxC_2$ has a six amino acid insertion inside the gene not found in any of the LpxCs of other species or in $LpxC_1$ of *B. cenocepacia* J2315.

Tertiary protein structure models were made (Figure 2.6) of $LpxC_1$ and $LpxC_2$ using Swissmodel in which *A. aeolicus* LpxC was used as a template. The two topologically similar domains, containing a five-stranded $\beta$-sheet and two $\alpha$-helices, found in *A. aeolicus* LpxC, could be recognised in both $LpxC_1$ and $LpxC_2$. Both enzymes contain the four residues known to form the active site, and both have a long hydrophobic tunnel leading out of the active site suitable for the fatty acid chain of the substrate. Using real-time PCR, I showed that both genes are expressed in the *B. cenocepacia* strains K56-2 and J2315 during exponential growth (results not shown).

### 2.2.2 The presence of $LpxC_2$ in the Bcc

To investigate a possible correlation between the presence of the $LpxC_2$ gene and resistance to CHIR-090, it was decided to continue the study by using the whole Bcc reference panel [35, 38], *B. cenocepacia* SAL-1 [183], the *E. coli* K-12, and

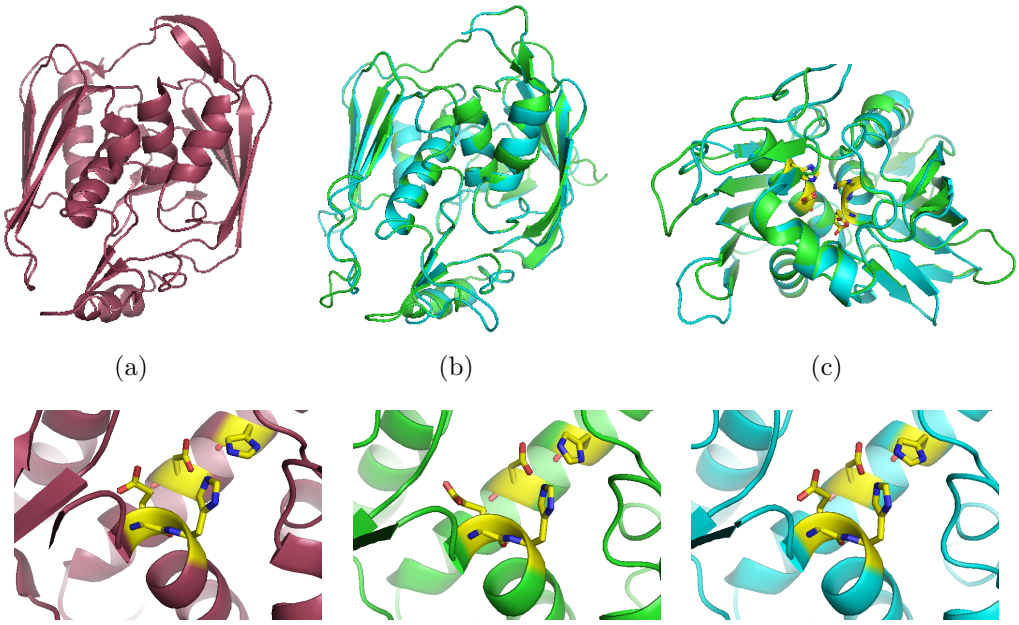


Figure 2.6: Structural models of *B. cenocepacia* J2315 $LpxC_1$ and $LpxC_2$ which were generated by Swissmodel and *A. aeolicus* LpxC (PDB code: 2IER) as a template. A, *A. aeolicus* LpxC; B and C, *B. cenocepacia* J2315 $LpxC_1$ (green) and $LpxC_2$ (blue) overlaid; D, active site of *A. aeolicus* LpxC; E, active site of $LpxC_1$; F, active site of $LpxC_2$.

*P. aeruginosa* PAO1 control strains.

DNA of all 46 Bcc strains was isolated, and the genomic DNA of all the Bcc strains were checked for the presence of *LpxC*$_2$ by PCR, using primers designed on high homology regions of sequenced *Burkholderia* species *LpxC*$_2$ genes. The presence of PCR products of the different Bcc species is summarised in Table 2.1 and shown in Appendix A.1. All *B. cepacia*, *B. stabilis*, and *B. anthina* strains possess the *LpxC*$_2$ gene. Most *B. cenocepacia* strains, two *B. ambifaria* strains, and one *B. pyrrocinia* (IX) strain also contain the gene.

With only a few exceptions (*B. stabilis* C7322, *B. anthina* C1765, and *B. anthina* J2552), a strong correlation was observed between the presence of *LpxC*$_2$ and resistance against CHIR-090. This supports the hypothesis that $LpxC_2$ can complement $LpxC_1$, or is responsible for CHIR-090 resistance. *B. stabilis* C7322

is the only strain that does contain the *LpxC*$_2$ gene but is not resistant to CHIR-090. This could be caused by a natural mutation in the gene, leading to a non-translated or inactive protein.

For the two *B. anthina* strains (C1765 and J2552) that show resistance but do not have the *LpxC*$_2$ gene, it might be that the concentration tested was too low to give zones of inhibition. The diameter of the inhibition zones of the other two *B. anthina* strains are amongst the lowest. Unfortunately, due to the limited amount of CHIR-090 I possessed, it was not possible to repeat the disc diffusion assay with higher concentrations of CHIR-090.

If both LpxC$_1$ and LpxC$_2$ can catalyse the same reaction and have both been shown to be expressed during exponential growth, then only one of the genes should be necessary for viability. Therefore, I attempted to create LpxC$_1$ and LpxC$_2$ knock-out strains. *B. cenocepacia* strain, K56-2 was used for this study, since *B. cenocepacia* J2315 is known to be poor as a recipient in transformation or conjugation. To create the knock out strains, I first used a pGpΩ plasmid [190], which inserts itself in the gene of interest, thereby disrupting it. However, repeated attempts to knock either of the genes out failed. This might be due to the fact that other genes lying downstream (in the same operon) as *LpxC*$_1$ or *LpxC*$_2$, are affected by the introduction of the pGpΩ plasmid and are necessary for viability, or that LpxC$_1$ and LpxC$_2$ can not fully complement each other and therefore are both necessary for viability. Subsequently I attempted to create a conditional *LpxC*$_2$ mutant using the pSc200 plasmid [98], which inserts itself upstream of the gene of interest, and introduces a rhamnose inducible promotor P$_{rhaB}$ to drive the expression of the gene. If LpxC$_2$ is responsible for resistance towards CHIR-090, Bcc strains should become susceptible to CHIR-090 when *LpxC*$_2$ is not expressed. The pSc200 plasmid was transferred to *B. cenocepacia* K56-2 by triparental mating and the correct insertion into the chromosome was confirmed by PCR. Next, a disc diffussion assay with 40 $\mu$g CHIR-090 was carried out on minimal media

supplemented with rhamnose to induce transcription of $LpxC_2$, or with glucose to suppress transcription. On both media, the *B. cenocepacia* K56-2 conditional mutant strain was resistant to CHIR-090 (no inhibition zones), as described for the wild-type strain in the previous section. A definite conclusion could not be drawn from this result due to the method used. The pSc200 plasmid introduces a promotor in front of the gene, enabling partially controlled expression, but "leaky" expression could still occur. Around the discs containing CHIR-090, a strong selection pressure might arise for cells that express $LpxC_2$ and "leaky" expression alone might be enough to cause resistance. Due to the limited amount of CHIR-090 available, this experiment was carried out only once.

### 2.2.3 Cloning and expression of $LpxC_1$ and $LpxC_2$

To characterise the enzymes encoded by $LpxC_1$ and $LpxC_2$, an attempt was made to clone both genes into expression plasmids for recombinant protein expression in *E. coli*. The $LpxC_1$ gene was amplified from genomic DNA of *B. cenocepacia* J2315 and cloned into the expression plasmid pET22b, giving pET22b_$LpxC_1$_J2315. Several attempts to amplify $LpxC_2$ from genomic DNA failed. Therefore, it was decided to purchase a synthetic gene encoding $LpxC_2$. This gene was also cloned into the expression plasmid pET22b, which was named pET22b_$LpxC_2$_J2315. Integrity of the correct plasmids was proven by restriction digests and by sequencing of the plasmids (results not shown).

For recombinant $LpxC_1$ and $LpxC_2$ expression, different cell lines, media, and growth conditions were tried.[4] In order to get good $LpxC_1$ expression, *E. coli* HMS174 (DE3) competent cells, transformed with pET22b_$LpxC_1$_J2315, were used. Expression was induced with 0.1 mM isopropyl $\beta$-D-1-thiogalactopyranoside (IPTG) for 18 hours at 20 $^o$C (Figure 2.7).

[4]Cell lines = *E. coli* HMS174 (DE3) and *E. coli* BL21 (DE3); media = LB broth and 2YT broth (with or without the addition of $Zn^{2+}$); growth conditions = temperature (20 or 37$^o$C, time (1, 3, 5, and 18 hours), and concentration of IPTG (0.1, 0.5, or 1 mM).

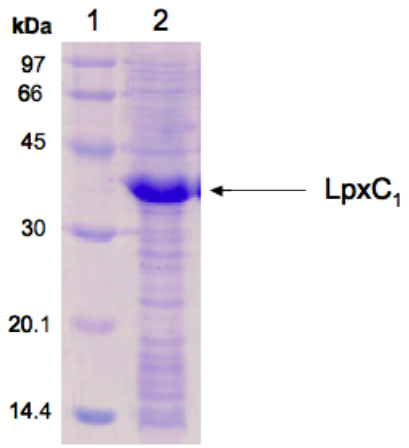


Figure 2.7: Recombinant $LpxC_1$ expression of by *E. coli* BL21 (DE3). Lane 1 = molecular weight marker; lane 2 = after 18 hours of induction.

Disappointingly, $LpxC_2$ was not expressed under any of the conditions tested. If expression of $LpxC_2$ is toxic to the expression cell lines, cell lysis might take place. However, the cell lines did not lyse when expression was induced. Also, the $LpxC_2$ gene does not contain any "rare" codons which would make it more difficult for standard expression cell lines to express the protein. Hence, there is no simple explanation why $LpxC_2$ is not recombinantly expressed in the *E. coli* cell lines used.

The enzyme and inhibition assay for LpxC used in previous studies makes use of enzymatically prepared [$\alpha$-$^{32}$P]UDP-monoacyl-GlcNac as a substrate [129, 141, 146]. The substrate and product ([$\alpha$-$^{32}$P]UDP-monoacyl-GlcN) can be separated by thin layer chromatography (TLC) and a phosphor-imager is used to detect the amount of product formed. Since the Campopiano lab is not equipped to perform this assay, the assays will be carried out by a collaborator in the lab of Prof. C. R. H. Raetz (Duke University, USA).

## 2.3 Conclusion

The limited options to successfully treat infections caused by resistant bacteria, and the rapid decline in the introduction of new antibiotics, has led to increasing interest in the chemical design of new drugs with novel antimicrobial activity. Enzymes involved in the lipid A biosynthesis pathway, in particular LpxC, have been recognised as attractive targets for new agents designed to treat infections caused by Gram-negative bacteria. The most potent inhibitor published so far, which is capable of inhibiting growth of several Gram-negative species, is the synthetic antibiotic CHIR-090.

The innate resistance of members of the Bcc to most classes of available antibiotics has been linked to their relatively large (∼8-9 Mbp) genomes which contain multiple antibiotic resistance genes [65]. In addition, the lipid A of the Bcc species has unique features compared to other Gram-negative bacteria. Unlike the endotoxins of other Gram-negative bacteria (e.g. *E. coli*, *S. typhimurium*, and *P. aeruginosa*), the inflammatory activity can not be neutralised by PmxB [191]. Moreover, the lipid A of the Bcc is always non-stoichometrically modified with L-Ara4N, and the outer Kdo residue of the inner core is replaced by a Ko residue. Because of the multi-drug resistance of the Bcc and the uniqueness of lipid A of the Bcc, I focused my investigation on the potential of antibiotics targeting lipid A biosynthesis to successfully treat Bcc infections, using CHIR-090 as a model antibiotic.

I showed that CHIR-090 can inhibit growth of some Bcc species, including one of the most prevalent Bcc species, *B. multivorans*. MICs were determined for eight *B. multivorans* strains and were found to be strain-dependent and ranged from 0.1 to >100 $\mu$g/ml. Despite the close taxonomic relationship of the Bcc, individual isolates displayed a remarkable difference in the sensitivity to CHIR-090 even within a single species. I attempted to understand why some species are resistant and others susceptible to CHIR-090. It was found that these differences between

species and strains are not caused by differences in LPS profile (smooth, rough, and deep-rough LPS). On the other hand, a strong correlation was observed between the presence of an ORF, encoding a putative LpxC ortholog ($LpxC_2$), and resistance to CHIR-090. I hypothesised that the two LpxC's ($LpxC_1$ and $LpxC_2$) can catalyse the same reaction, but that only $LpxC_1$ is inhibited by CHIR-090. However, so far it has not been possible to prove that $LpxC_2$ is responsible for resistance. To confirm this hypothesis, future research could focus on the *in vitro* characterisation of $LpxC_1$ and $LpxC_2$. The enzymes of lipid A biosynthesis, including LpxC, are known to be encoded by single copy genes in all sequenced Gram-negative genomes [142]. Hence, if $LpxC_1$ and $LpxC_2$ are capable of catalysing the same reaction in the Bcc, this would also be the first example of encoding two proteins that catalyse the same reaction within the lipid A biosynthesis.

To the best of my knowledge, this CHIR-090 study is the first to report an agent against *Burkholderia* targeted at the LPS biosynthetic pathway. I showed that new drugs targeting this pathway have a potential to treat Bcc infections. However, this potential is likely to be species- and strain-dependent.
New compounds targeting LpxC based on CHIR-090 have proven to be active and will be patented in future [192]. Unfortunately, CHIR-090 itself does not seem to be a potential therapeutic agent. CHIR-090 was produced by CHIRON, a biotech company in California, acquired by Novartis in 2006. According to Prof. C. R. H. Raetz it was 'dropped' from CHIRON's clinical trials for reasons that were withheld by the company [192].

It has recently been reported that the Bcc display species- and strain-dependent susceptibility or resistance to biocides with most isolates being highly resistant to agents that are found in hand-washes and disinfectants [193]. LiPuma and colleagues reported the *in vitro* inhibitory activity of a novel nanoemulsion (NB-401) against a panel of 75 *Burkholderia* isolates which included 10 *B. multivorans*

and 20 *B. cenocepacia* isolates [194]. The NB-401 MICs were strain-specific and ranged from 31.2 to 125 $\mu$g/ml and <15.6 to 500 $\mu$g/ml, respectively. This suggests that agents specifically interfering with *Burkholderia* LPS biosynthesis should be further explored and that they may, possibly in combination with nanoemulsions, provide a breakthrough in the treatment of CF-related infections.

# Chapter 3

# An Old Antibiotic with a Novel Use: D-cycloserine fights the Bcc

**Part of this chapter will be submitted for publication:**

Manuscript in preparation.

As described in the previous chapters, there is an urgent need for antibiotics that are capable of eradicating Bcc infections, either as monotherapy or in combination with additional drugs to obtain a synergistic effect. The majority of approaches to find new drugs has been to search for (entirely) novel compounds. This is typically being accomplished either by mass screening of natural products to identify antibiotic activity or by designing "new" antibiotics, for example CHIR-090. The approach described in this chapter explores the potential and novel use of the "old" antibiotic, cycloserine (CS), to treat Bcc infections.

CS, discovered around 1955, specifically inhibits PLP-dependent enzymes and, as mentioned in the first chapter, two enantiomers exist, D-cycloserine (DCS) and L-cycloserine (LCS), illustrated in Figure 3.1. DCS is a natural product that was isolated from *Streptomyces lavendulae* and *Streptomyces garyphalus* [195],

whereas LCS was originally isolated from *Erwinia uredovora* [196] and is now prepared synthetically.

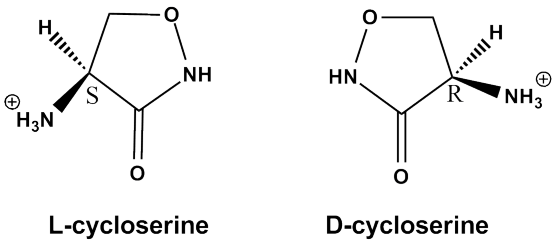


Figure 3.1: The two cycloserine enantiomers, LCS (left) and DCS (right).

DCS (also known as Seromycin) is an "old" antibiotic used as a second line drug to treat multiple drug-resistant *M. tuberculosis* infections as well as neurological disorders. To my knowledge, neither of the CS enantiomers have been investigated as antibiotics in the treatment of Bcc lung infections.

In *M. tuberculosis*, the primary targets of DCS are D-alanyl-D-alanine synthetase and D-alanine racemase, both necessary for viability. However, CS is a broad-range inhibitor, reacting with many PLP-dependent enzymes in the cell. Since this thesis focuses on the lipid A biosynthesis and aminoarabinose modification pathways as drug targets, I chose to study *in vitro* CS inhibition with the only PLP-dependent enzyme, ArnB, involved in these pathways.

## 3.1 CS activity against the Bcc

To investigate the potential of CS in treatment of Bcc infections, the *in vitro* antimicrobial activity of CS towards Bcc species was tested. Minimal inhibitory (MIC) and bactericidal (MBC) concentrations were determined for CS, and synergistic studies were performed with front-line antibiotics used in the current treatment of Bcc infections.

### 3.1.1 MIC

MICs of CS were determined for all strains of the Bcc reference panel [35, 38]. As described for CHIR-090 in the previous chapter, MIC data was generated using the internationally accepted BSAC methodology [184] for other Gram-negative pathogens. The quality control strains *P. aeruginosa* ATCC27853, *P. aeruginosa* ATCC10145, and *E. coli* ATCC25922 species were included, as recommended by the guidelines. ISA plates contained two-fold dilutions of DCS (range 0-1000 $\mu$g/ml) or LCS (range 0-128 $\mu$g/ml) and MICs were defined as the lowest concentrations of CS where no visual growth could be observed.

LCS did not inhibit the growth of any of the strains tested in the tested concentration range. All MICs of LCS are >128 $\mu$g/ml, including the control strains *P. aeruginosa* and *E. coli*. However, in the same study LCS showed activity against two *Sphingomonas* strains (results not shown), indicating that the observed lack of growth inhibition by LCS was not caused by an experimental error.

In contrast to that observed with LCS, the growth of all Bcc and control strains was inhibited within the range of DCS concentrations tested. MICs of DCS against the Bcc are shown in Table 3.1 and varied between 2 and 128 $\mu$g/ml. Interestingly, with one exception, namely *B. vietnamiensis* FC441, DCS proved to be more active against Bcc strains than *P. aeruginosa* strains. As previously described for the LpxC inhibitor CHIR-090 [197], the individual strains within the nine Bcc reference species displayed different susceptibility to DCS. The three epidemic *B. cenocepacia* ET12 lineage strains (J2315, K56-2 and BC-7) showed the highest MICs. The MIC for *B. cenocepacia* SAL-1, the deep-rough K56-2 derivative [183], was similar to the parental strain, indicating that as for CHIR-090, the LPS profile does not influence the susceptibility toward DCS. *B. multivorans* 249-2, derived from ATCC17616, displayed a higher MIC value than the parental strain. This is in contrast to what was found for CHIR-090, where *B. multivorans*

Table 3.1: MIC values of D-cycloserine against the Bcc reference panel and control strains.

| **Strain** | **MIC** ($\mu$g/ml) | **Strain** | **MIC** ($\mu$g/ml) |
|---|---|---|---|
| ***B. cepacia* (I)** | | ***B. dolosa* (VI)** | |
| ATCC25416 | 32 | AU0645 | 32 |
| ATCC17759 | 32 | CEP021 | 32 |
| CEP509 | 64 | E12 | 4 |
| LMG17991 | | STM1441 | 16 |
| ***B. multivorans* (II)** | | ***B. ambifaria* (VII)** | |
| C5393 | 4 | AMMD | 8 |
| LMG13010 | 8 | ATCC53266 | 8 |
| C1575 | 32 | CEP0996 | 4 |
| CF-A1-1 | 32 | | |
| JTC | 32 | | |
| C1962 | 16 | | |
| ATCC17616 | 16 | | |
| 249-2 | 32 | | |
| ***B. cenocepacia* (III)** | | ***B. anthina* (VIII)** | |
| J2315 | 64 | W92 | 4 |
| BC7 | 64 | C1765 | 4 |
| K56-2 | 64 | J2552 | 16 |
| C5424 | 16 | AU1293 | 16 |
| C6433 | 32 | | |
| C1394 | 32 | | |
| PC184 | 16 | | |
| CEP511 | 32 | | |
| J415 | 16 | | |
| ATCC17765 | 16 | | |
| SAL-1 | 64 | | |
| ***B. stabilis* (IV)** | | ***B. pyrrocinia* (IX)** | |
| LMG14292 | 4 | ATCC15958 | 4 |
| C7322 | 16 | ATCC39277 | 4 |
| LMG14086 | 2 | BC011 | 16 |
| LMG18888 | 16 | C1469 | 8 |
| ***B. vietnamiensis* (V)** | | ***E. coli*** | |
| PC259 | 64 | ATCC25922 | 64 |
| LMG16232 | 32 | ***P. aeruginosa*** | |
| FC441 | 128 | ATCC27853 | 128 |
| LMG10929 | 32 | ATCC10145 | 128 |

249-2 showed an extremely low MIC value (0.1 $\mu$g/ml) compared to the parental strain (6.25 $\mu$g/ml). The three *B. ambifaria* strains were amongst the most susceptible Bcc strains with MICs of 4-8 $\mu$g/ml. *B. stabilis* strain LMG14086 showed the lowest (2 $\mu$g/ml) MIC of all Bcc strains.

In a previous study, clinical (multiple drug-resistant) isolates of *M. tuberculosis* and the type strain H37Rv showed MICs of DCS ranging from 25 to 75 $\mu$g/ml [198]. In my study, the MICs of DCS against the Bcc are in the same range or even lower, suggesting that DCS might have a clinically useful activity against the Bcc.

### 3.1.2 Bactericidal and synergistic activity of DCS

To determine the bactericidal or bacteriostatic activity of DCS towards the Bcc, a panel of relevant strains was assembled (Table 3.2). This panel consisted of six strains of the two most clinically relevant species, *B. multivorans* and *B. cenocepacia*, together with a *P. aeruginosa* and an *E. coli* control strain.

MICs for the eight strains tested were examined in IS broth containing two-fold dilutions of DCS (range 0-500 $\mu$g/ml). After incubating the strains overnight with DCS, the MIC was determined as the first concentration at which no turbidity or visual growth could be observed. The MIC concentration and a two-fold higher concentration was used as an inoculum to plate on non-antibiotic containing agar plates and survival of the strains (confluent growth) was checked the following day. The DCS concentration at which no survival was observed is given in Table 3.2 as the MBC.

The MICs in broth corresponded to the MICs found on agar plates. DCS was found to be bactericidal towards the Bcc. All MBCs were within 1 dilution of the respective MICs, except for *B. cenocepacia* K56-2 which had an MIC value of 64 $\mu$g/ml but still showed confluent growth after incubation in 128 $\mu$g/ml DCS. Interestingly, LiPuma and colleagues reported that the nanoemulsion NB-

Table 3.2: MIC and MBC values ($\mu$g/ml) of DCS against a panel of clinically relevant strains.

| Strain | Source/reference | MIC | MBC |
|---|---|---|---|
| ***E. coli*** | | | |
| ATCC25922 | ATCC | 64 | 64 |
| ***P. aeruginosa*** | | | |
| ATCC10145 | ATCC | 128 | 128 |
| ***B. multivorans*** | | | |
| C5393 | Vancouver CF clinic [185] | 4 | 8 |
| C1575 | Glasgow Epidemic [60] | 32 | 64 |
| ATCC17616 | Environmental strain [47] | 16 | 32 |
| ***B. cenocepacia*** | | | |
| J2315 | Edinburgh Epidemic [26] | 64 | 128 |
| K56-2 | Toronto CF clinic [63] | 64 | >128 |
| ATCC17765 | Urinary tract infection [47] | 16 | 32 |

401 showed MBCs typically within two-fold of the MIC value, but also reported a single *B. cenocepacia* strain exception [194]. However, LiPuma et al did not indicate which *B. cenocepacia* strain showed a different profile.

In the treatment of multiple drug-resistant Bcc infections, as well as other Gram-negative infections, such as *P. aeruginosa*, antibiotics are usually not used as single agents but rather in combination with other antibiotics. Therefore, I investigated the synergistic activity of DCS with seven front-line antibiotics presently used to treat Bcc infections: minocycline, ceftazidime, tobramycin, meropenem, chloramphenicol, trimethoprim, and ciprofloxacin. A panel of strains was assembled, including three *B. multivorans* strains, three ET12 lineage *B. cenocepacia* strains, one *B. dolosa* strain, and two control strains (*P. aeruginosa* and *E. coli*). Synergistic activity was tested by a double disc diffusion assay. One filter disc was impregnated with DCS and the other with one of the above-mentioned antibiotics. The diameter and shape of the zones of inhibition were evaluated after

overnight incubation. No clear change in size or shape of the inhibition zones could be observed for all seven antibiotics when used alone or together with DCS (results not shown). Hence, it was concluded that with the method used, DCS did not act synergistically or antagonistically with any of these seven clinically-used antibiotics. It should be noted that many methods of antibiotic synergy testing against bacteria have been described but no reproducible guidelines for synergy testing against the Bcc have been reported. It is known, however, that the results of synergy tests dependent on the method applied, the concentrations of antibiotics used, and duration of drug exposure [199]. Therefore, the synergistic or antagonistic mode of action of DCS with these antibiotics cannot be excluded.

## 3.2 ArnB: a possible intracellular DCS target

Encouraged by the antimicrobial activity studies of DCS against the Bcc, it was decided to study DCS inhibition of the ArnB enzyme *in vitro*.

In a recent study by the Campopiano group and collaborators showed that in contrast to *S. typhimurium*, the putative genes (including *ArnB*) involved in L-Ara4N synthesis and LPS modification are essential for viability to *B. cenocepacia* K56-2 [98]. Moreover, the lipid A structures described for different Bcc species indicate that, in contrast to other Gram-negative bacteria, lipid A is always non-stoichiometrically substituted with L-Ara4N [28]. When combined, those findings suggest that the L-Ara4N biosynthetic pathway could be a rational target for antibiotic therapy. Also, from those studies I learned that the Bcc has, in addition to the broad range of intracellular DCS targets, a possible unique target, namely ArnB.

Thomas Vargues, a former PhD student from the Campopiano group, recently cloned, expressed, and purified ArnB of *B. cenocepacia* J2315 and performed initial *in vitro* inhibition studies with CS [200]. In this section, the optimisation

of his work and additional inhibition studies on the *B. cenocepacia* J2315 ArnB enzyme are described.

### 3.2.1 Expression and purification of ArnB-His6

The expression plasmid pET22b_ArnB_J2315, expressing ArnB with a C-terminal 6 His tag, was kindly given by Thomas Vargues. Integrity of the plasmid was proven by a restriction digest and by sequencing of the plasmid (results not shown).

The method of ArnB-His6 purification was adapted from the method described previously [200], with some modifications. For recombinant ArnB-His6 expression, *E. coli* BL21(DE3) competent cells, transformed with pET22b_ArnB_J2315, were used. Expression was induced with 0.5 mM IPTG for 5 hours at 37 $^{o}$C (Figure 3.2, Lane 3). ArnB-His6 was expressed as a soluble protein and purified using IMAC nickel affinity (Figure 3.2, Lane 4) and size exclusion chromatography (Figure 3.2, Lane 5). As judged by SDS-PAGE, ArnB-His6 was purified to near homogeneity after these two chromatography steps. A yield of 15 mg of pure recombinant ArnB-His6 protein was generally obtained from one litre of *E. coli* BL21 (DE3) culture. Based on the elution profile of the size exclusion chromatography column, ArnB-His6 behaved as a monomeric protein (Figure 3.2), in contrast to the homodimeric *Salmonella* ArnB [156]. Molecular weight of the protein (theoretical mass = 43,252 Da) was confirmed by MALDI-TOF mass spectometry (Appendix A.4).

Prior to further studies, ArnB-His6 was saturated with the PLP co-factor. The purified enzyme was dialysed against an excess of PLP overnight after which the un-bound PLP was removed using a PD10-column.

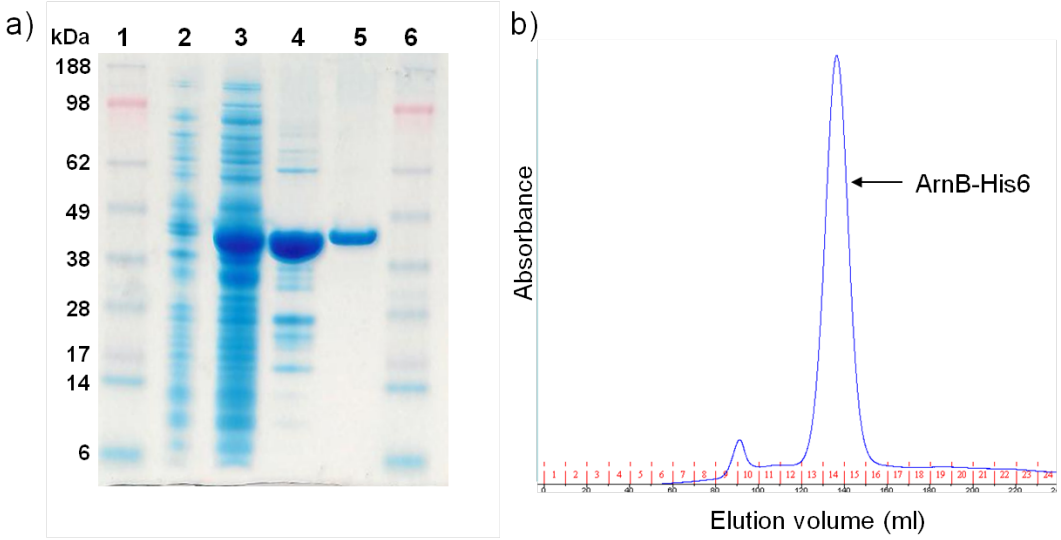


Figure 3.2: ArnB purification profile. a) All consecutive expression and purification steps were analysed by SDS-PAGE. Lane 1 and 6 show the molecular weight marker, lane 2 = *E. coli* BL21 before induction, lane 3 = the cell free extract after IPTG induction, lane 4 = the Ni-NTA chromatography elution fraction, and lane 5 = fractions 13-15 of the S-200 size exclusion column. b) The elution profile of ArnB-His6 running through the S-200 size exclusion column.

### 3.2.2 ArnB-His6 activity studies

As described in the introduction, ArnB is a transaminase that catalyses the amino group transfer from glutamic acid to UDP-Ara4O, yielding UDP-L-Ara4N and $\alpha$-ketoglutarate [150]. The catalysed reaction consists of two half reactions (Figure 3.3). In the first half reaction, the amino group of L-glutamate is donated to the active site of the protein. In the second half, the amino group is transferred from the active site to the substrate UDP-Ara4O. Since the substrate, UDP-Ara4O, is not (commercially) available, enzyme activity and inhibition studies could only be performed on the first half reaction.

Enzyme assays could be carried out using UV-Vis spectroscopy. The holo-enzyme (E-PLP) has absorption maxima of 415 nm and 328 nm (Figure 3.4), corresponding to the ketoenamine and enolimine forms of E-PLP.

To test for activity of ArnB-His6, the natural amine donor, L-glutamate, was

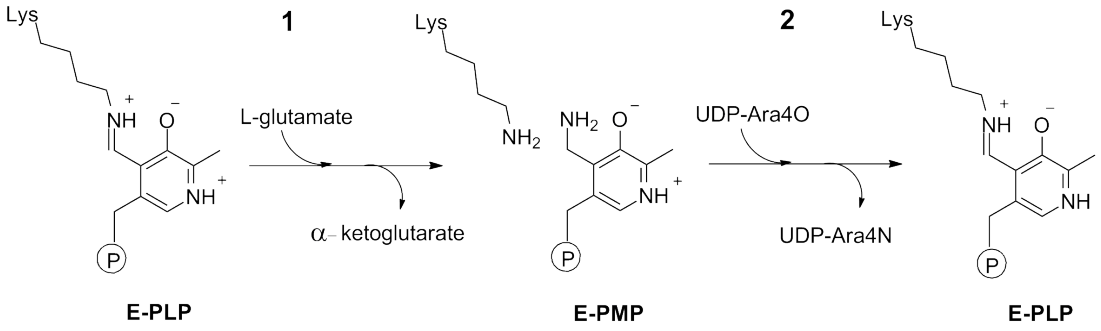


Figure 3.3: The two half reactions of ArnB. Adapted from [150].

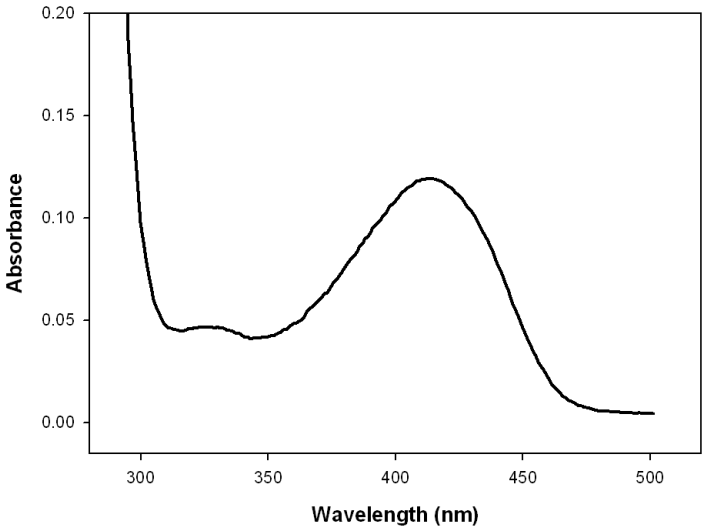


Figure 3.4: Absorbance spectrum of ArnB-His6 in the E-PLP form.

added to the enzyme. After addition of L-glutamate, at 415 nm absorbance, the peak of the internal aldimine was within seconds decreased to ∼30% and an increase of a new peak with a $\lambda_{max}$ at 334 nm could be observed (Figure 3.5). This increase in peak size of 334 nm can be assigned to the transfer of the amine group to ArnB-His6, forming the E-PMP complex.

After completion of the enzymatic reaction with L-glutamate, regeneration of the enzyme to its E-PLP state was attempted by dialysis in an excess of fresh PLP overnight. The unbound PLP was removed before a new assay was carried out. A scan was taken of the "regenerated" enzyme before the addition of L-glutamate and directly after the addition of L-glutamate. A good recovery of

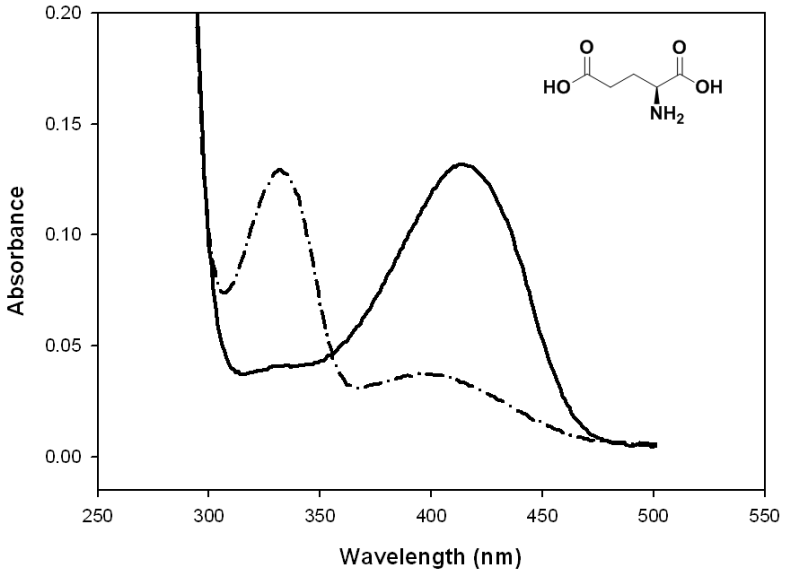


Figure 3.5: Absorbance spectra of ArnB-His6 activity. ArnB-His6 (14 $\mu$M) E-PLP enzyme (solid line) and 1 minute after incubation with 500 $\mu$M L-glutamate (dashed-dotted line).

the enzyme to E-PLP could be observed (Appendix A.5). However, even after overnight dialysis, a significant amount of the enzyme remained in the E-PMP form. The recovered enzyme was reacted again with L-glutamate in a the same fashion as before dialysis and E-PLP was formed.

The above purification procedure and activity assay for ArnB-His6 worked well when a potassium phosphate- or ammonium acetate buffer was used for all purification steps and assays. However, when the phosphate buffer was replaced by Tris buffer (same pH) the elution profile of the size exclusion column was less defined and the protein lost activity (results not shown). Since Tris has an amine group it might be that the buffer reacts with the PLP co-factor in the active site of the protein and thereby interferes with the activity assay.

### 3.2.3 Cycloserine inhibition of ArnB-His6

Both CS enantiomers, LCS and DCS, have been described as inhibitors of a wide range of PLP-dependent enzymes. Depending on the targeted enzyme and conditions tested (e.g. pH of buffers) CS inhibition can be reversible or not. Inhibition with CS has been described for several transaminases (e.g. D-amino acid transaminase [201]), decarboxylases (e.g. dialkylglycine decarboxylase [202]), and racemases (e.g. alanine racemase [203]). In contrast to most enzyme inhibitors that typically form covalent interactions with the protein, CS binds covalently to the PLP co-factor and the interaction with the enzyme itself is non-covalent. Therefore, enzyme activity can be restored for many CS-inhibited enzymes (e.g. D-amino acid transferases [201] and for bacterial serine palmitoyltransferase [204]) by dialysis against an excess of fresh PLP that can replace the CS-bound PLP in the active site. However, the time required to restore activity by dialysis is generally on a scale that is not of physiological relevance [205].

The ArnB of *S. typhimurium* has been shown to be inhibited by LCS enantiomer [156]. When LCS was added to ArnB-His6, an instantaneous decrease of the internal aldimine peak at 415 nm was observed and a new peak appeared with a $\lambda_{max}$ at 328 nm. Additionally, a shoulder between 365 and 395 nm can be observed (Figure 3.6). The UV-Vis spectra did not show any significant changes after ∼10 minutes and the time of incubation (8 or 24 hours) did not influence the spectra.

An analogous change in absorbance has been described for *S. typhimurium* ArnB [156]. Ten minutes after the addition of LCS to the enzyme, when no further change in absorbance spectra could be observed, L-glutamate was added to the reaction mixture. This addition of L-glutamate did not cause changes in the absorbance spectra, indicating that the enzyme was inhibited. However, it should be noted that the peak that arises when ArnB-His6 reacts with LCS (328 nm) lies only 6 nm away from the $\lambda_{max}$ of the E-PMP (334 nm) peak, which might

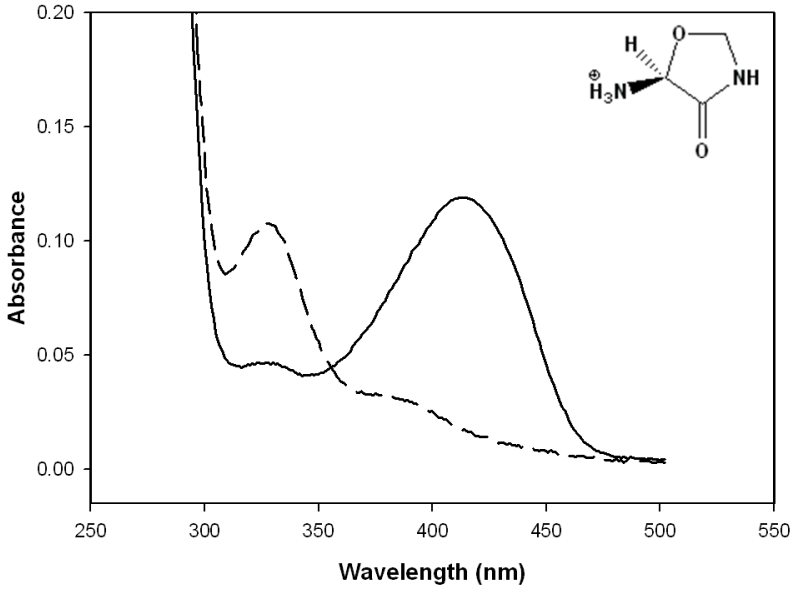


Figure 3.6: Absorbance spectra of ArnB-His6 in the E-PLP form (solid line) and 10 minutes after addition of 1 mM LCS (dashed line).

make it difficult to observe any changes in the spectrum.

The absorbance spectrum of ArnB-His6 changed in the presence of DCS (Figure 3.7). However, the completion of the reaction took considerably longer for DCS than for LCS, and the spectra of DCS and LCS when reacted with ArnB-His6 differ greatly. When DCS is added, both E-PMP peaks at 415 and 328 nm were reduced in size over time and a new peak appeared with a $\lambda_{max}$ of 372 nm. After ∼20 minutes, the E-PMP peaks completely disappeared. However, when L-glutamate was added at this point, some ArnB-His6 activity remained and rise of the E-PLP peak at 334 nm could be observed (results not shown). After incubating DCS with ArnB-His6 for over 30 minutes, a broad shoulder on the 372 nm peak appeared (Figure 3.7) and the $\lambda_{max}$ was shifted to 360 nm. After ∼3 hours, no significant change in the spectrum could be observed. When L-glutamate was added after prior incubation with DCS, no change in the spectrum was observed, indicating that ArnB-His6 was inhibited.

For alanine racemase, it has been reported that UV-Vis spectra for both CS

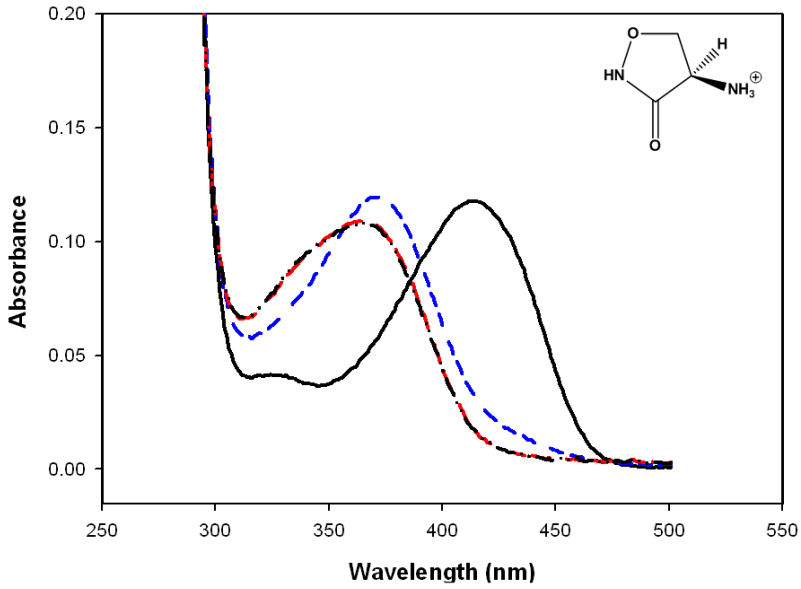


Figure 3.7: Absorbance spectra for ArnB-His6 in the E-PLP (solid line) form, 20 minutes (blue dashed line) and 3 hours (red dashed line) after addition of 1 mM DCS. After 3 hours of incubation with DCS, 500 $\mu$M L-glutamate was added and a scan was taken after an additional 10 minutes (black dashed-dotted line).

enantiomers reacted with the enzyme are similar [203]. In contrast, for ArnB-His6, both enantiomers show different absorbance profiles when incubated with the enzyme and none of the peaks formed had the same $\lambda_{max}$ as the E-PMP peak (Figure 3.8). This suggests that both enantiomers do not act as amine donors but pursue different reaction pathways dependent upon CS chirality. A difference in reaction pathway of LCS and DCS has been described for several enzymes, including dialkylglycine decarboxylase [202] and bacterial serine palmitoyltransferase [204].

Several mechanisms of CS inhibition have been reported and seem to differ between enzymes. So far, it is not possible to predict the mechanism of inhibition based on differences or similarities in the absorption spectra between enzymes. The crystal structure of *S. typhimurium* ArnB with LCS in the active site showed that LCS binds the co-factor by replacing the lysine-PLP aldimine bond by an LCS-PLP amine bond (Figure 3.9). The LCS-PLP adduct showed that the LCS

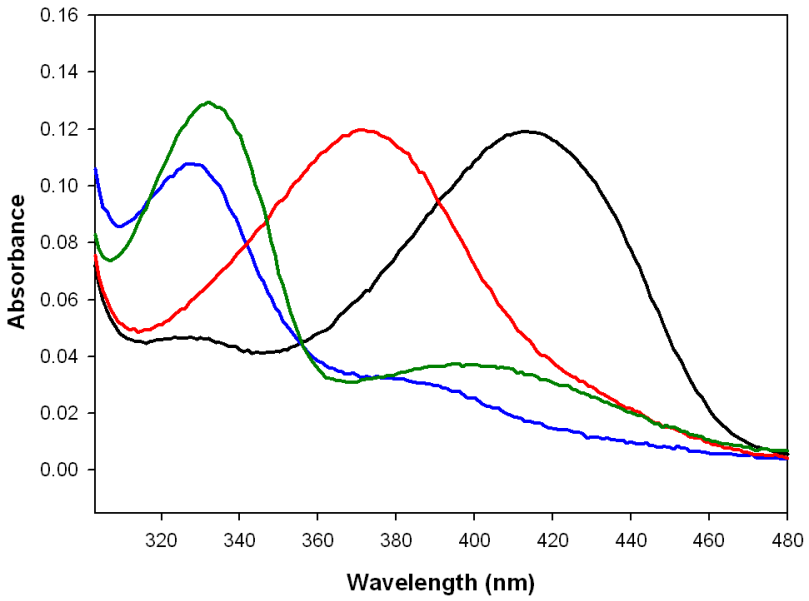


Figure 3.8: Absorbance spectra for ArnB-His6 in the E-PLP form (black), 10 minutes after addition of 500 $\mu$M L-glutamate (green), 1 mM DCS (red), or 1 mM LCS (blue).

ring stays in its cyclic form [156], as described in the case of alanine racemace CS inhibition [203]. Recently, it has been published for the bacterial serine palmitoyltransferase, that LCS inhibition of the enzyme shows a similar UV-absorption profile as published for *S. typhimurium* ArnB. However, in that study, PLP-LCS or PLP-DCS adducts could not be identified by mass spectrometry or enzyme crystallography where the CS ring was still in its cyclic form. A new CS inhibition mechanism involving the opening of the ring followed by decarboxylation of the opened ring was proposed [204]. Similar mechanisms involving the opening of the ring have been proposed in other previous studies [206]. Furthermore, in a study on serine palmitoyltransferase, it was found that both CS enantiomers show different absorption spectra when inhibiting the enzyme, but the same PLP-adduct was isolated from enzymes inhibited with both LCS and DCS [204]. Both UV-absorption profiles presented here for CS-inhibited ArnB-His6 are similar to the absorption profiles published for the serine palmitoyltransferase enzyme.

To test for the reversibility of CS inhibition, the inhibited protein was dialysed

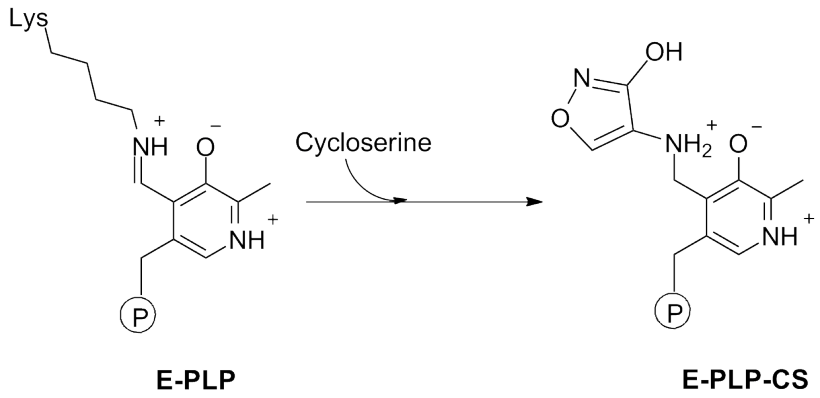


Figure 3.9: Proposed inhibition mechanism of LCS of *S.typhimurium* ArnB.

overnight in an excess of fresh PLP. The unbound co-factor was then removed using a PD-10 column. A UV-Vis spectrum of the enzyme was taken after dialysis and activity of the protein was tested by adding L-glutamate. For both LCS- and DCS-inhibited proteins, activity could be partly recovered by dialysis (Appendix A.7), however, a significant amount of ArnB-His6 still has LCS or DCS bound after dialysis.

To gain further insight into the mechanism of inhibition of both enantiomers, several methods were attempted to isolate the PLP-DCS and PLP-LCS adducts for mass spectrometry analysis. We tried to denature the enzyme, leaving the adduct in solution by: 1) adding 8 M urea (with or without boiling), 2) by increasing the pH from 7.5 to 12 [206], and 3) by filtering the protein, using a 3 kD spin filter. Unfortunately, none of those attempts was successful. Though CS is non-covalently bound into the active site, the combined affinity of the PLP-CS may be very high, as described for other non-covalent inhibitors [205].

### 3.2.4 Inhibition studies with $\beta$-chloroalanine and propargylglycine

PLP-dependent enzymes have been extensively studied and many inhibitors of this class of enzymes have been described. Therefore, based on previous ArnB studies in *S. typhimurium* ArnB [156], I decided to test for the inhibitory activity of other well known PLP-dependent enzyme inhibitors. Two inhibitors, gabaculine and ibotenic acid, were tested in previous studies for inhibition of ArnB-His6 [200], but neither of those showed reactivity towards ArnB-His6. Thus, ArnB-His6 reactivity with $\beta$-chloro-D-alanine ($\beta$CDA) and L-propargylglycine (L-PPG) was tested.

#### Inhibition studies with $\beta$-chloro-D-alanine

A powerful synergistic activity (MIC of DCS was reduced from 50 to 2.5 $\mu$g/ml) of DCS and $\beta$CDA against *M. tuberculosis* has been reported [207]. Therefore it was decided to test if $\beta$CDA could inhibit ArnB-His6.

Similar to CS, $\beta$CDA is an alanine analogue that can inhibit alanine racemase and a range of D- and L-amino transferases. However, a difference between CS and $\beta$CDA is that inhibition with $\beta$CDA is irreversible due to the fact that the PLP-cofactor remains covalently bound to the enzyme after inhibition (Figure 3.10). $\beta$CDA binds to the active site where it can displace the lysine-PLP aldimine bond by a $\beta$CDA-PLP aldimine bond. Formation of the quinonoid intermediate takes place by deprotonation in the $\alpha$-position of $\beta$CDA, followed by the reprotonation of the quinonoid and release of HCl to form an aminoacrylate aldimine species. The lysine residue displaces the aminoacrylate-PLP amine bond and aminoacrylate is released. The free aminoacrylate can nucleophilically attack the co-factor to form a stable covalent bond, thereby inhibiting the enzyme, or it diffuses out of the active site where it is spontaneously degraded to ammonia and

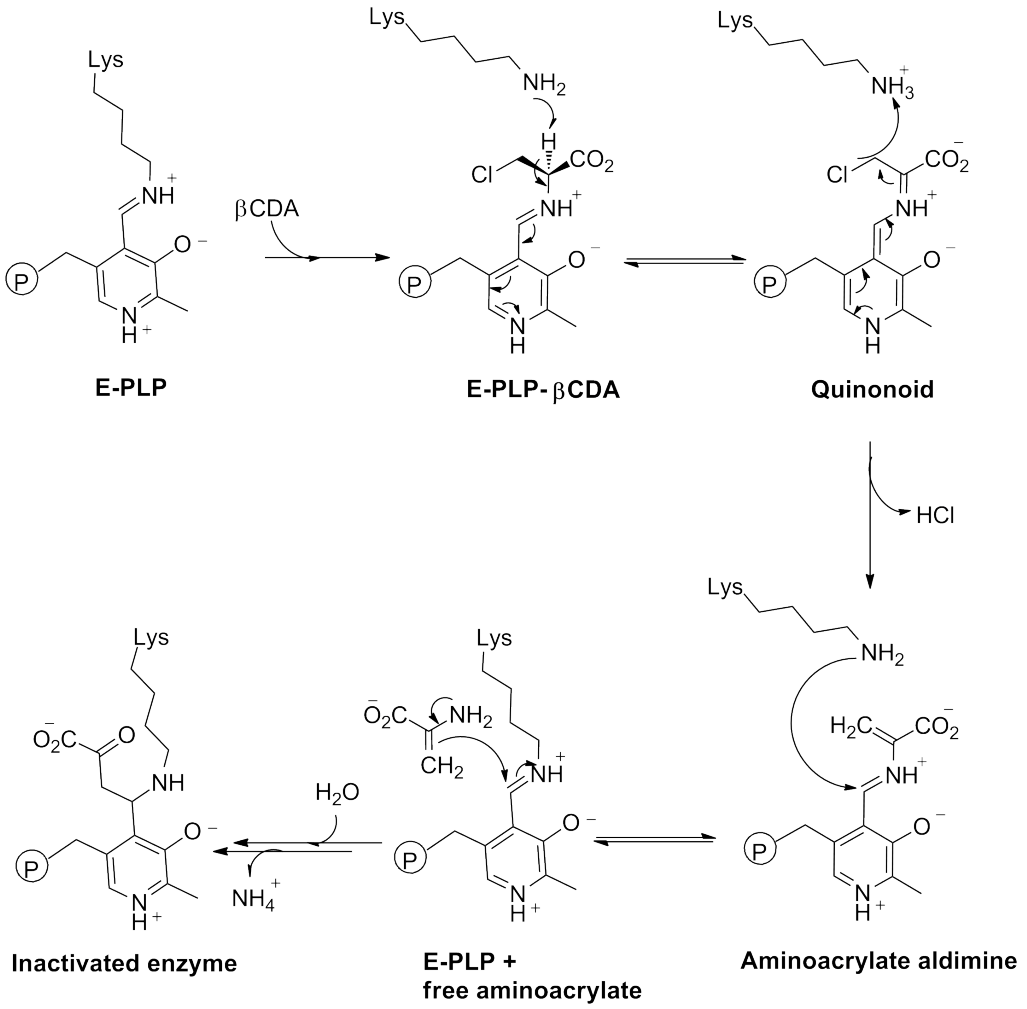


Figure 3.10: Mechanism of inhibition of PLP-dependent enzymes by $\beta$CDA. Adapted from [205].

pyruvate [205, 208].

ArnB-His6 (14 $\mu$M final concentration) was incubated with different concentrations of $\beta$CDA (500 $\mu$M, 1 mM, and 2 mM) for one minute and UV-Vis spectra were generated (Figure 3.11). An increase in peak size could be observed with a $\lambda_{max}$ of 326 nm. However, in contrast to the activity and inhibition assays shown for L-glutamate, DCS, and LCS, the 415 nm internal aldimine peak did not significantly decrease. This suggests that $\beta$CDA is binding to ArnB-His6, and that the enzyme uses $\beta$CDA as a substrate, thereby regenerating the enzyme into an active form, a phenomenon that has been reported for several other aminotrans-

ferases [208, 209]. As described above, when $\beta$CDA is used as a substrate by aminotransferases, pyruvate and ammonia are released.

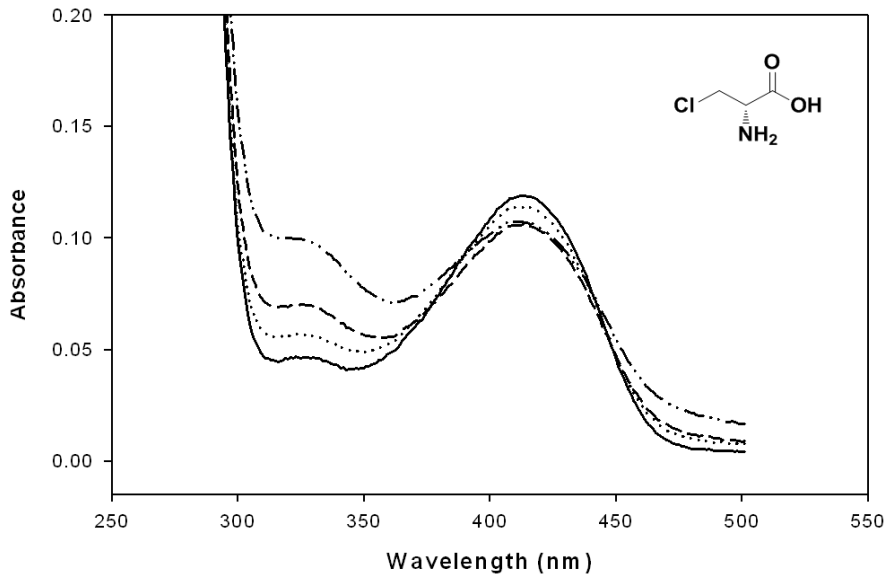


Figure 3.11: Absorbance spectra for ArnB in the E-PLP (solid line) form and 1 minute after addition of 500 $\mu$M (dotted line), 1 mM (dashed line), and 2 mM (dashed-dotted line) $\beta$CDA.

To confirm that ArnB-His6 uses $\beta$CDA as a substrate and pyruvate is indeed released, a coupled assay with lactate dehydrogenase (LDH) was performed (Figure 3.12a). The assay was activated by the addition of $\beta$CDA to ArnB-His6, and the reaction was followed by UV-Vis (Figure 3.11). After completion of the reaction, NADH was added to the reaction mixture, thereby increasing the absorbance at 340 nm. A new reaction was then initiated by addition of LDH to the reaction mixture. LDH uses pyruvate as a substrate to form L-lactate, utilising the co-factor NADH to NAD+. The decrease of absorbance at 340 nm was followed over time by UV-Vis (Figure 3.12b). As controls, NADH and LDH were added to a reaction mixture that only contained ArnB-His or $\beta$CDA.

Figure 3.12b clearly shows that pyruvate is released when ArnB-His6 is incubated with $\beta$CDA, and therefore it was concluded that $\beta$CDA acts as a substrate and not as an effective inhibitor of ArnB-His6.

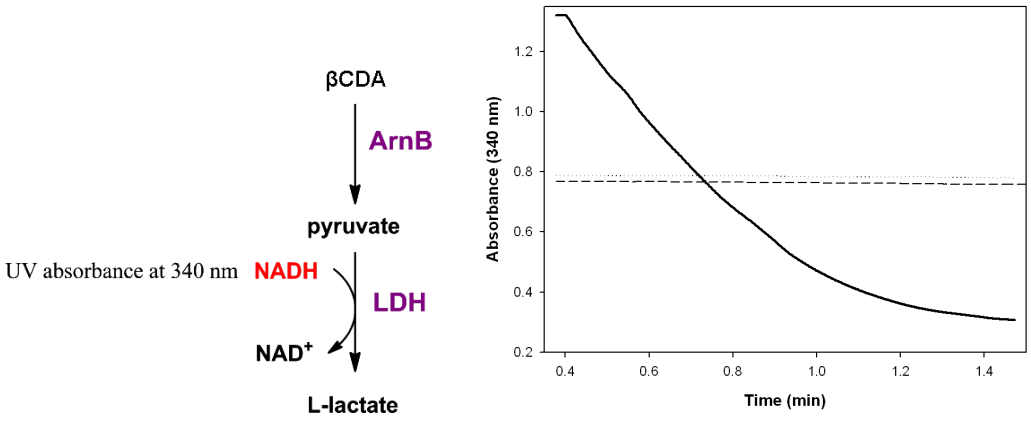


(a) (b)

Figure 3.12: a) ArnB-His6-$\beta$CDA activity assay. ArnB-His6 uses $\beta$CDA as a substrate and pyruvate is released. LDH uses pyruvate as a substrate to form L-lactate, utilising the co-factor NADH to NAD+. b) Decay of absorbance at 340 nm after the addition of NADH and LDH to the ArnB-His6- $\beta$CDA reaction mixture (solid line), to ArnB-His6 (dashed line) and to $\beta$CDA (dotted line).

### Inhibition studies with L-propargylglycine

L-PPG is an irreversible inhibitor of PLP-dependent enzymes. Unlike CS and $\beta$CDA, L-PPG forms a covalent bond with one of the amino acids in in the active site of the protein (Figure 3.13). Similar to the natural substrate of the enzymes, L-PPG binds in the active site where it can displace the lysine-PLP aldimine bond by a L-PPG-PLP aldimine bond. Formation of the quinonoid intermediate takes place by deprotonation in the $\alpha$-position of L-PPG, followed by the reprotonation of the quinonoid species to generate a ketimine. In this case the ketimine is not hydrolysed, but the acetylene moiety of L-PPG isomerises to form an allene. This highly reactive allene is nucleophilically attacked by a residue in the active site and a stable covalent bond is created [205, 208].

When 500 $\mu$M L-PPG was added to 14 $\mu$M ArnB-His6, it was observed that ArnB-His6 reacted with L-PPG after $\sim$10 and that a new peak developed at 324 nm. However, it took $\sim$16-24 hours till the reaction was completed (Figure 3.14).

The data suggests that ArnB-His6 is reacting with L-PPG, but that the reaction is

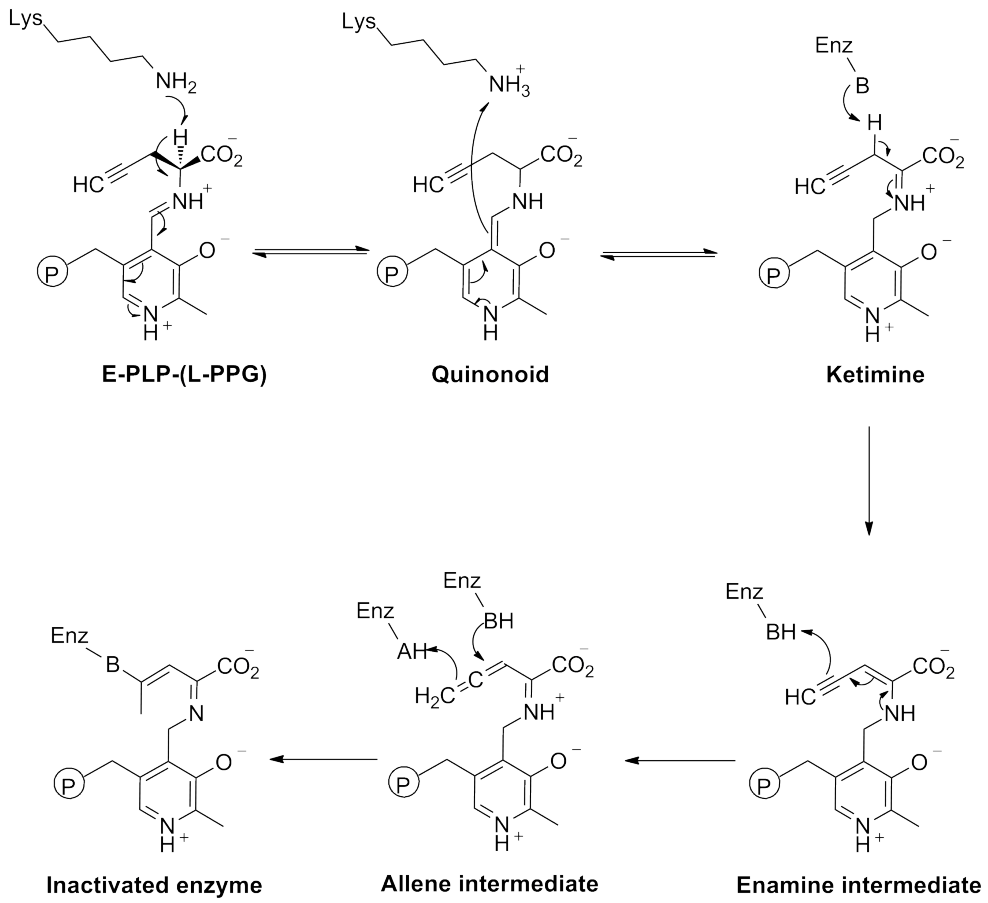


Figure 3.13: Mechanism of inhibition of PLP-dependent enzymes by L-PPG. Adapted from [205].

very slow. Further studies were not performed due to severe solubility problems, which arose when a higher concentration of L-PPG was added to the enzyme. After completion of the reaction with 500 $\mu$M L-PPG ($\sim$16-24 hours at 25 $^{o}$C), the protein precipitated when L-glutamate was added to the reaction mixture. In addition, it was not possible to dialyse the L-PPG bound ArnB-His6 in fresh PLP-buffer since under these conditions the protein was also sensitive to precipitation.

## 3.3 Conclusion

Bcc species have the potential to cause rapidly lethal "Cepacia syndrome" in CF individuals and treatment of such infections is virtually impossible. Most antimi-

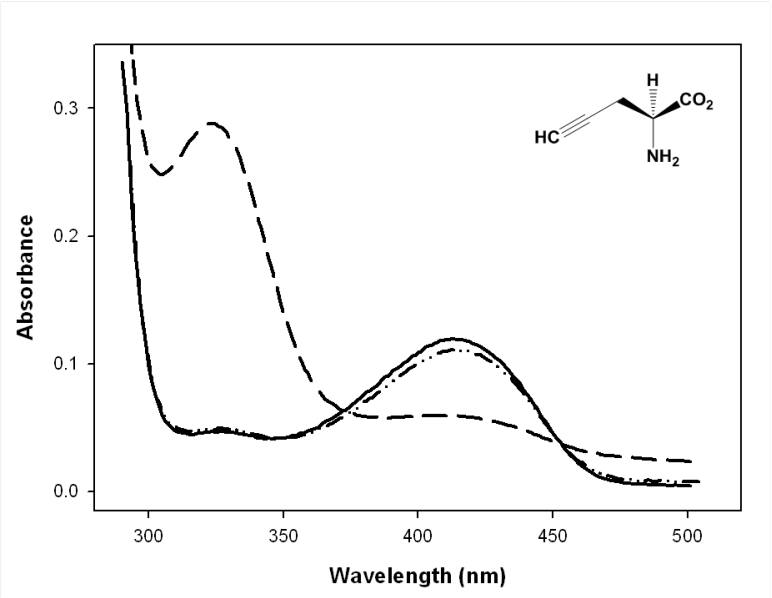


Figure 3.14: Absorbance spectra for ArnB in the E-PLP (solid line) form, 10 minutes (dashed-dotted line), and 24 hours (dashed line) after addition of L-PPG.

crobial research has focused on finding natural products with novel antimicrobial activity, modification of existing drugs, or on the chemical design of new drugs. In this chapter, I followed a different path, by investigating the potential role that the "old" antibiotic Seromycin (DCS) might play in the treatment of Bcc infections.

Interestingly, we demonstrated that DCS could inhibit growth of all strains in the Bcc reference panel, and acted bactericidally against five out of six Bcc species tested; this included the highly virulent strains *B. cenocepacia* J2315 and *B. multivorans* C1575. DCS is a drug that is already in use in the treatment of multiple drug-resistant *M. tuberculosis* and the Bcc strains tested showed MICs in a similar range or even lower than previously published for clinical isolates of *M. tuberculosis*. These results indicate that, *in vitro*, Bcc strains are at least as susceptible towards DCS as *M. tuberculosis* strains, and that DCS might be of clinical use in the treatment of Bcc infections. The site of infection of the Bcc in the lungs is similar to the site of infection of *M. tuberculosis*. Also, both species can survive intracellularly, which implies that DCS is capable or reaching the Bcc species *in*

*vivo* at bactericidal concentrations.

Although it is 'early days,' as the following statement shows, there is certainly a clinical need for an effective therapy against Bcc infections.

> "**Seromycin? Not heard of it, but willing to try anything for Cepacia syndrome.**" *Dr. Alistair Innes, chest physician at Western General Hospital, Edinburgh. Personal communication 2010.*

These results suggest that DCS (Seromycin) could be considered as an additional antibiotic in the treatment of lethal Bcc infectious of the CF lung. Conversely, care should be taken with the severe side effects, such as hallucination, confusion, and depression, reported for DCS in the treatment of tuberculosis. One option would be that, for the present, and as for *M. tuberculosis* infections, DCS should only be considered as a second line drug. Future research could then focus on efficient delivery of the drug, possibly as an aerosol, to limit the toxic side effects.

This section of the thesis has demonstrated that the L-Ara4N biosynthesis pathway might be a reasonable target for antimicrobial therapy against the Bcc. ArnB uses PLP as a co-factor. Therefore, ArnB of *B. cenocepacia* J2315 was chosen as the enzyme to study the *in vitro* CS inhibition and the potential of antibiotics targeting the L-Ara4N biosynthesis pathway. It was shown that ArnB-His6 activity could be inhibited by both LCS and DCS and the differences in the inhibition spectra were highlighted. LCS also showed a similar inhibition profile to that described for *S. typhimurium* ArnB [156]. Though both enantiomers showed reactivity towards ArnB-His6, only DCS showed antimicrobial activity against the Bcc. At present, a conclusive interpretation of those results cannot be provided, but the data could be explored by further research. In addition, as isolation of the PLP-LCS or PLP-DCS adducts was not achieved, the mechanism of inhibition of both CS enantiomers remains to be clarified.

Unlike other enzyme inhibitors that form covalent interactions with the protein,

both CS enantiomers form a stable covalent interaction with the PLP co-factor, but the interaction with the enzyme is non-covalent. Therefore, enzyme activity can be restored for many CS inhibited enzymes by dialysis against an excess of PLP [204, 201], including ArnB-His6. However, the time it takes to restore activity by dialysis is generally on a scale that is not of physiological relevance [205].

Though ArnB-His6 is inhibited *in vitro* by DCS, I do not have any evidence that DCS targets ArnB intracellularly if used against the Bcc. If DCS targets ArnB intracellularly I would expect that when the Bcc is grown in the presence of DCS, to observe accumulation of membranous material. Interestingly, this phenotype has recently been described for strain *B. cenocepacia* XAO12, a conditional *ArnB* mutant of *B. cenocepacia* K56-2 [98]. This hypothesis is being further investigated by the group of Prof. Miguel Valvano (Infectious Diseases Research Group, University of Western Ontario), who have the expertise and the resources for this research.

Of the two other PLP-dependent enzyme inhibitors tested, L-PPG might be a slow inhibitor of ArnB-His6 and could be further explored; however solubility issues might hamper this research. For the well-known PLP-dependent enzyme inhibitor $\beta$CDA, I proved that it cannot inhibit ArnB-His6, but that ArnB-His6 uses $\beta$CDA as a substrate.

# Chapter 4

# L-Ara4N Specificity of Lipid A Transport: LptA & LptB

**LPS isolated for the studies described in this chapter was also used for published collaborative work:**

Ganesh V., Bodewits K., Bartholdson SJ., Natale D., Campopiano D. J., Mareque-Rivas J. C. Effective binding and sensing of lipopolysaccharide: combining complementary pattern recognition receptors. *Angew. Chem. Int. Ed.* **2009**, 48, 356-60

In the previous chapter, I explored ArnB as a drug target and showed that ArnB can be inhibited by some PLP-dependent enzyme inhibitors. Also, it is known that the ORFs in the putative L-Ara4N operon are essential for *B. cenocepacia* survival [98]. The question remains, however, why L-Ara4N is necessary for viability in *B. cenocepacia*. A possible explanation is that non-stoichometrically attached L-Ara4N is necessary for membrane stability and that loss of it cannot be compensated for in a different manner. Secondly, it could be that the necessity of L-Ara4N depends on the growth conditions of *B. cenocepacia*, and that it is essential under laboratory conditions tested, but not in all environmental niches. A third explanation might be that L-Ara4N is essential for lipid A transport and

that L-Ara4N-deficient mutants fail to transport lipid A. This last hypothesis seems to be most likely since it is consistent with the accumulation of membranous material inside the cell observed in the conditional lethal *ArnB* and *ArnT* mutant strains [98]. It was previously noted that the phenotype of the *B. cenocepacia* *ArnB* and *ArnT* mutant strains was very similar to the phenotype observed for *E. coli* mutant with defects in the OM LptD/LptE transport complex [98, 174]. I observed that the phenotype of *B. cenocepacia* *ArnB* and *ArnT* mutant strains was strikingly similar to a conditional lethal *E. coli* *LptA/LptB* mutant (Figure 4.1) [165].

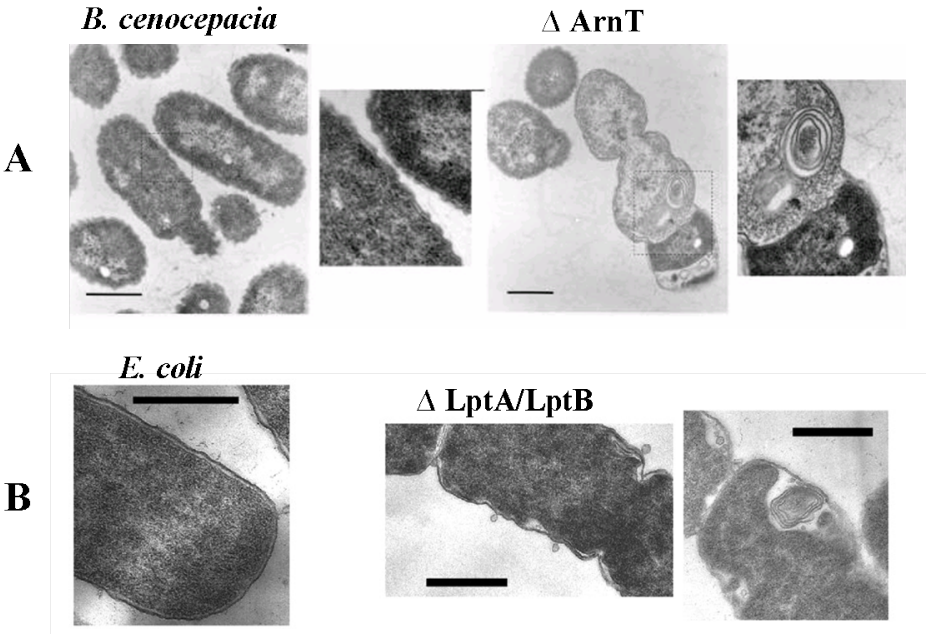


Figure 4.1: Electron microscopy images of *B. cenocepacia* K56-2 (A) wild type strain and a conditional lethal ArnT mutant knock-out strain [98], and (B) *E. coli* wild type and the conditional lethal LptA/LptB mutant [165].

In this chapter, the LptA and LptB homologs of *B. cenocepacia* J2315 are characterised *in vitro* to explore if either of these proteins are specific for L-Ara4N-modified lipid A. Moreover, LptB of *E. coli* has recently received renewed interest as a target for new antimicrobial agents. Therefore, I tested two kinase inhibitors for their ability to inhibit *B. cenocepacia* LptB.

## 4.1 LptA (LPS transport protein A)

LptA is a soluble periplasmic protein that has been shown to bind lipid A and facilitates lipid A transport through the periplasm. LptA from *E. coli* has been characterised [171] and the x-ray crystal structure has been solved [178]. Characterisation of the *B. cenocepacia* LptA homolog has not yet been attempted. Genome analysis indicated that the putative *B. cenocepacia LptA* (BCAL0815) and *LptB* (BCAL0814) genes are located in the same operon (Figure 4.2), as found in *E. coli* [165]. *LptA* lies upstream of *LptB* and the genes overlap by 4 bp. As in *E. coli*, the genes share an operon with *kdsD* and *kdsC*, both encoding proteins involved in the biosynthesis of Kdo sugars (found in the inner core of lipid A). In contrast to *E. coli*, *LptC* (*YrbK*) and *YrbG* (unknown function) are not found in the *B. cenocepacia* operon. Moreover, upstream of *LptA* a hypothetical gene of unknown function is located, which to date does not have any homologs in non-*Burkholderia* species.

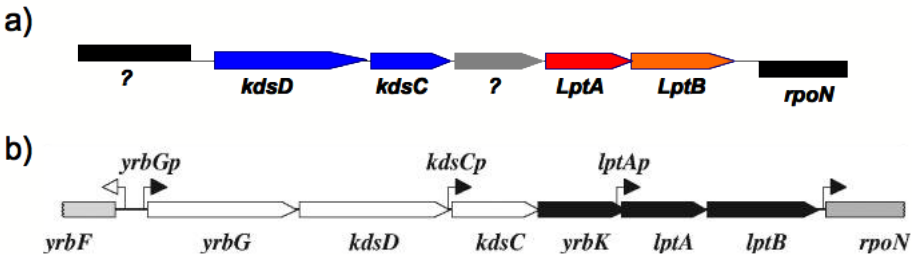


Figure 4.2: Genetic organization of the (putative) operon where *LptA* and *LptB* are located: (a) in *B. cenocepacia* J2315 (www.burkholderia.com); and (b) in *E. coli* [165].

The *B. cenocepacia* LptA sequence is 24% identical to *E. coli* LptA (Appendix A.10). Like the *E. coli* LptA protein, $\text{LptA}_{BCAL0815}$ has a putative N-terminal signal sequence of 46 bp facilitating the transport of the protein across the IM to the periplasm.

### 4.1.1 Cloning, expression, and purification of LptA-His6

In order to characterise the *B. cenocepacia* J2315 LptA protein, *LptA* was amplified from genomic DNA and cloned into the IPTG-inducible expression plasmid pET22b, giving pET22b_LptA_J2315. To aid purification, a C-terminal 6 His tag was introduced, as previously described for the purification of *E. coli* LptA. The recombinant LptA-His6 was exressed in *E. coli* HMS174 (DE3) cells transformed with the pET22b_LptA_J2315 plasmid. Expression of LptA-His6 was obtained after an hour of induction. A longer induction time was avoided to reduce cell lysis. LptA-His6 was solublised and purified using IMAC nickel affinity and size

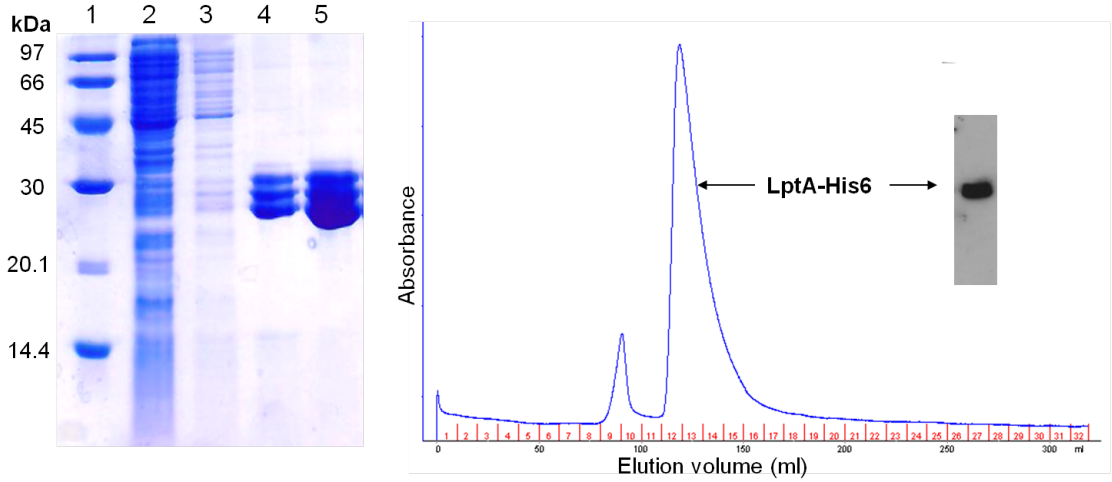


Figure 4.3: LptA-His6 purification profile. a) All consecutive expression and purification steps were analysed by SDS-PAGE. Lane 1 = molecular weight marker, lane 2 = *E. coli* HMS174 after induction, lane 3 = the cell free extract, lane 4 = the Ni-NTA chromatography elution fraction, and lane 5 = fractions 12-15 of the S-300 size exclusion column. b) The elution profile of LptA-His6 purified using a S-300 size exclusion column and the Western Blot analysis after purification.

exclusion chromatography (Figure 4.3). The protein was purified to near homogeneity as judged by SDS-PAGE and its identity was verified by Western Blot with a anti-polyhistidine monoclonal antibody. Size exclusion chromatography showed that LptA-His6 behaved as a mixture of tetrameric and octomeric proteins. The oligomerisation status of LptA-His6 differs from *E. coli* LptA,

which has been showing to be a monomeric protein [171]. The molecular weight of purified LptA-His6 was confirmed by MALDI-TOF mass spectrometry (Appendix A.9), and showed that the 46 amino acid long signal peptide (M1-A46) was cleaved off (predicted MW= 20.4 kD, Appendix A.8). Interestingly, by SDS-PAGE analysis of the purified LptA-His6, the presence of three protein species of different molecular weight was observed. However, MALDI-TOF mass spectrometry of the same sample showed only one molecular ion. A similar observation has been described for *E. coli* LptA, where two bands are seen by SDS-PAGE analysis. It was hypothesised that this is caused by conformational differences causing altered electrophoretic migration characteristics of part of the purified protein [171].

### 4.1.2 LptA-His6 LPS binding assay

To confirm that the *B. cenocepacia* LptA-His6 homolog is able to bind LPS and to explore its specificity a LptA-His6-LPS binding assay was carried out. The method used was adapted from the published *E. coli* LptA-LPS binding assay [171]. Firstly, I chose to test the ability of LptA-His6 to bind L-Ara4N modified deep-rough LPS. Therefore, LPS was isolated from *B. cenocepacia* SAL-1, using the hot phenol-water method (Figure 4.4). Commercially available $Kdo_2$-lipid A (unmodified) of *E. coli* was used as a control. As judged by gel-electrophoresis, discussed below, the isolation of SAL-1 LPS was successful.[1]

Purified LptA-His6 was incubated with $Kdo_2$-lipid A (unmodified) or *B. cenocepacia* SAL-1 LPS to allow binding of the protein to the putative ligands. The protein was re-purified from the mixture using IMAC nickel affinity chromatography. Then, the protein and ligands were analysed by gel-electrophoresis and silver-staining to see whether the two different LPS's would co-elute with the

[1]This LPS was also used for a collaborative study of which the publication can be found attached to this thesis [210].

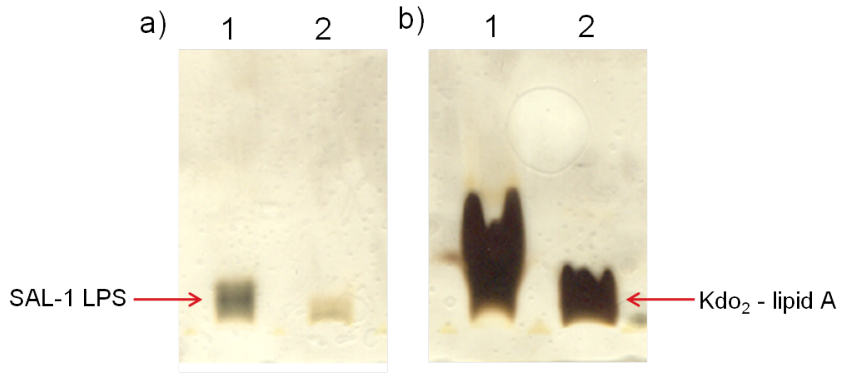


Figure 4.4: LPS isolated from *B. cenocepacia* SAL-1 (a) and *E. coli* $Kdo_2$-lipid A (b) analysed by gel-electrophoresis followed by silver-staining. 1 = 10 $\mu$L of a 1 mg/ml solution; 2 = 10 $\mu$L of a 0.1 mg/ml solution.

protein (Figure 4.5). In these studies, a control was included where the protein was incubated with LPS-free water.

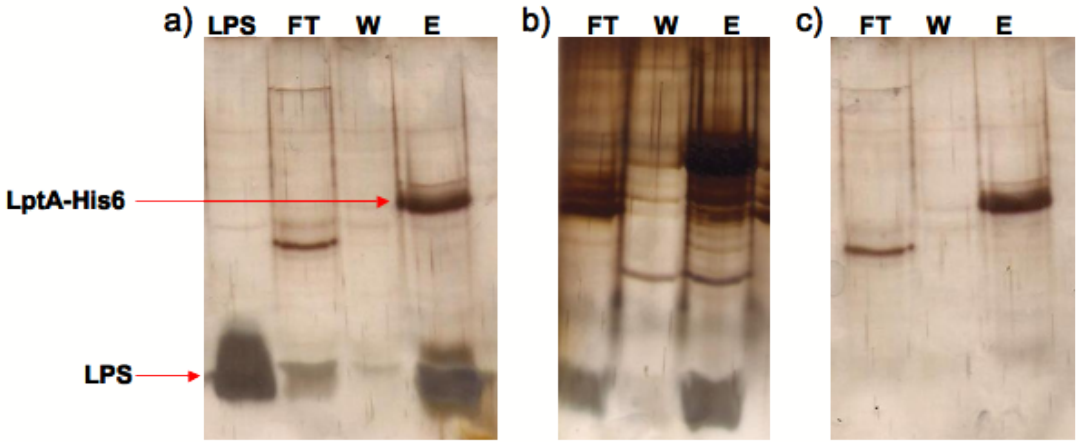


Figure 4.5: (a) *E. coli* $Kdo_2$-lipid A and (b) *B. cenocepacia* SAL-1 LPS binding by LptA-His6. LPS and LptA-His6 was examined by SDS-PAGE followed by silver-staining. FT = flow-through; W = washed (5 times); E = elutions. (c) Control without LPS.

As shown in Figure 4.5, both types of LPS tested co-eluted with the protein, indicating that both can bind to LptA-His6. Therefore, I concluded that *B. cenocepacia* LptA can bind unmodified and modified LPS and is not L-Ara4N-specific. Since I only tested $Kdo_2$-lipid A and deep-rough LPS, it was decided to test if LptA-His6 can bind rough- and smooth LPS as well. Smooth LPS was isolated

from *E. coli* AY103 [152], an ArnT knock-out strain (kindly given by Prof. C. R. H. Raetz, Duke University). This LPS was isolated using a published tri-reagent method [211]. As shown in Figure 4.6, the smooth LPS displays the typical ladder-like profile when analysed by SDS-PAGE. The LptA-His6-LPS binding assay was repeated with this smooth LPS and I could observe that the LPS co-elutes with LptA-His6. However, instead of the ladder-like profile a typical deep-rough LPS profile was observed in the elution fraction. This could indicate that LPS containing the O-antigen region does not bind to LptA-His6. However, this phenomenon was not explored further and a conclusive answer cannot be drawn.

A previous PhD student in the Campopiano group, Josephin Bartholdson, isolated deep-rough LPS from *B. cenocepacia* J2315, using the hot phenol-water method [212]. Therefore, it was decided to use this LPS to explore if LptA-His6 can bind this type of LPS. As shown in Figure 4.6, LptA-His6 can bind rough LPS and the typical two-banded pattern of *B. cenocepacia* J2315 co-elutes with the protein.

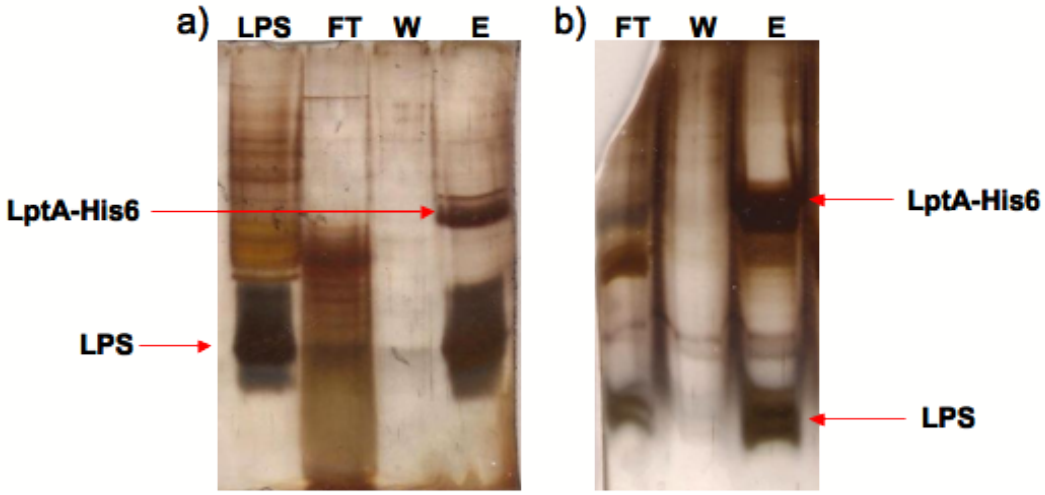


Figure 4.6: *E. coli* AY103 smooth LPS (a) and *B. cenocepacia* J2315 rough LPS (b) binding by LptA-His6. LPS and LptA-His6 was examined by SDS-PAGE followed by silver-staining. FT = flow-through; W = washed (5 times); E = elutions.

The LptA-His6-LPS binding assays were all carried out directly after purifica-

tion of the protein, which was necessary due to the instability of the protein. LptA-His6 degrades within hours after purification. Repeatedly, a ∼4 kDa fragment would cleave off the C-terminus, leading to precipitation of the protein. The cleavage after ∼4 kDa was confirmed with MALDI-TOF analysis (Appendix A.9). This degradation suggested that a protease was co-purified with LptA-His6. However, several attempts to add additional protease inhibitors to the purification buffers, such as phenylmethylsulfonyl fluoride (PMSF), EDTA, leupeptin, or tosyl phenylalanyl chloromethyl ketone (TPCK), failed to stabilise the protein. EDTA was the only inhibitor tested which could slow down the decomposition but not completely prevent it. The fact that this decrease in decomposition was effected by a complexing ligand hints at the presence of a metalloproteinase. Several attempts to explore the binding affinity of ligand and protein in more detail, by isothermal titration calorimetry (ITC) and dynamic light scattering (DLS), failed due to this protein instability (data not shown).

## 4.2 LptB (LPS transport protein B)

LptB is a soluble cytoplasmic ATP-ase that forms a complex with LptC, LptF, and LptG, and most likely delivers energy for the extraction of lipid A molecules out of the phospholipid-bilayer of the IM. To date, no structural information is available on the LptB from any organism. However, previous studies have yielded kinetic characterisation of the *E. coli* isoform [168, 169]. Herein, I show the characterisation of the *B. cenocepacia* J2315 LptB homolog *in vitro*.

### 4.2.1 Cloning, expression, and purification of LptB-His6

The *LptB* homologous gene (BCAL0814) was amplified from genomic *B. cenocepacia* J2315 DNA. Then I constructed a plasmid able to express a C-terminal

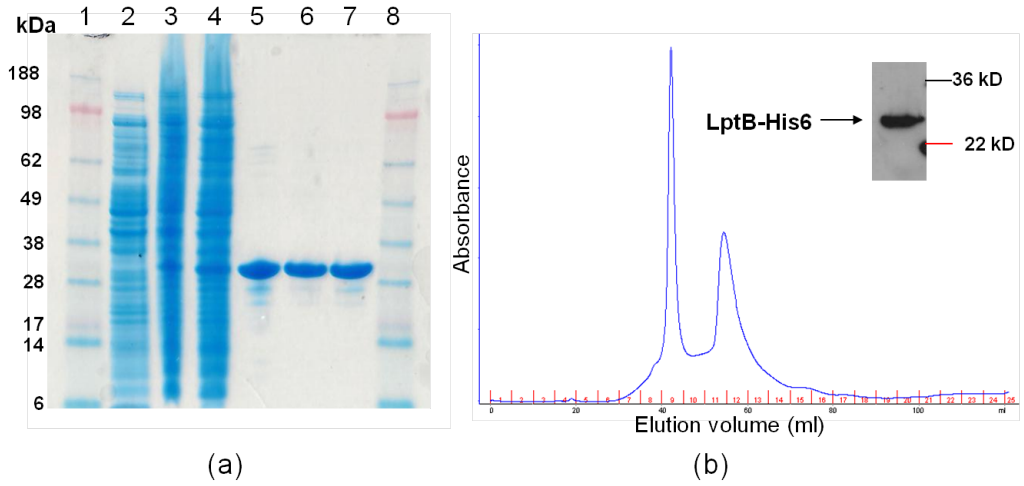


Figure 4.7: LptB-His6 purification profile. a) All consecutive expression and purification steps were analysed by SDS-PAGE. Lane 1 and 8 = molecular weight marker, lane 2 = *E. coli* BL21 before induction, lane 3 = after induction, lane 4 = the cell free extract, lane 5 = the Ni-NTA chromatography elution fraction, lane 6 = fraction 9 of the S-75 size exclusion column, and lane 7 = fractions 11-13 of the S-75 size exclusion column. b) The elution profile of LptB-His6 purified with a S-75 size exclusion column and the Western Blot analysis after purification.

6 His tagged version of LptB under the control of the IPTG-inducible promoter, pET22b_LptB_J2315. The recombinant LptB-His6 was exressed in *E. coli* BL21 (DE3) cells transformed with the pET22b_LptB_J2315 plasmid.

The purification condition of the *E. coli* LptB-His6 isoform were published recently [169], and I adopted the same strategy with some modifications to purify *B. cenocepacia* LptB-His6. Though LptB-His6 does not have any membrane-spanning domains, it is known to be associated to the IM. Therefore, it was necessary to solubilise LptB-His6 by adding glycerol and DTT to the purification buffers. Then, LptB-His6 was purified to near homogeneity using IMAC nickel affinity and size exclusion chromatography (Figure 4.7). The identity of the purified protein was confirmed by Western Blot. The yield obtained was typically ~8 mg of pure recombinant LptB-His6 per litre of induced *E. coli* BL21 (DE3) cells. Judging from the elution profile of the size exclusion chromatography col-

umn, LptB-His6 was purified as a mixture of monomeric and dimeric protein. (Figure 4.7). The monomer molecular weight (predicted MW = 28.2 kDa) of the protein was confirmed by MALDI-TOF mass spectometry (Appendix A.12). The two peaks from the size exclusion chromatograhy column were assayed independently and showed identical activity (results not shown).

### 4.2.2 Kinetic analysis of LptB-His6

To measure LptB-His6 activity, a similar assay was used as described for the *E. coli* homolog [169]. An assay was used in which the production of ADP by LptB-His6 is continuously detected using a pyruvate kinase (PK)- lactate dehydrogenase (LDH) assay (Figure 4.8). Reactions were monitored by measuring the decrease in NADH concentration in the reaction mixture over time at the analytical wavelength of 340 nm.

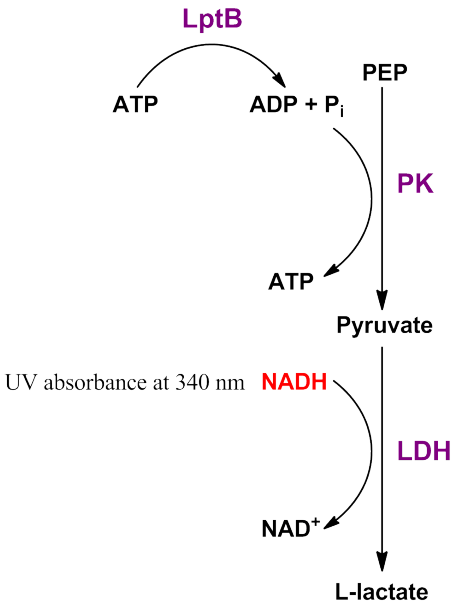


Figure 4.8: LptB activity assay. LptB hydrolysis ATP to ADP and free phosphate. PK catalyses the transfer of a phosphate group from PEP to ADP, regenerating ATP and pyruvate. LD uses pyruvate as a substrate to form L-lactate, utilising the co-factor NADH to $NAD^+$. NADH absorbs UV light at a wavelength of 340 nm. The decrease in NADH absorbance is proportional to the amount of ATP hydrolysed.

The assay was performed with variable concentrations of substrate and data was plotted using the Michaelis-Menten equations (Figure 4.9). The initial reaction rate was calculated by measuring the decrease in absorbance at 340 nm. The molar extinction coefficient of NADH at 340 nm is 6220 $M^{-1}$ $cm^{-1}$. The data was processed using SigmaPlot software and the $V_{max}$, $K_M$ and Hill coefficient were obtained from the graph. The kinetic parameter $k_{cat}$ was calculated from the values obtained from the graph. The $k_{cat}$ value was found to be 5.71 $min^{-1}$. The $K_M$ was found to be 0.88 mM, with a Hill coefficient of 1.6. A Hill coefficient of >1 indicates that a cooperative reaction takes place, indicating that LptB acts as a dimer. Our values are comparable to the kinetic parameters found for the *E. coli* LptB of which the $k_{cat}$ is 6.2 $min^{-1}$ and the $K_M$ is 0.56 mM with a Hill coefficient of 1.5 [169].

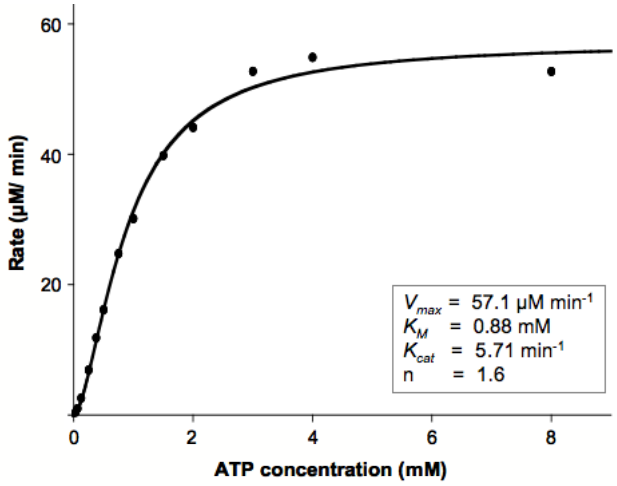


Figure 4.9: Kinetic analysis of LptB-His6. Michaelis-Menten representation, generated with SigmaPlot software.

Some ATP-ases can be activated or inhibited by their substrate. I explored, whether the presence of LPS had an effect on LptB-His6 activity and if LptB-His6 showed a specificity towards L-Ara4N modified LPS. Therefore I measured the activity of LptB-His6 in the presence of variable concentrations of LPS. The LPS's tested included commercially available *E. coli* $Kdo_2$-lipid A (unmodified), deep-rough LPS isolated from *B. cenocepacia* SAL-1 (L-Ara4N-modified), rough

LPS isolated from *B. cenocepacia* J2315, and smooth LPS isolated from *E. coli* AY103. It was found that the presence of LPS in all concentrations tested did not have any effect on the activity of LptB-His6 (data not shown). Previously, it has been shown that the presence of $Kdo_2$-lipid A also did not affect the activity of *E. coli* LptB [168].

In the same study, it was shown that *E. coli* LptB could be inhibited with orthovanadate ($VO_4$), a well-known inhibitor of a number of ATP-ases. Furthermore, during a high-throughput inhibition study of two commercially available kinase inhibitor libraries, two compounds were found to inhibit *E. coli* LptB [169]. I decided to test inhibition by orthovanadate and one of the inhibitors (inhibitor 2) found during the high-throughput study (Chapter 1, Figure 1.17) of *B. cenocepacia* LptB-His6. During my studies I could not observe any inhibition of LptB-His6 by either $VO_4$ or inhibitor 2, not even after pre-incubation with the enzyme for $\sim$2 hours. It should be noted that the highest concentrations of inhibitor tested were 22 $\mu$M for inhibitor 2 and 8 mM for orthovanadate. It was impossible to increase the concentrations of the inhibitors in my assay since as with NADH both inhibitors absorb at 340 nm. However, at the concentrations I tested *E. coli* LptB was clearly inhibited [168, 169] and the *B. cenocepacia* enzyme was not.

## 4.3 Conclusion

In this chapter, I have tried to explain why L-Ara4N is necessary for viability in *B. cenocepacia*, but not in other gram-negative bacteria, such as *E. coli* and *S. typhimurium*. To answer this question, I characterised two proteins *in vitro* involved in lipid A transport in *B. cenocepacia*, namely LptA and LptB. These proteins were picked as targets since I observed a striking similarity in phenotype between *B. cenocepacia ArnB* and *ArnT* conditional lethal mutant strains [98] and the conditional lethal *E. coli* LptA/LptB mutant [165]. Therefore, it could

be hypothesised that either LptA or LptB might show specificity to L-Ara4N-modified LPS.

Both proteins were successfully cloned, expressed, and purified. The previously putative *B. cenocepacia* LptA homolog did bind LPS *in vitro* as expected. However, this LptA was able to bind all types of LPS offered, like the *E. coli* isomer, and was not specific for L-Ara4N-modified LPS.

The LptB homolog of *B. cenocepacia* showed ATP-ase activity *in vitro* and the kinetic parameters that were found are in a similar range as the values described in a very recent analysis of *E. coli* LptB. It was attempted to inhibit *B. cenocepacia* LptB with two inhibitors that were shown to be active against *E. coli* LptB, but in both cases no inhibition could be observed. This suggests that there are differences in structure between the *E. coli* and *B. cenocepacia* LptB enzyme, and that *E. coli* LptB inhibitors are not necessarily likely to be active against *B. cenocepacia*. As with the *E. coli* LptB, the presence of any LPS (L-Ara4N-modified or not) in the reaction mixture, had no influence on the activity of LptB. Therefore, I concluded that LptA and LptB are not L-Ara4N-specific.

To my knowledge, this was the first study on *B. cenocepacia* proteins involved in lipid A transport. However, the question still remains, why L-Ara4N is necessary for viability. Future research could focus on the other proteins involved in lipid A transport, such as the OM LptD/E complex.

# Chapter 5

# Conclusions

*Burkholderia cepacia* complex (Bcc) consists of a group of closely related *Burkholderia* species that are opportunistic pathogens in patients with cystic fibrosis (CF) [12, 16, 17]. Though the risk of infection by Bcc species is relatively low, it is of great concern with regard to CF patients. This because of four reasons: 1) infection by Bcc leads, in approximately 20% of individuals, to Cepacia syndrome, a syndrome which in most cases is lethal [25]; 2) Bcc infections can be transmissible from one patient to another [12] and have caused several epidemic outbreaks in history [26, 27]; 3) successful treatment of Bcc infections is problematic due to the inherent resistance of Bcc species to most classes of antibiotics; 4) Bcc infection makes it necessary to segregate infected individuals from the rest of the CF population, which has a great impact on the psychological well-being of the patient [28].

Most Bcc species produce a wide variety of virulence factors that might cause Cepacia syndrome, but none of these factors has been established as the main causative agent [12]. The virulence factor I focused on during these studies was LPS, which can, beside stimulating an immune response directly, be responsible for the high resistance of Bcc species against polycationic compounds. Lipid A (also known as endotoxin) is the hydrophobic anchor of lipopolysaccaride (LPS)

and is the bio-active component of LPS. The lipid A structure and composition of Bcc members is distinct from the lipid A of other Gram-negative bacteria investigated today. One of several unique characteristics of the lipid A of the Bcc, is the permanent attachment of 4-amino-4-deoxy-L-arabinose (L-Ara4N) to the lipid A molecule [28]. Also, the genes involved in L-Ara4N biosynthesis are necessary for viability in *B. cenocepacia* [98]. In this thesis I presented research on lipid A biosynthesis, modification, and transport in the Bcc and highlighted promising antimicrobial targets.

Enzymes involved in the lipid A biosynthesis pathway, in particular LpxC, have been recognised as attractive targets for new agents designed to treat infections caused by Gram-negative bacteria [128]. The most potent inhibitor published so far, which is capable of inhibiting growth of several Gram-negative species, is the synthetic antibiotic CHIR-090. CHIR-090 showed good antimicrobial activity against several Gram-negative bacteria, such as *E. coli* and *P. aeruginosa*. CHIR-090 is a slow, tight binding inhibitor of LpxC [144, 146], the enzyme the catalyses the first irreversible step of the lipid A biosynthesis pathway. I explored the potential of antibiotics targeting lipid A biosynthesis to treat Bcc infections by investigating the activity of CHIR-090 against the Bcc. I showed that CHIR-090 can inhibit growth of some Bcc species, including one of the most prevalent Bcc species, *B. multivorans*. MICs were determined for eight *B. multivorans* strains and were found to be strain-dependent and ranged from 0.1 to >100 $\mu$g/ml. Despite the close taxonomic relationship of the Bcc, individual isolates displayed a remarkable difference in the sensitivity to CHIR-090 even within a single species.The species- and strain-specific sensitivity towards CHIR-090 was further explored and a strong correlation was found between the presence of a unique open reading frame, named $LpxC_2$, and the occurrence of resistance. I showed that new drugs targeting this pathway have a potential to treat Bcc infections. However, this potential is likely to be species- and strain-dependent. To the best of my knowledge, this CHIR-090 study is the first to report an agent

against *Burkholderia* targeted at the LPS biosynthetic pathway.

To address the problem of multiple drug-resistance of the Bcc, I explored the potential and novel use of the "old" antibiotic, cycloserine (CS), to treat Bcc infections. CS is a pyridoxal 5′-phosphate (PLP)-dependent enzyme inhibitor that binds to the PLP co-factor in the active site. CS is used as a second line of defense against *M. tuberculosis*. Antimicrobial activity assays against the Bcc were performed with both CS enantiomers, L-cycolserine (LCS) and D-cycloserine (DCS). LCS did not show any growth inhibitory activity against the Bcc. DCS on the other hand could inhibit growth of all strains of the Bcc reference panel and acted bactericidal towards the Bcc. DCS displayed MICs between 2 and 128 $\mu$g/ml, which are in the same range or lower than previously published for clinical isolates of *M. tuberculosis*. These results indicate that, *in vitro*, Bcc are at least as susceptible towards DCS as *M. tuberculosis*, and that DCS might be of clinical use in the treatment of Bcc infections. Since this thesis focuses on the lipid A biosynthesis and aminoarabinose modification pathways as drug targets, *in vitro* CS inhibition with the only PLP-dependent enzyme, ArnB, involved in these pathways was studied. Recombinant ArnB from *B. cenocepacia* J2315 was inhibited reversibly by DCS. ArnB was further explored as a promising drug-target in the Bcc, by using the other well known PLP dependent enzyme inhibitors $\beta$-chloro-D-alanine and L-propargylglycine, but only CS could been identified as an inhibitor so far.

The last topic covered in this thesis included lipid A transport and L-Ara4N modification. I observed a striking similarity between the electron microscopic images of the previously published *B. cenocepacia ArnB* and *ArnT* conditional mutant strains [98] and the conditional lethal *E. coli* LptA/LptB mutant [165]. Therefore, it could be hypothesised that either LptA or LptB might show specificity to L-Ara4N-modified LPS. I explored and characterised two proteins which are involved in lipid A transport: LptA, the periplasmic lipid A binding protein, and LptB, the cytoplasmic ATP-ase. LptA was found to be able to bind

LPS *in vitro*. LptA could bind both modified and unmodified lipid A *in vitro*. Furthermore, LptA could bind deep-rough-, rough-, and smooth- LPS, similar to that described for *Escherichia coli* LptA. Therefore I concluded that LptA is not L-Ara4N-specific. Recombinant *B. cenocepacia* LptB was expressed, purified and the kinetic parameters were determined *in vitro*. The kinetic parameters were found to be in a similar range as the values decribed for *E. coli* ($k_{cat} = 5.71$ min$^{-1}$ and $K_M = 0.88$ mM). The ATP-ase activity of LptB was not influenced by the presence of any forms of LPS (modified or non-modified), suggesting the absence of a regulatory protein domain that influences activity by LPS. Therefore, I concluded that both *B. cenocepacia* J2315 LptA and LptB are not L-Ara4N-specific.

# Chapter 6

# Materials & Methods

## 6.1 Materials

All chemicals and reagents were purchased from Sigma Aldrich, Fisher Scientific, Biorad or Oxoid unless otherwise stated. DNA primers were purchased from Sigma Aldrich. All restriction enzymes were purchased from New England Biolabs. Competent cells were purchased from Promega, Invitrogen or Novagen. All pET expression plasmids were purchased from Novagen. The (conditional) knock out plasmids, pGpΩ plasmid and pSc200, and the *Burkholderia cenocepacia* SAL-1 were given by Prof. M. A. Valvano (Department of Microbiology and Immunology, University of Western Ontario, London, Ontario, Canada). *E. coli* AY103 was given by Prof. C. H. R. Raetz (Department of Biochemistry, Duke University Medical Center, Durham, North Carolina, USA). All chromatography columns and affinity raisins were purchased from GE-Healthcare or Qiagen.

### 6.1.1 Cell lines, growth media, and antibiotics

All competent *E. coli* cell lines used in these studies are listed in Table 6.1.

Table 6.1: Competent *E. coli* cell lines.

| ***E.coli* strain** (source) | **Relevant Characteristics** |
|---|---|
| **DH5$\alpha$** (Novagen) | F$^-$ $\phi$80d*lacZ*$\Delta$M15 ($\Delta$*lac*2YA-*arg*F)U169 *end*A1 *rec*A1 *hsd*R17($r_k^-m_k^+$) *pho*A supE44 thi-1 $\Delta$*gyr*A96 *rel*A1 |
| **JM109** (Promega) | *end*A1 *rec*A1 *gyr*A96 *thi* *hsd*R17($r_k^-m_k^+$) *rel*A1 *sup*E44 $\Delta$(*lac-pro*AB), [F$'$ *tra*D36 *pro*AB, *laq*I$^q$Z$\Delta$M15] |
| **TOP10** (Invitrogen) | F$^-$ $_{mcrA}$ $\Delta$(*mrr-hsdRMS-mcr*BC) $\phi$80d*lacZ*$\Delta$M15 $\Delta$LacX74 deoR *rec*A1 araD139 $\Delta$*ara-leu*7697 *gal*U *gal*K *rps*L *end*A1 *nup*G |
| **Bl21 (DE3)** (Novagen) | F$^-$ ompT *hsd*$S_b$ ($r_B^-m_B^-$) *gal dcm* (DE3) |
| **HMS174 (DE3)** (Novagen) | F$^-$ *rec*A1 *hsd*R17($r_{K12}^-m_{K12}^+$) (DE3) (RIF$^R$) |
| **GT115** (Invitrogen) | F$^-$ $_{mcrA}$ $\Delta$(*mrr-hsdRMS-mcr*BC) $\phi$80d*lacZ*$\Delta$M15 $\Delta$LacX74 *rec*A1 *end*A1 $\Delta$*dcm*, *uiad* ($\Delta$*MluI*)::*pir*-116, $\Delta$*sbcC-sbcD* |

**Luria-Bertani (LB)** broth contained 1% bacto-tryptone, 0.5% bacto-yeast extract, and 1% NaCl (pH7.5). LB agar was purchased from Invitrogen or Sigma.

**Terrific Broth (TB)** contained 1.2% bacto-tryptone, 2.4% bacto-yeast extract, 4 ml glycerol, and 17 mM $KH_2PO_4$/ 72 mM $K_2HPO_4$ (autoclaved separately).

**2YT broth** contained 1.6% bacto-tryptone, 1% bacto-yeast extract, and 0.5% NaCl (pH7.5).

**S-Gal agar** was obtained from Sigma.

**SOC** contained 2% bacto-tryptone, 0.5% bacto-yeast extract, 0.05% NaCl, 0.5% $MgSO_4$, and 3.2% glucose (pH7.5).

**Nutrient agar, Isosensitest (IS) broth, IS agar, Mueller Hinton (MH) broth, and MH agar** were purchased from Oxoid.

**Antibiotics:** When required cultures were supplemented with the following antibiotics (final concentrations): ampicillin, 100 $\mu$g/ml; kanamycin 50 $\mu$g/ml; gentamycin, 50 $\mu$g/ml; tetracycline, 50 $\mu$g/ml; and trimethoprim 50 $\mu$g/ml. All

strains were grown at 37 $^{o}$C unless stated otherwise.

## 6.2 General Methods

### 6.2.1 Introduction of plasmid DNA into bacterial cells

#### Transformation of competent *E. coli* cells

Competent cells were defrosted on ice, 3 $\mu$L of plasmid DNA was added, and incubated on ice for 30 minutes. The cells were heat-shocked for 30 seconds at 44 $^{o}$C, and allowed to close by incubation on ice for 2 minutes. 250 $\mu$L LB or SOC medium was added, the cells were agitated (250 rpm) for an hour at 37 $^{o}$C, spread on LB agar containing the appropriate antibiotic, and incubated overnight at 37 $^{o}$C.

#### Tri-parental mating

*E. coli* DH5$\alpha$ or *E. coli* GT115 was transformed (as described above) with the knock-out plasmid to become a donor strain. The helper strain was created by transforming the pRK2013 plasmid into *E. coli* DH5$\alpha$. The donor-, and helper-strains were grown overnight in 10 ml SOB broth with appropriate antibiotic selection. Recipient strains were grown overnight in 10 ml LB. All overnight cultures were pelleted. The helper- and donor- strain were both resuspended in 3 ml PBS, of which 1 ml of each was used to resuspend the recipient strain. The mixture was washed 3 times with PBS and resuspended in 2 ml LB. 200 $\mu$L was pipetted onto a 0.12 $\mu$M cellulose filter, which was placed onto a SOB agar plate without any antibiotic selection. The plate was incubated upright overnight at 37 $^{o}$C. The filter was washed in 10 ml LB, of which 200 $\mu$L was spread on a LB agar plate containing two different antibiotics. The first antibiotic used

corresponded to the antibiotic resistance cassette of the knock-out plasmid. The second antibiotic was an antibiotic where the recipient strain is naturally resistant to but kills the donor and helper strain (in these studies on *Burkholderia* species, gentamycin was used). After 2 days, surviving colonies were spread on fresh LB plates containing the same antibiotics. The presence of the plasmid or insertion of the construct into the genome was confirmed by PCR.

### 6.2.2 DNA & RNA

#### Isolation of genomic DNA

Chromosomal DNA was isolated using alkaline lysis extraction. Bacterial colonies were scraped from a plate and mixed into 20 $\mu$L lysis buffer (2.5 ml 10% SDS, 5 ml 1 M NaOH, 92.5 ml $dH_2O$), which was then heated to 95 $^oC$ for 15 minutes. After a quick spin in a centrifuge, 180 $\mu$L $dH_2O$ was added. It was centrifuged for 5 minutes at 13,000 rpm, and stored at -20 $^oC$.

#### DNA gel electrophoresis

1.2% or 4% agarose was added to TAE buffer and heated in a microwave until dissolved. The molten agarose was cooled to approximately 50 $^oC$, ethidium bromide was added to a final concentration of 5 $\mu$g/ml. The molten agarose was poored into the casting and allowed to set at room temperature. DNA loading dye (Novagen) was added to the DNA samples and the gel was ran in TAE buffer at 100 V for 30-60 minutes.

#### DNA purification

For isolation of DNA restriction fragments or PCR products from 1.2% agarose gels, the Qiagen Gel Extraction kit was used. Plasmids were isolated from *E. coli*

cells using the Qiagen Miniprep kit. Both extractions were carried out according to the protocol of the manufacturer.

### Polymerase chain reaction (PCR)

All PCR reactions were carried out in a Techne TC-3000 hot-lid Thermal Cycler. Proofstart polymerase (Qiagen) was used for the PCR reactions unless otherwise stated. The total reaction volume was 50 $\mu$L, containing 10 $\mu$M forward and reverse primer, 4 $\mu$L genomic DNA (isolated as described above), 5 $\mu$L buffer, 10 $\mu$L solution Q, 200 $\mu$M dNTPs, 1 $\mu$L polymerase, and $dH_2O$. Typically, the reaction was cycled 35 times, denaturing at 95 $^o$C for 30 seconds, followed by annealing (specific temperatures are given for every primer-set) for 30 seconds, and elongation at 72 $^o$C for 1 minute per 1000 bp. For cloning into pGEM-T-Easy (Promega), which requires the addition of a poly(A) tail on both ends of the PCR product, a puReTaq Ready-To-Go bead (GE Healthcare) was added after the PCR reaction. The mixture was heated to 95 $^o$C for 5 minutes, followed by an elongation step of 10 minutes at 72 $^o$C.

### Restriction digests

For a small scale restriction digest (total volume of 10 $\mu$L), 1 $\mu$L 10 x appropriate buffer was added to 8 $\mu$L of plasmid DNA, which was then mixed with 0.5 $\mu$L of each endonuclease required. The mixture was incubated for at least 1 hour at 37 $^o$C before analysis by DNA gel electrophoresis.

For a large scale restriction digest the total volume of the reaction was 50 $\mu$L (43 $\mu$L plasmid DNA, 5 $\mu$L buffer, and 1 $\mu$L of each endonuclease). The procedure was identical as described for the small scale restriction digest.

### Sequencing

The cloned plasmids were sequenced using a PCR-based method. The sequencing reaction contained 5 $\mu$L plasmid (50-100 ng), 1 $\mu$L forward or reverse primer (final concentration was 3.2 $\mu$M), 2 $\mu$L BigDye Terminator v3.1 5x sequencing buffer (Applied Biosystems), and 2 $\mu$L BigDye. The reaction was cycled 30 times, 95 $^o$C for 30 seconds, 45 $^o$C for 15 seconds, and 60 $^o$C for 4 minutes. The primers used to sequence the pET expression- and pGEM-T-Easy plasmids are listed in Table 6.2. Sequencing of the reaction product was carried out by Genepool sequencing service, Institute for Cell and Molecular Biology, University of Edinburgh. Sequencing data was analysed by Contig Express & Vector NTI Advance $^{TM}$ V9 software package (Invitrogen).

Table 6.2: Sequencing primers for the pET expression plasmids and pGEM-T-Easy.

| **Primer** | **Sequence 5$'$ to 3$'$** |
|---|---|
| pGEM T7 For (forward primer) | TAATACGACTCACTATAGGG |
| pGEM T7 Rev (reverse primer) | ATTTAGGTGACACTATAGAA |
| pET For (forward primer) | TAATACGACTCACTATAGGG |
| pET Rev (reverse primer) | ATTTAGGTGACACTATAGAA |

### Cloning

All PCR products were cloned into a pGEM-T-Easy vector, before further cloning into an expression or knock-out plasmid. To do so, the purified DNA PCR product was ligated into the pGEM-T-Easy plasmid, using either T4 DNA ligase (Promega) or Quick time ligase (Roche) according to the instructions of the manufacturer. The ligation product (3 $\mu$L) was transformed into *E. coli* JM109 competent cells and spread on S-Gal/Amp plates, which allows for blue- (no insert) white (insert)- colony screening. White colonies were picked, grown overnight

in 5 ml LB/Amp, and the plasmid was isolated. The pGEM-T-Easy plasmids were screened for the right insert by performing a small scale restriction digest. Typically, restriction sites were incorporated in all forward- and reverse- primers. Hence, the plasmid was restricted with the two corresponding endonucleases. When possible, a second restriction digest was performed using an endonuclease cleaving inside the gene of interest. The plasmids which showed the expected digest profiles were sequenced. When sequencing confirmed the right insert (without mutations), a large scale restriction digest was carried out of the pGEM-T-Easy plasmid and the recipient plasmid. The digest products were separated by DNA gel electrophoresis and purified. The insert and the recipient plasmid were ligated and transformed into competent *E. coli* TOP10 or DH5$\alpha$ cells.

### *RecA* & RFLP analysis

To confirm the identity of all Bcc strains used in this study, DNA was isolated and the *RecA* gene was amplified using the primers BCR1 and BCR2 (Table 6.3). The PCR consisted of 30 cycles: 30 seconds at 94 $^o$C, 5 seconds at 58 $^o$C, and 60 seconds at 72 $^o$C; and a final extension of 10 minutes at 72 $^o$C. 10 $\mu$L of PCR product was ran on a 1.2% agarose gel (1 kb ladder) and 10 $\mu$L was restricted overnight with *HaeIII* and ran on a 4% agarose gel (100 bp ladder).

Table 6.3: *RecA* amplification primers.

| **Primer** | **Sequence 5$'$ to 3$'$** |
|---|---|
| BCR 1 | TGACCGCCGAGAAGAGCAA |
| BCR 2 | CTCTTCTTCGTCCATCGCCTC |

### 6.2.3 Protein

#### Protein expression

Proteins were expressed in expressing *E. coli* cell lines (BL21(DE3) or HMS174(DE3)).

**Small scale expression.** To determine the expression conditions of the different proteins, a small scale induction of the expression plasmid was performed. A single colony of the expressing cell line was grown overnight in 5 ml LB broth. The cells were diluted down 1/10 in 5 ml fresh broth and grown to an $A_{600}$ of ∼0.6-0.8. To trigger transcription of the *lac* operon, different concentrations (0.1 mM, 0.5 mM, 1.0 mM) of isopropyl $\beta$-D-1-thiogalactopyranoside (IPTG) were added. The cells were grown for an additional 5 hours (unless stated otherwise) at 37 $^{o}$C and 500 $\mu$L samples were taken after 1 hour, 3 hours, and 5 hours. The samples were spun down, and protein expression was analysed by sodium dodecyl sulfate polyacrylamide gel electrophoresis (SDS-PAGE).

**Large scale expression.** A single colony of the expressing cell line was grown overnight in 250 ml LB medium containing the appropriate antibiotic. The overnight cultures were diluted into 4 L fresh medium to an $A_{600}$ of ∼0.1 and grown to an $A_{600}$ of ∼0.6-0.8 at 37 $^{o}$C. Protein expression was induced by adding IPTG to the cell culture, and the cells were grown for an additional amount of hours, at the optimised temperature needed for protein expression. The cells were harvested by centrifugation at 4,000 rpm and the pellets were stored at -20 $^{o}$C.

#### SDS-PAGE

SDS-PAGE mini gels (15% acrylamide) were used to analyse proteins based on their molecular weight. SDS-PAGE gels, loading buffer, staining solution and destaining solution were prepared according to the Laemmeli protocol. Samples

for analysis by SDS-PAGE were prepared by addition of appropriate volume of loading buffer, followed by boiling the sample for 5 minutes, and centrifugation (13,000 rpm, 5 min). The low molecular weight (LMW) marker (GE Healthcare) or SeeBlue-Plus2-prestained standard (Invitrogen) was used as a reference for size. Gels were typically run for 60 minutes, 200 V and 180 mA.

**Western Blot**

Western Blot analysis was performed to positively identify expressed and/ or purified His6 tagged proteins. After running a SDS-PAGE mini gel the gel and the nitrocellulose membrane (Hybond-ECL, Amersham) were placed into transfer buffer (150 mM TRIS, 150 mM glycine, and 10% MeOH) for 10 minutes. Six slightly larger Whatman filter papers were soaked into transfer buffer. The filter papers, nitrocellulose membrane, and SDS-PAGE gel were placed on top of each other (from bottom to top: 3 times filter paper, nitrocellulose membrane, gel, and 3 times filter paper) in the blotting machine (Trans-Blot SD Semi-Dry Transfer Cell (Bio-Rad)) and blotted for 40 minutes, 15 V, and 150 mA. The membranes were incubated overnight in blocking solution (0.1% $\text{Tween}_{20}$ and 5% milk powder dissolved PBS), with agitation at 4 $^{o}$C. The membranes were washed 6 times for 5 minutes with washing solution (0.1% $\text{Tween}_{20}$ in PBS). Membranes were incubated with blocking solution, containing 1:3000 $\mu$L Anti-His antibody (Roche) for an hour, after which they were washed 6 times with washing solution and incubated with blocking solution, containing 1:3000 Anti-Mouse antibody. The membranes were washed 6 times with washing solution, were dried and covered with ECL Plus Western Blotting Detection System solution (GE Healthcare). The membrane was dried and the western blot was developed using KODAK BioMax XAR film in a Hypercassette (Amersham).

#### Cell lysis by sonication

The cell pellet was defrosted on ice and resuspended in lysis buffer (composition is specified per protein) till a homogeneous suspension was obtained. The suspension was sonicated on ice for 15 cycles (30 seconds on, 30 seconds off) using a soniprep 150. The cell debris and supernatant were separated by centrifugation (15,000 rpm, 20 minutes, 4 $^{o}$C).

#### MALDI-TOF analysis of proteins

Proteins, in concentrations of typically 1 mg/ml, were co-crystallised with sinapinic acid (10 mg synapinic acid in 500 $\mu$L $H_2O$, 400 $\mu$L acetonitrile and 100 $\mu$L 3% trifluoroacetic acid (TFA)) as a matrix, directly on MALDI plate. Spectra were measured on a Voyager DE-STR MALDI-TOF mass spectrometer and analysed using the DataExplorer software (Applied Biosystems).

### 6.2.4 LPS

#### LPS extraction using hot-phenol

A single colony of the desired strain was picked and grown in 5 ml LB broth at 37 $^{o}$C overnight. This 5 ml of culture was used to inoculate 4 L LB broth and was grown overnight at 37$^{o}$C. The cells were harvested by centrifugation (9,000g for 20 minutes). When LPS of *Burkholderia* strains was isolated, the pellet was boiled for 10 minutes to kill the cells (for transport purposes). For other strains this step was omitted. The cell pellets were stored at -20 $^{o}$C.
The pellet was resupended in 50 ml cold EDTA solution (0.05 M $Na_2HPO_4$*$7H_2O$, 50 mM EDTA, pH 7). The cells were sonicated on ice for 15 minutes, 30 seconds on, 30 seconds off. The mixture was transferred to a conical flask, 15 mg lysozyme was added, and stirred overnight at 4 $^{o}$C. The mixture was transferred to a 37 $^{o}$C

shaker and heated for 20 minutes. 20 mg RNAse, 0.4 mg DNAse, and 25 ml of 0.04 M $MgCl_2$*$6H_2O$ was added and incubated for half an hour at 37 $^oC$. The mixture was then heated up to 60 $^oC$ in a waterbath. After reaching 60 $^oC$, both the mixture and a bottle with 75 ml phenol were heated to 65 $^oC$ in the waterbath. The mixture was added to the hot phenol, stirred manually for 15 minutes at 65 $^oC$, and incubated on ice for 15 minutes. To separate the water and phenol phases, the mixture was centrifuged (9,000 g, 20 minutes, at 4 $^oC$). After separation, the phenol phase was transferred to dialysis tubing. The filled dialysis tubing was placed in bucket filled with ∼7 L water and dialysed with a constant flow of fresh water for 3 days. The samples were transferred to new falcon tubes and kept at -80 $^oC$ overnight. The samples were lyophilised and stored at -20 $^oC$. By running a SDS-PAGE gel the presence of LPS was confirmed. Before using it for my experiments the LPS was cleaned up. The LPS was resuspended in LPS-free $dH_2O$, ultra-centrifuged at 100,000 g, and lyophilised.

**LPS extraction using Tri-reagent**

A single colony of the desired strain was picked and grown in 1 L 2YT broth overnight. The cells were harvested by centrifugation (9,000 g for 20 minutes). The cell-pellet was lyophilised. The dried cells were resuspended into 10 ml Tri-reagent and incubated for 20 minutes at room temperature. Chloroform (3 ml) was added and incubated for 10 minutes at room temperature. To separate the aqueous phase and the organic phase, the samples were centrifuged for 15 minutes at 12,000 g. The aqueous phase (upper) was transferred to a new tube and the organic phase was re-extracted 3 times by adding 10 ml $dH_2O$, incubate 10 minutes at room temperature and centrifuge for 15 minutes at 12,000 g. The aqueous phases of all extractions were combined and lyophilized. Then, 25 ml of 375 mM MgCl in 95% EtOH was used to re-dissolve the dried material, cooled down to 0 $^oC$ (in -20$^oC$ freezer), and spun down at 12,000 g for 15 minutes. The

supernatant was discarded and the pellet (conaining the LPS) was resuspended in 7 ml of $dH_2O$ and lyophilized. By running a SDS-PAGE gel the presence of LPS was confirmed and used for further experiments.

## 6.3 CHIR-090 & LpxC methods

### 6.3.1 Bacterial strains and growth conditions

To determine the sensitivity of members of the Bcc to CHIR-090, using the disc diffusion assay, a panel of relevant strains was assembled against which CHIR-090 was tested (Tabl 2.1). This panel included the Bcc experimental strain panel [35, 38], together with *B. cenocepacia* SAL1 [183], *P. aeruginosa* PAO1, and *E. coli* K12 MG1655.

For MIC determination of CHIR-090 against *B. multivorans*, the selected panel of species consisted of the eight *B. multivorans* strains of the experimental strain panel [38, 35]. As positive control strains *E. coli* ATCC25922, *P. aeruginosa* ATCC27853, and *P. aeruginosa* ATCC10145 were used as suggested by the BSAC guidelines [184].

All strains were typically grown on nutrient agar, unless otherwise stated. Before doing disc diffusion tests and MIC determinations, the strains were recovered from storage (-80 $^o$C freezer) by growing them 3 times on fresh nutrient plates and allow them to grow at 37 $^o$C overnight. Prior to experiments, the identity of the Bcc strains was confirmed by *RecA*/ RFLP analysis (described above).

### 6.3.2 Antibiotic susceptibility testing of CHIR-090

#### Antibacterial disk diffusion tests

Single colonies of each organism were picked and grown overnight in 5 ml IS broth and sub-cultured (1/10) the next day in fresh IS broth. The strains were grown for an additional 2 hours at 37 $^{o}$C to mid-log phase and then diluted with saline (0.85% NaCl) to an $A_{600}$ of 0.1. This culture was spread on IS agar plates to provide a lawn of confluent growth. The remaining liquid was suctioned of the plates and the plates were allowed to dry for 1 hour at room temperature. Then, the discs, containing CHIR-090, were placed on top of the agar.
CHIR-090 was dissolved in dimethyl sulfoxide (DMSO), and six stock solutions were prepared (0-, 0.25-, 1.25-, 2.5-, 5-, and 10 mg/ml CHIR-090). Six sterile Whatmann filter paper disks were dotted with 0-, 1-, 5-, 10-, 20-, or 40 $\mu$g CHIR-090 by adding 4$\mu$L of the correct stock solution. After dotting, the filter disks were directly placed on top of the agar plates. The plates were incubated for 18 hours at 37 $^{o}$C and the diameters of the inhibition zones were measured.

#### MIC determination

MIC data was generated for all *B. multivorans* strains of the Bcc reference panel as described in the BSAC guidelines [184]. Single colonies of the strains were picked and grown overnight in 10 ml nutrient broth + 0.5% yeast extract. The next day, cultures were diluted 1/10 in fresh broth and grown for an additional 2 hours at 37 $^{o}$C to mid-log phase. All strains were diluted 1/10 in saline (0.85% NaCl). Those dilutions were used in conjunction with a multipoint inoculator (Denley) to spot $\sim 10^4$ colony forming units (cfu) onto the CHIR-090 containing ISTA plates. Due to the limited amount of CHIR-090 available, plates were poured with 10 ml ISTA, instead of the standard 20 ml volume. The plates containing different concentrations of CHIR-090 ranging from 0 to 100 $\mu$g/ml (0-, 0.006-, 0.0125-,

0.025-, 0.05-, 0.1-, 0.2-, 0.4-, 0.8-, 1.6-, 3.2-, 6.4-, 12.5-, 25-, 50-, 100 $\mu$g/ml), were inoculated, allowed to dry, and incubated at 37 $^{o}$C for 18 hours. MICs were calculated as the lowest concentration of antibiotic where no growth could be observed.

### 6.3.3 *LpxC*$_2$: genome analysis and genetic modification

#### *LpxC*$_2$ presence check in the Bcc genomes

All Bcc strains within the Bcc reference panel were checked for the presence of the *LpxC*$_2$ gene in the genome. DNA was isolated of all Bcc strains using the alkaline lysis extraction method described in section 5.2.2. A DNA sequence alignment was made with all the *LpxC*$_2$ gene sequences available in the *Burkholderia* database (www.burkholderia.com) at the time these studies were performed, also including LpxC$_2$ genes of *Burkholderia* species that do not belong to the Bcc. PCR primers were designed on high homology regions of the genes (Table 6.4), amplifying a 321 bp fragment. Furthermore, it was confirmed that the primer sequences were specific (low sequence homology to other regions in the genome).

Table 6.4: Primers amplifying a 321 bp fragment of *LpxC*$_2$.

| **Primer** | **Sequence 5′ to 3′** |
|---|---|
| *LpxC*$_2$_FW | TTCGGCGASATGCACTGGGA |
| *LpxC*$_2$_Rev | CCGGAAYTTCATRTCGTGGCT |

Samples were prepared as follows: 1 puReTaq Ready-To-Go beads (GE Healthcare), 1 $\mu$l forward primer, 1 $\mu$l reverse primer, 3 $\mu$l total genomic DNA, and 20 $\mu$l $H_2O$. The reactions were initiated with a hot-start of 5 minutes at 95 $^{o}$C and cycled 40 times at 95 $^{o}$C for 30 seconds, 55 $^{o}$C for 30 seconds, and 72 $^{o}$C for 30 seconds.

### Inactivation of Bcc genes using (conditional) knock-out plasmids

Insertional inactivation of $LpxC_1$ and $LpxC_2$ in *B. cenocepacia* K56-2 was attempted using the suicide pGpΩTp plasmid, as described previously [190]. A ∼300 bp fragment inside of the target genes was amplified and cloned into the pGpΩTp plasmid. *E. coli* GT115 cells were transformed with the plasmid. The construct was introduced into *B. cenocepacia* K56-2 by tri-parental mating, using *E. coli* GT115 as the donor strain. Surviving colonies were verified by PCR using a forward primer at the beginning of the gene and the RSF1300 primer, which is specific for the plasmid. To note is that with this procedure no colonies were obtained with the correct insertion.

Conditional inactivation of $LpxC_2$ in *B. cenocepacia* K56-2 was attempted using the pSC200 plasmid, as described previously [98]. The first 300 bp of $LpxC_2$, starting at ATG, were cloned into the pSc200 plasmid (using the NdeI and XbaI restriction sites). *E. coli* GT115 cells were transformed with the plasmid. Transformed cells were streaked onto LB agar plates containing 0.2% glucose and trimethoprim. The construct was introduced into *B. cenocepacia* K56-2 by tri-parental mating, using *E. coli* GT115 as the donor strain, and LB plates containing 0.2% rhamnose. Surviving colonies were verified by PCR using a forward primer upstream of the site of insertion and the RSF1300 primer, which is specific for the plasmid. The conditional $LpxC_2$ mutant *B. cenocepacia* strain created was grown on LB containing 0.2% rhamnose, until the mutant was further explored. Then the mutant strain was streaked 3 times on LB agar containing 0.2% glucose (no rhamnose) to test for survival. Then, a disc diffusion assay was carried out with 40 $\mu$g CHIR-090 (as described above) using LB agar containing 0.2% glucose (no rhamnose).

### 6.3.4 $LpxC_1$ & $LpxC_2$: cloning and expression

DNA was isolated from *B. cenocepacia* J2315 using the alkaline lysis method descibed previously. The *LpxC*$_1$ gene (BCAL3455) was amplified with the primers listed in Table 6.5, using PCR (annealing temperature was 55 $^o$C). The cloning procedure as described in section 3.2.2 was followed. The *LpxC*$_1$ gene was cloned into the expression plasmid pET22b (using the NdeI and EcoRI restriction sites), giving pET22b_LpxC$_1$_J2315 (Figure 6.1). The construct contains an IPTG inducible promotor for controlled expression, and expresses LpxC$_1$ without a fusion tag.

Table 6.5: *LpxC*$_1$ amplification primers.

| **Primer** | **Sequence 5′ to 3′** |
|---|---|
| *LpxC*$_1$_FW | AATCAAGACGAAGAAGCATATGTTGAAGCA |
| *LpxC*$_1$_Rev | CTTTTTTTATCGCTCGAGCTGAACGCCGGTC |

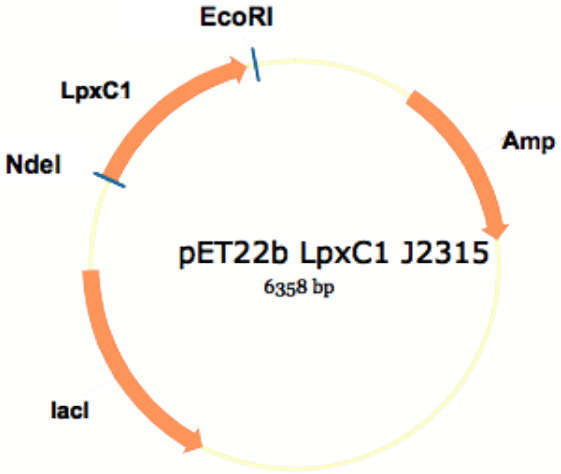


Figure 6.1: Plasmid map of pET22b_LpxC$_1$_J2315.

A synthetic gene (cloned into pUC57) encoding LpxC$_2$ was ordered from GenScript. The synthetic gene was cloned into the expression vector pET22b (using the NdeI and XhoI restriction sites), giving pET22b_LpxC$_2$_J2315 (Figure 6.2).

The plasmid contains an IPTG inducible promotor, and as for pET22b_LpxC$_1$_J2315, should express LpxC$_2$ without a fusion tag.

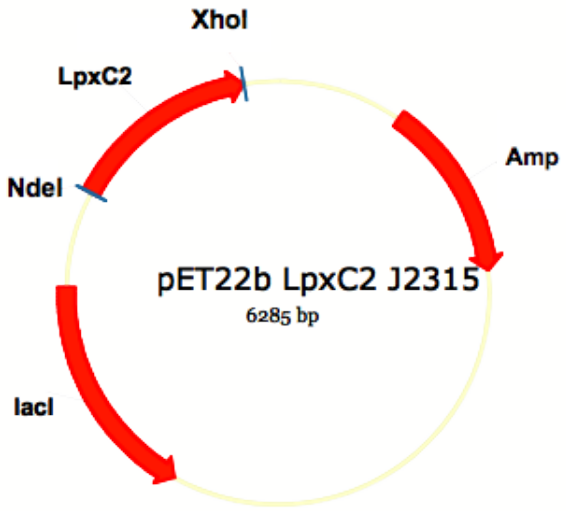


Figure 6.2: Plasmid map of pET22b_LpxC$_2$_J2315.

A small scale expression was carried out to confirm expression of the plasmids pET22b_LpxC$_1$_J2315 and pET22b_LpxC$_2$_J2315, as described in section 3.2.3. Protein expression was induced in *E. coli* HMS174 (DE3) and BL21 (DE3) cells. Different temperatures (e.g. 37 $^o$C, 30 $^o$C, and 18 $^o$C) and times (e.g. 3-,5-,18 hours) of expression were tested.

## 6.4 Cycloserine & ArnB methods

### 6.4.1 Antibiotic susceptibility and synergy testing of cycloserine

#### MIC determination

MIC data was generated for all Bcc strains within the Bcc reference panel [35, 38] as described in the BSAC guidelines [184]. The same procedure was followed as

described in section 5.3.2 for CHIR-090. The plates contained different concentrations of LCS (Sigma Aldrich) or DCS (Duchefa Biochemie) ranging from 0 to 128 $\mu$g/ml (0-, 0.06-, 0.125-, 0.25-, 0.5-, 1-, 2-, 4-, 8-, 16-, 32-, 64-, 128 $\mu$g/ml) for LCS and from 0 to 1000 $\mu$g/ml (0-, 0.06-, 0.125-, 0.25-, 0.5-, 1-, 2-, 4-, 8-, 16-, 32-, 64-, 128-, 250-, 500-, 1000 $\mu$g/ml), were inoculated, allowed to dry, and incubated at 37 $^o$C for 18 hours.

**MBC determination**

MBCs were determined for a selection of strains, including: three *B. multivorans* strains (C5393, C1575 and ATCC17616), three *B. cenocepacia* strains (J2315, K56-2 and ATCC17765) and the two control strains *E. coli* ATCC25922 and *P. aeruginosa* ATCC10145. Single colonies of the strains were picked and grown overnight in 10 ml nutrient broth + 0.5% yeast extract. The next day, cultures were diluted 1/10 in fresh broth and grown for an additional 2 hours at 37 $^o$C to mid-log phase. Serial dilutions of DCS were made (ranging from 0 to 500 $\mu$g/ml final concentration; 0-, 2-, 4-, 8-, 16-, 32-, 64-, 128-, 250-, 500 $\mu$g/ml) in 0.9 ml of IS broth in WR tubes. The mid-log phase cultures were diluted 1/100 cells/ml and 100 $\mu$L was added to each dilution of antibiotic. The broths were incubated overnight at 37 $^o$C without agitation. The next day, 50 $\mu$L of the first (MIC concentration) and second serial dilution where no growth could be observed was plated onto a nutrient agar plate (without antibiotics) and grown at 37 $^o$C overnight. When no growth could be observed the following day DCS was called bactericidal and when a confluent lane of growth could be observed DCS was called bacteriostatic. MBCs were determined as the lowest concentration of DCS were no growth could be recovered.

### 6.4.2 DCS synergy studies

For synergy studies a selection of Bcc strains was used; three *B. multivorans* strains LMG13010, C1576 and ATCC17616; three *B. cenocepacia* strains K56-2, Sal-1 and J2315; *B. dolosa* AU0645; two control strains P. aeruginosa ATCC10145 and E. coli ATCC25922. Synergy studies of DCS (100 $\mu$g) were performed with chloramphenicol (30 $\mu$g), trimethoprim (5 $\mu$g), tobramycin (10 $\mu$g), meropenem (10 $\mu$g), minocycline (30 $\mu$g), ceftazidime (30 $\mu$g) and ciprofloxacin (5 $\mu$g). A disc diffusion test (as described for CHIR-090) was done with single antibiotic discs on IS agar. The radius of the killing zones was measured of the individual antibiotics. When no zone of inhibition was observed for one of the strains, the strain was excluded for that particular antibiotic in the next step. Then, a double disc diffusion test was carried out. One filter disc was impregnated with DCS and the other with one of the above-mentioned antibiotics. The two discs were placed together on the agar plates at a distance that equaled the sum of the radii of the two individual antibiotics. The plates were incubated for 18 hours at 37 $^{o}$C and the zones of inhibition were examined.

### 6.4.3 Expression and purification of ArnB-His6

The plasmid pET22b_ArnB_J2315 (Figure 6.3) was created by Thomas Varques (PhD student Campopiano lab). It contains an IPTG inducible promotor for controlled expression, and expresses ArnB with a C-terminal His6 fusion tag. To express ArnB-His6, *E. coli BL21* (DE3) was transformed with pET22b_ArnB_J2315 and a large scale grow (see section 1.2.3) was carried out. Expression of ArnB was induced for 5 hours by adding 0.5 mM IPTG. The cell pellet was resuspended in Buffer A (20 mM Kphos, 150 mM NaCl and 25 $\mu$M PLP) containing 100 $\mu$g/ml lysozyme and a protease inhibitor tablet (Roche diagnostic, GmbH complete EDTA free). The cells were disrupted by sonication and unbroken cells

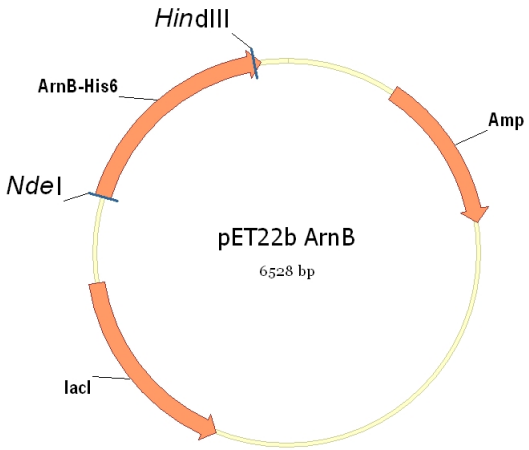


Figure 6.3: Plasmid map of pET22b_ArnB_J2315.

and cell debris were removed by centrifugation at 12,000 g for 30 minutes. The soluble lysate was applied to a 1 ml polypropylene column loaded with 1 ml Ni-NTA Superflow resin (Qiagen) that had been pre-equilibrated with Buffer A containing 20 mM imidazole. After loading the column it was washed with 100 column volumes (cv) of Buffer A containing 20 mM imidazole. ArnB-His6 was eluted off in 20 cv Buffer A containing 200 mM imidazole. The eluate was concentrated to a volume of ∼1 ml using a 30.000 Da MWCO vivaspin column (Sartorius Stedim Biotech). ArnB-His6 was further purified by size exclusion chromatography using a calibrated HiPrep 26/60 Sephacryl S-200 column (GE Healthcare). The column was equilibrated with 1 cv Buffer A, the protein was loaded onto the column, and 1 cv of Buffer A was run through at 1 ml/min. 10 ml fractions were collected and analysed by SDS-PAGE. Fractions containing pure ArnB were pooled and stored at -80 $^{o}$C in Buffer A containing 20% glycerol.

The molecular mass of ArnB-His6 estimated from the S-200 column elution volume and the molecular mass was confirmed by MALDI-TOF analysis.

### 6.4.4 ArnB-His6 activity and inhibition assay

Prior to the assays, ArnB-His6 was defrosted and dialysed overnight in Buffer A containing an excess of PLP (e.g 100 $\mu$M). Dialysis buffer was refreshed three times. To remove the unbound PLP, the dialysed sample was concentrated to a volume of 1.5 ml and loaded on a PD-10 column (GE-Healthcare), that was pre-equilibrated with Buffer A. ArnB-His6 was eluted of the column with 5 ml Buffer A. The protein concentration was determined by taking the absorbency in an Cary 50 UV visible photospectrometer (Varian) at 280 nm. All assays were carried out in a final volume of 500 $\mu$L Buffer A containing 14 $\mu$M ArnB-His6, in a UV visible photospectrometer at 25 $^{o}$C measuring between a wavelength of 200 and 800 nm, using a quartz cuvette. Spectra were analysed using Cary WinUV software (Varian), and graphs were generated using Sigma Plot software.
The reversibility of the (inhibition) reactions was tested by dialysis. 2 ml of completed reaction mixture (E-PLP) was dialysed overnight against 250 ml Buffer A containing 100 $\mu$M fresh PLP. Than the protein was loaded on a PD-10 column to remove unbound PLP. The protein was eluted in 5 ml Buffer A and concentrated to the required protein concentration for the assays. Then, a new reaction with L-glutamate was carried out as described below.

#### ArnB-His6 and L-glutamate

A scan was taken of the holo-enzyme (E-PMP) before the start of the assay. Reactions were initiated by the addition of 500 $\mu$M L-glutamate. Scans were taken every six seconds till no change in absorbance spectra was observed.

#### ArnB-His6 inhibition by CS

A scan was taken before the reaction (showing the holo-enzyme). Reactions were initiated with 1 mM DCS or 1 mM LCS. Scans were taken every minute till the

reaction completed. After completion of the reaction, two additional experiment were performed: 1) When there was no change in spectra observed anymore, 500 $\mu$M L-glutamate was added to the completed reaction mixture to check for any change in spectra (activity); 2) The reversibility of DCS and LCS inhibition was tested as described above.

**ArnB-His6 inhibition by $\beta$CDA**

A scan was taken before the initiation of the reaction. The reactions were initiated by the addition of 500 $\mu$M, 1 mM, or 2 mM $\beta$CDA. Scans were taken every minute till no change in spectra could be observed. To test if $\beta$CDA was inhibiting the enzyme or was used as a substrate by the enzyme, we scanned for the release of pyruvate in the reaction mixture. After completion of the reaction, a scan was taken at 340 nm, 150 $\mu$M NADH was added to the reaction mixture and the expected increase of absorbance was confirmed at 340 nm. Then, 0.4 U/ml LDH was added to the reaction mixture and the decrease in absorbance at 340 nm was measured over time. As controls for this experiment, NADH and LDH were added in the same concentrations to Buffer A containing 2 mM $\beta$CDA or buffer A containing 14 $\mu$M ArnB-His6 and the absorbance at 340 nM was measured over time.

**ArnB-His6 inhibition by L-PPG**

A scan was taken before the initiation of the reaction. The reactions were initiated by the addition of 500 $\mu$M L-PPG. Scans were taken after 10 minutes, 1 hour, 5 hours, and 24 hours. When there was no change in spectra observed anymore, 500 $\mu$M L-glutamate was added to the completed reaction mixture to check for any change in spectra (activity), and the reversibility was tested by dialysis against fresh PLP, as described above.

## 6.5 LptA &LptB methods

### 6.5.1 Cloning, expressing and purification of LptA

Plasmid pET22b_LptA_J2315 (Figure 6.4) expresses LptA of *B. cenocepacia* J2315 with a C-terminal His6 tag upon IPTG induction. pET22b_LptA_J2315 was constructed by PCR amplifying the LptA open reading frame (BCAL0815) from genomic DNA with primers $\text{LptA}_{FW1}$ and $\text{LptA}_{REV1}$ (Table 6.6). *LptA* was cloned into pET22b using the NdeI-XhoI restriction sites. A large scale ex-

Table 6.6: *LptA* amplification primers.

| **Primer** | **Sequence 5′ to 3′** |
|---|---|
| *LptA*_FW | GACCATATGAACGAACCGTTCCCTCGACAG |
| *LptA*_Rev | GGCGGTTCGGAAGCGCTCGAGTTGGCCCGG |

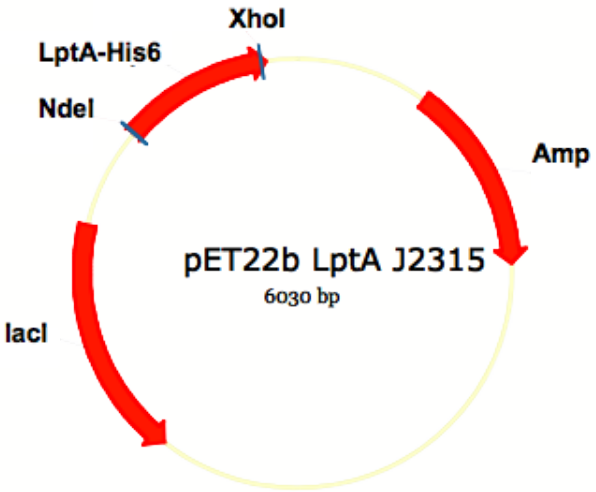


Figure 6.4: Plasmid map of pET22b_LptA_J2315.

pression was carried out using *E. coli* HMS174 (DE3) cells carrying the plasmid pET22b_LptA_J2315 in TB, containing 5 times the recommended amount of glycerol. The cells were induced for 1-1.5 hours with 0.1 mM IPTG at 37 $^{o}$C. The cells were harvested by centrifugation and stored at -20 $^{o}$C until purification.

All the following steps were performed at 0-4 $^{o}$C. The pellet was resuspended into Buffer B (20 mM $Na_2HPO_4$ (pH 7.5), 300 mM NaCl) containing a protease inhibitor tablet (Roche) and 20 mM imidazole, and the cells were disrupted by sonication. Unbroken cells and cellular debris was removed by centrifugation. LptA-His6 was purified with nickel affinity chromatography by adding 1 ml Ni-NTA raisin to the supernatant and was gently mixed for 1 hour. The protein bound Ni:NTA beads were loaded into a 1 ml polypropylene column using a periplastic pump. The raisin was washed with 30 cv Buffe  B containing 20 mM imidazole and the protein was eluted in 15 cv 250 mM imidazole containing Buffer B. The elution fraction was dialysed against Buffer C (25 mM HEPES (pH 7.5, 150 mM NaCl) and LptA-His6 was further purified by size exclusion chromatography using a calibrated HR 26/60 Sephacryl S-300 column (GE Healthcare). The column was equilibrated with 1 cv Buffer C, the protein was loaded onto the column, and 1 cv of Buffer C was run through at 1 ml/min. 10 ml fractions were collected and analysed by SDS-PAGE. Fractions containing LptA-His6 were pooled and used for further studies. The oligomerisation status of LptA-His6 was estimated from the S-300 column elution volume and the molecular mass was confirmed by MALDI-TOF analysis.

### 6.5.2 LptA: LPS binding assays

The LPS used in this study was prepared in the following way: Smooth LPS of *E. coli* AY103 was isolated using the tri-reagent method, as described in section 5.2.4. Rough LPS of *B. cenocepacia* J2315 was isolated using the the hot water-phenol mehod. Deep-rough LPS of *B. cenocepacia* Sal-1was isolated using either the tri-reagent or hot water-phenol mehod. *E. coli* $Kdo_2$-lipid A was purchased from Avanti Polar Lipids.

The *in vitro* LPS binding assay was carried out in a similar fashion as described previously [171] with some modifications. Purified LPS (300 $\mu$g) or purchased

$Kdo_2$-lipid A (100 $\mu$g) was added to 500 $\mu$l Buffer C containing 0.5 mg/ml LptA-His6. The mixture was incubated at room temperature for 1 hour with agitation. Then, Ni-NTA raisin was added to the sample and was gently mixed for 10 minutes. The protein bound Ni:NTA beads were washed 5 times with 1 mL Buffer C to remove unbound LPS. Then, the protein and Ni:NTA beads were separated by adding 500 $\mu$l Buffer C containing 300 mM imidazole. The samples were analysed by SDS-PAGE followed by silverstaining (according to the protocol of the manufacturer, Sigma).

### 6.5.3 Cloning, expressing and purification of LptB

Plasmid pET22b_LptB_J2315 (Figure 6.5) expresses LptB of *B. cenocepacia* J2315 with a C-terminal His6 tag upon IPTG induction. pET22b_LptB_J2315 was constructed by PCR amplifying, using QIAGEN proofstart polymerase and TAQ bead extension, the LptB open reading frame (BCAL0814) from genomic DNA with primers $LptB_{FW1}$ and $LptB_{REV1}$ (Table 6.7). The PCR product was cloned into the recombinant protein expression plasmid pET22b, using the NdeI-HindIII restriction sites. *E. coli* BL21 carrying the plasmid pET22b_LptB_J2315 was

Table 6.7: *LptB* amplification primers.

| **Primer** | **Sequence 5′ to 3′** |
|---|---|
| *LptB*_FW | CCAGGGAGCGCCGGGCATATGAACGCGCTT |
| *LptB*_Rev | GCCACGAGGAGGAAGCTTCATGCGGAAGTG |

grown at 37 $^o$C in LB broth to an $A_{600}$ of 0.6-0.8. The cells were induced with 0.1 mM IPTG and grown for an additional 18 hours at 18 $^o$C. The cells were harvested by centrifugation and stored at -20 $^o$C until purification. The purification condition of the *E. coli* LptB-His6 protein were published recently [169], and the same strategy was adapted with some modifications. The LptB-His6 ex-

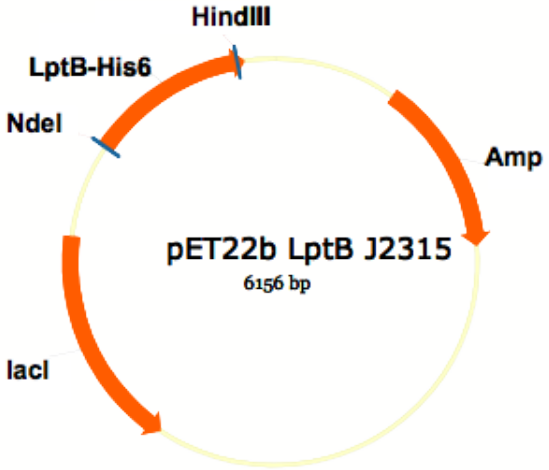


Figure 6.5: Plasmid map of pET22b_LptB_J2315.

pressing cells were resuspended in LptB lysis buffer (∼4 ml/ gram of cell paste). LptB buffer contained 50 mM HEPES buffer (pH 7.5), 10% glycerol, 150 mM potassium chloride (KCl), 1mM dithiothreitol (DTT), 5 mM magnesium chloride (MgCl). For LptB lysis buffer, 1 mM phenylmethylsulphonyl (PMSF), 100 $\mu$g/ml lysozyme and 2 Units/ml DNAseI (Roche) was added.

The cells were incubated on ice for 30 minutes, followed by sonication. Cell debris was removed by centrifugation and the cell free extract was pressed through a 0.45 $\mu$M filter. A 1 ml polypropylene column was loaded with  ml Ni-NTA Superflow resin (Qiagen). The column was pre-washed with 10 cv LptB buffer, and equilibrated with 10 cv LptB buffer plus 20 mM imidazole. The cell free extract was passed through the column at 0.75 ml/min using a periplastic pump. The column was washed at 1.5 ml/min with 100 cv of LptB buffer containing 20 mM imidazole and the protein was eluted at 0.75 ml/min with 15 cv LptB buffer plus 300 mM imidazole. The eluate was dialysed against LptB buffer for 2 hours to remove the imidazole, and concentrated to a volume of ∼1 ml using a 10,000 Da MWCO vivaspin column (Sartorius Stedim Biotech).

The protein was further purified using the calibrated Superdex 75, 16-60 HR, a size exclusion chromatography column (GE Healthcare). The column was equilibrated with 1 cv (120 ml) LptB buffer. The protein was loaded onto the column

after which 1 cv at a flow rate 1 ml/min of LptB buffer ran through the column to elute the protein. Fractions of 5 ml were collected and analysed by SDS-PAGE.

### 6.5.4 LptB-His6 activity, kinetic analysis and inhibition

#### LptB-His6 activity assay

The LptB-His6 enzyme was assayed using a coupled, three enzyme system, with LptB-His6, pyruvate kinase, and lactate dehydrogenase. The conditions described for *E. coli* LptB [169] were adapted with slight modifications. The LptB-His6 reaction mixture consisted off (final concentrations): 100 mM HEPES, 10% glycerol, 150 mM KCl, 5 mM MgCl, 1 mM DTT, 10 $\mu$M LptB (based on absorbance at 280 nm), 3.31 U/ml pyruvate kinase (PK), 4.03 U/ml lactate dehydrogenase (LDH), 0.25 mg/ml BSA, 4 mM phospo(enol) pyruvic acid (PEP) and 0.3 mM NADH. The assays were carried out in a UV visible photospectrometer (Varian) at 25 $^{o}$C measuring at a wavelength of 340 nm. For the assay 400 $\mu$L of reaction mixture was used per reaction, using 500 $\mu$L quartz cuvettes. Reactions were initiated by the addition of ATP (50 $\mu$L) in the reaction cuvette. The decrease in NADH absorbance at 340 nm was measured over time, which is proportional to the amount of ATP hydrolyzed. All assays were carried out in triplo, and as a control the mixture was measured without the addition of ATP.

#### Kinetic analysis of LptB-6His

Using the LptB-His6 activity assay conditions as described above, the LptB-His6 kinetics were determined by altering the final ATP concentrations (8 mM, 4 mM, 3 mM, 2 mM, 1.5 mM, 1 mM, 750 $\mu$M, 500 $\mu$M, 375 $\mu$M, 250 $\mu$M, 125 $\mu$M, 62.5 $\mu$M, 31.25 $\mu$M, and 0 (blank)). The initial rate of reaction (-slope) was

calculated from a linear portion of the plot, using kinetics software (Varian). The extinction coefficient of NADH at 340 nm is $\varepsilon = 6220\ M^{-1}\ cm^{-1}$ in a 1 cm path quartz cuvette. Sigma-plot software was used to fit the data by non-linear regression.

The Hill-coefficient, which is useful to characterise the cooperative behavior of oligomeric enzymes, can be calculated using the following formula:

$$Y_s = \frac{[S]^n}{K + [S]^n} \tag{6.1}$$

Were $n$= Hill constant, K= the dissociation constant, [S]= the free (unbound) substrate concentration, and $Y_s$= fraction of occupied sites where the substrate can bind. The quantity of $n$ increases with the degree of cooperativity. When n= 1, the substrate-binding reaction is non-cooperative. If n= <1, the substrate-binding reaction is negative-cooperative. And in case n= >1 the, he substrate-binding reaction is positively-cooperative, indicating that the enzyme acts as a dimer. The Hill coefficient can also be graphically determined (Sigma Plot software) by rearranging equation 6.1 to equation 6.2.

$$\log\left(\frac{Y_s}{1 - Y_s}\right) = n \log[S] - \log K \tag{6.2}$$

**LptB-His6 inhibition studies**

Inhibition studies of LptB-6His were performed under the conditions as described above. The final ATP concentrations used to measure inhibition were 2 mM, 1 mM and 0.5 mM respectively.

**Sodium orthovanadate:** The final concentrations of sodium orthovanadate (Sigma) in the reaction mixture were adapted from published data on *E. coli*

LptB [168]. Concentrations tested were 8 mM, 4 mM, 2 mM, 1 mM, 0.5 mM, 0.25 mM, and 0.12 mM, with pre-incubation times of inhibitor and enzyme (reaction mixture without ATP) ranging from 0 to 60 minutes at 25 $^{o}$C. The initial rate of reaction was compared with and without inhibitor.

**Inhibitor 2:** Inhibitor 2 (5-[1-[5-(4-Fluoro-2-hydroxy-phenyl)-furan-2-yl]-meth-(Z)-ylidene]-thiazolidine-2,4-dione) was purchased from Axon MedChem. The final concentrations of inhibitor tested in the reaction mixture was adapted from published data on *E. coli* LptB-His6 [169]. Concentrations tested were 22 $\mu$M, 18 $\mu$M, 12 $\mu$M, 6 $\mu$M, 3 $\mu$M, and 1 $\mu$M, with pre-incubation times of inhibitor and enzyme (reaction mixture without ATP) ranging from 0 to 120 minutes at 25 $^{o}$C. The initial rate of reaction was compared with and without inhibitor.

**LptB-6His activity stimulation by its "substrate"**

The ATP-ase activity of LptB-6His was measured in the presence and absence of purchased $Kdo_2$-lipid A, isolated LPS from the two *B. cenocepacia* strains, J2315 and SAL-1, and the two mutated *E. coli* strains AY103 (ArnT knock out) and MST100 (pmrA overexpressing) [152]. Concentrations tested were 20 $\mu$g/ml, 2 $\mu$g/ml, 200 ng/ml, 20 ng/ml, and 2 ng/ml. The initial rate of reaction was compared within and without the presence of LPS.

# Bibliography


[1] Andersen, D. H. *Am J Dis Child* **1938,** *56,* 344-399.

[2] Darling, R. C.; di Sant'Agnese, P. A. *Am. J. M. Sc.* **1953,** *225,*.

[3] Davis, P. B.; di Sant'Agnese, P. A. *Chest* **1984,** *85,* 802-809.

[4] Shwachman, H.; Leubner, H.; Catzel, P. *Adv Pediatr* **1955,** *7,* 249–323.

[5] Gibson, L. E.; Cooke, R. E. *Pediatrics* **1959,** *23,* 545–549.

[6] Kerem, B.; Rommens, J. M.; Buchanan, J. A.; Markiewicz, D.; Cox, T. K.; Chakravarti, A.; Buchwald, M.; Tsui, L. C. *Science* **1989,** *8,* 1073-80.

[7] Riordan, J. R.; Rommens, J. M.; Kerem, B.; Alon, N.; Rozmahel, R.; Grzelczak, Z.; Zielenski, J.; Lok, S.; Plavsic, N.; Chou, J. L.; Drumm, M. L.; Lannuzzi, M. C.; Collins, F. S.; Tsui, L. C. *Science* **1989,** *8,* 1066-73.

[8] Rommens, J. M.; Lannuzzi, M. C.; Kerem, B.; Drumm, M. L.; Melmer, G.; Dean, M.; Rozmahel, R.; Cole, J. L.; Kennedy, D.; Hikada, N.; Zsiga, M.; Buchwald, M.; Riordan, J. R.; Tsui, L. C. *Science* **1989,** *8,* 1059-1065.

[9] "Cystic Fibrosis Mutation Database", http://www.genet.sickkids.on.ca/cftr/app, 2010.

[10] Bear, C. E.; Li, C.; Kartner, N.; Bridges, R. J.; Jensen, T. J.; Ramjeesingh, M.; Riordan, J. R. *Cell* **1992,** *68,* 809-818.

[11] Gadsby, D. C.; Vergani, P.; Csanady, L. *Nature* **2006,** *23,* 477-483.

[12] Govan, J. R.; Hughes, J. E.; Vandamme, P. *J Med Microbiol* **1996,** *45,* 395–407.

[13] Miller, M.; Gilligan, P. *J. Clin. Microbiol* **2003,** *41,* 4009-4015.

[14] Hutchison, M. L.; Govan, J. R. *Microbes Infect* **1999,** *1,* 1005–1014.

[15] Foweraker, J. *Br. Med. bull* **2009,** *89,* 93-110.

[16] Mahenthiralingam, E.; Urban, T. A.; Goldberg, J. B. *Nat Rev Microbiol* **2005,** *3,* 144–156.

[17] Chiarini, L.; Bevivino, A.; Dalmastri, C.; Tabacchioni, S.; Visca, P. *Trends Microbiol* **2006,** *14,* 277–286.

[18] Corral, D. M.; Coates, A. L.; Yau, Y. C. W.; Tellier, R.; Glass, M.; Jones, S. M.; Waters, V. J. *Can Respir J* **2008,** *15,* 237–239.

[19] Barth, A. L.; de Abreu E Silva, F. A.; Hoffmann, A.; Vieira, M. I.; Zavascki, A. P.; Ferreira, A. G.; da Cunha, L. G. J.; Albano, R. M.; de Andrade Marques, E. *J Clin Microbiol* **2007,** *45,* 4077–4080.

[20] Asiah, K.; Hanifah, Y. A.; Norzila, M. Z.; Hasniah, L.; Rusanida, A. *J Paediatr Child Health* **2006,** *42,* 217–218.

[21] Holland, D. J.; Wesley, A.; Drinkovic, D.; Currie, B. J. *Clin Infect Dis* **2002,** *35,* e138-40.

[22] Miralles, I. S.; Maciel, M. d. C. A.; Angelo, M. R. F.; Gondini, M. M.; Frota, L. H. F.; dos Reis, C. M. F.; Hofer, E. *Rev Inst Med Trop Sao Paulo* **2004,** *46,* 51–54.

[23] O'Carroll, M. R.; Kidd, T. J.; Coulter, C.; Smith, H. V.; Rose, B. R.; Harbour, C.; Bell, S. C. *Thorax* **2003,** *58,* 1087–1091.

[24] Cheng, A. C.; Currie, B. J. *Clin Microbiol Rev* **2005,** *18,* 383–416.

[25] Isles, A.; Maclusky, I.; Corey, M.; Gold, R.; Prober, C.; Fleming, P.; Levison, H. *J Pediatr* **1984,** *104,* 206–210.

[26] Govan, J. R.; Brown, P. H.; Maddison, J.; Doherty, C. J.; Nelson, J. W.; Dodd, M.; Greening, A. P.; Webb, A. K. *Lancet* **1993,** *342,* 15–19.

[27] LiPuma, J. J.; Dasen, S. E.; Nielson, D. W.; Stern, R. C.; Stull, T. L. *Lancet* **1990,** *336,* 1094–1096.

[28] De Soyza, A.; Silipo, A.; Lanzetta, R.; Govan, J. R.; Molinaro, A. *Innate Immun* **2008,** *14,* 127–144.

[29] Davis, P. B. *AJRCCM* **2006,** *173,* 475-482.

[30] Grimwood, K.; Kidd, T. J.; Tweed, M. *J Cyst Fibros* **2009,** *8,* 291–293.

[31] Burkholder, W. H. *Phytopathology* **1950,** *40,* 115-117.

[32] Yabuuchi, E.; Kosako, Y.; Oyaizu, H.; Yano, I.; Hotta, H.; Hashimoto, Y.; Ezaki, T.; Arakawa, M. *Microbiol Immunol* **1992,** *36,* 1251–1275.

[33] Baldwin, A.; Mahenthiralingam, E.; Thickett, K. M.; Honeybourne, D.; Maiden, M. C. J.; Govan, J. R.; Speert, D. P.; Lipuma, J. J.; Vandamme, P.; Dowson, C. G. *J Clin Microbiol* **2005,** *43,* 4665–4673.

[34] Coenye, T.; Vandamme, P.; Govan, J. R.; Lipuma, J. J. *J Clin Microbiol* **2001,** *39,* 3427-36.

[35] Coenye, T.; Vandamme, P.; LiPuma, J. J.; Govan, J. R. W.; Mahenthiralingam, E. *J Clin Microbiol* **2003,** *41,* 2797–2798.

[36] Vandamme, P.; Holmes, B.; Vancanneyt, M.; Coenye, T.; Hoste, B.; Coopman, R.; Revets, H.; Lauwers, S.; Gillis, M.; Kersters, K.; Govan, J. R. *Int. J. Syst. Bacteriol* **1997,** *47,* 1188-200.

[37] Vanlaere, E.; Lipuma, J. J.; Baldwin, A.; Henry, D.; Brandt, E. D.; Mahenthiralingam, E.; Speert, D.; Dowson, C.; Vandamme, P. *Evol Microbiol* **2008,** *58,* 1580-90.

[38] Mahenthiralingam, E.; Coenye, T.; Chung, J. W.; Speert, D. P.; Govan, J. R.; Taylor, P.; Vandamme, P. *J Clin Microbiol* **2000,** *38,* 910-913.

[39] McArthur, J.; Kovacic, D.; Smith, M. *Proc Natl Acad Sci U S A* **1988,** *85,* 9621–9624.

[40] Falkiner, F. R. *J Antimicrob Chemother* **1998,** *41,* 429–431.

[41] Burns, J. L.; Jonas, M.; Chi, E. Y.; Clark, D. K.; Berger, A.; Griffith, A. *Infect Immun* **1996,** *64,* 4054–4059.

[42] Perotto, S.; Bonfante, P. *Trends Microbiol* **1997,** *5,* 496–501.

[43] Lamothe, J.; Thyssen, S.; Valvano, M. A. *Cell Microbiol* **2004,** *6,* 1127–1138.

[44] Saini, L. S.; Galsworthy, S. B.; John, M. A.; Valvano, M. A. *Microbiology* **1999,** *145 ( Pt 12),* 3465–3475.

[45] Saldias, M. S.; Valvano, M. A. *Microbiology* **2009,** *155,* 2809–2817.

[46] Keith, K. E.; Killip, L.; He, P.; Moran, G. R.; Valvano, M. A. *J Bacteriol* **2007,** *189,* 9057–9065.

[47] Stanier, R. Y.; Palleroni, N. J.; Doudoroff, M. *J Gen Microbiol* **1966,** *43,* 159–271.

[48] Lessie, T. G.; Hendrickson, W.; Manning, B. D.; Devereux, R. *FEMS Microbiol Lett* **1996,** *144,* 117–128.

[49] O'Sullivan, L. A.; Mahenthiralingam, E. *Lett Appl Microbiol* **2005,** *41,* 8–11.

[50] Mahenthiralingam, E.; Baldwin, A.; Dowson, C. G. *J Appl Microbiol* **2008,** *104,* 1539–1551.

[51] Koenig, D. W.; Pierson, D. L. *Water Sci Technol* **1997,** *35,* 59–64.

[52] Beckman, W.; Lessie, T. G. *J Bacteriol* **1979,** *140,* 1126–1128.

[53] Berg, G.; Eberl, L.; Hartmann, A. *Environ Microbiol* **2005,** *7,* 1673–1685.

[54] Mahenthiralingam, E. Unpublished data.

[55] Govan, J. R.; Vandamme, P. *Microbiology* **1998,** *144 ( Pt 9),* 2373–2375.

[56] Parke, J. L.; Gurian-Sherman, D. *Annu Rev Phytopathol* **2001,** *39,* 225–258.

[57] LiPuma, J. J.; Spilker, T.; Coenye, T.; Gonzalez, C. F. *Lancet* **2002,** *359,* 2002–2003.

[58] McDowell, A.; Mahenthiralingam, E.; Moore, J. E.; Dunbar, K. E.; Webb, A. K.; Dodd, M. E.; Martin, S. L.; Millar, B. C.; Scott, C. J.; Crowe, M.; Elborn, J. S. *J Clin Microbiol* **2001,** *39,* 4247–4255.

[59] Govan, J. R. W.; Brown, A. R.; Jones, A. M. *Future Microbiol* **2007,** *2,* 153–164.

[60] Whiteford, M. L.; Wilkinson, J. D.; McColl, J. H.; Conlon, F. M.; Michie, J. R.; Evans, T. J.; Paton, J. Y. *Thorax* **1995,** *50,* 1194–1198.

[61] Speert, D. P.; Henry, D.; Vandamme, P.; Corey, M.; Mahenthiralingam, E. *Emerg Infect Dis* **2002,** *8,* 181–187.

[62] Johnson, W. M.; Tyler, S. D.; Rozee, K. R. *J Clin Microbiol* **1994,** *32,* 924–930.

[63] Darling, P.; Chan, M.; Cox, A. D.; Sokol, P. A. *Infect Immun* **1998,** *66,* 874–877.

[64] Vandamme, P.; Holmes, B.; Coenye, T.; Goris, J.; Mahenthiralingam, E.; LiPuma, J. J.; Govan, J. R. W. *Res Microbiol* **2003,** *154,* 91–96.

[65] Holden, M. T. G. *et al. J Bacteriol* **2009,** *191,* 261–277.

[66] Herasimenka, Y.; Benincasa, M.; Mattiuzzo, M.; Cescutti, P.; Gennaro, R.; Rizzo, R. *Peptides* **2005,** *26,* 1127–1132.

[67] Bartholdson, S. J.; Brown, A. R.; Mewburn, B. R.; Clarke, D. J.; Fry, S. C.; Campopiano, D. J.; Govan, J. R. W. *Microbiology* **2008,** *154,* 2513–2521.

[68] Baldwin, A.; Sokol, P. A.; Parkhill, J.; Mahenthiralingam, E. *Infect Immun* **2004,** *72,* 1537–1547.

[69] Mahenthiralingam, E.; Simpson, D. A.; Speert, D. P. *J Clin Microbiol* **1997,** *35,* 808–816.

[70] Peeters, E.; Nelis, H. J.; Coenye, T. *J Antimicrob Chemother* **2009,** *64,* 801–809.

[71] Park, B. S.; Song, D. H.; Kim, H. M.; Choi, B.-S.; Lee, H.; Lee, J.-O. *Nature* **2009,** *458,* 1191–1195.

[72] Miller, S. I.; Ernst, R. K.; Bader, M. W. *Nat Rev Microbiol* **2005,** *3,* 36–46.

[73] Shaw, D.; Poxton, I. R.; Govan, J. R. *FEMS Immunol Med Microbiol* **1995,** *11,* 99–106.

[74] Hughes, J. E.; Stewart, J.; Barclay, G. R.; Govan, J. R. *Infect Immun* **1997,** *65,* 4281–4287.

[75] Zughaier, S. M.; Ryley, H. C.; Jackson, S. K. *Infect Immun* **1999,** *67,* 1505–1507.

[76] De Soyza, A.; Ellis, C. D.; Khan, C. M. A.; Corris, P. A.; Demarco de Hormaeche, R. *Am J Respir Crit Care Med* **2004,** *170,* 70–77.

[77] Glauert, A. M.; Thornley, M. J. *Annu Rev Microbiol* **1969,** *23,* 159–198.

[78] Silhavy, T. J.; Kahne, D.; Walker, S. *Cold Spring Harb Perspect Biol* **2010,** *2,* a000414.

[79] Nikaido, H. *Microbiol Mol Biol Rev* **2003,** *67,* 593–656.

[80] Madigan, M. T.; Martinko, J. M. *Biology of microorganisms (Brock);* Pearson Education, Inc: Pearson Prentice Hall, Upper Saddle River, NJ07458, 11 ed.; 2006.

[81] Raetz, C. R. H.; Whitfield, C. *Annu Rev Biochem* **2002,** *71,* 635–700.

[82] Belunis, C. J.; Clementz, T.; Carty, S. M.; Raetz, C. R. *J Biol Chem* **1995,** *270,* 27646–27652.

[83] Meredith, T. C.; Aggarwal, P.; Mamat, U.; Lindner, B.; Woodard, R. W. *ACS Chem Biol* **2006,** *1,* 33–42.

[84] Trent, M. S. *Biochem Cell Biol* **2004,** *82,* 71–86.

[85] Raetz, C. R. H.; Reynolds, C. M.; Trent, M. S.; Bishop, R. E. *Annu Rev Biochem* **2007,** *76,* 295–329.

[86] Guo, L.; Lim, K. B.; Poduje, C. M.; Daniel, M.; Gunn, J. S.; Hackett, M.; Miller, S. I. *Cell* **1998,** *95,* 189–198.

[87] Trent, M. S.; Stead, C. M.; Tran, A. X.; Hankins, J. V. *J Endotoxin Res* **2006,** *12,* 205–223.

[88] Carty, S. M.; Sreekumar, K. R.; Raetz, C. R. *J Biol Chem* **1999,** *274,* 9677–9685.

[89] Groisman, E. A. *J Bacteriol* **2001,** *183,* 1835–1842.

[90] Ohl, M. E.; Miller, S. I. *Annu Rev Med* **2001,** *52,* 259–274.

[91] Hancock, R. E. *Lancet* **1997,** *349,* 418–422.

[92] Hancock, R. E.; Chapple, D. S. *Antimicrob Agents Chemother* **1999,** *43,* 1317–1323.

[93] Cox, A. D.; Wilkinson, S. G. *Mol Microbiol* **1991,** *5,* 641–646.

[94] Isshiki, Y.; Kawahara, K.; Zahringer, U. *Carbohydr Res* **1998,** *313,* 21–27.

[95] Gronow, S.; Noah, C.; Blumenthal, A.; Lindner, B.; Brade, H. *J Biol Chem* **2003,** *278,* 1647–1655.

[96] Silipo, A.; Molinaro, A.; Ierano, T.; De Soyza, A.; Sturiale, L.; Garozzo, D.; Aldridge, C.; Corris, P. A.; Khan, C. M. A.; Lanzetta, R.; Parrilli, M. *Chemistry* **2007,** *13,* 3501–3511.

[97] Silipo, A.; Molinaro, A.; Cescutti, P.; Bedini, E.; Rizzo, R.; Parrilli, M.; Lanzetta, R. *Glycobiology* **2005,** *15,* 561–570.

[98] Ortega, X. P.; Cardona, S. T.; Brown, A. R.; Loutet, S. A.; Flannagan, R. S.; Campopiano, D. J.; Govan, J. R. W.; Valvano, M. A. *J Bacteriol* **2007,** *189,* 3639–3644.

[99] Ierano, T.; Silipo, A.; Sturiale, L.; Garozzo, D.; Brookes, H.; Khan, C. M. A.; Bryant, C.; Gould, F. K.; Corris, P. A.; Lanzetta, R.; Parrilli, M.; De Soyza, A.; Molinaro, A. *Glycobiology* **2008,** *18,* 871–881.

[100] Vinogradov, E. V.; Bock, K.; Petersen, B. O.; Holst, O.; Brade, H. *Eur J Biochem* **1997,** *243,* 122–127.

[101] Vinogradov, E. V.; Muller-Loennies, S.; Petersen, B. O.; Meshkov, S.; Thomas-Oates, J. E.; Holst, O.; Brade, H. *Eur J Biochem* **1997,** *247,* 82–90.

[102] Vinogradov, E. V.; Lindner, B.; Kocharova, N. A.; Senchenkova, S. N.; Shashkov, A. S.; Knirel, Y. A.; Holst, O.; Gremyakova, T. A.; Shaikhutdinova, R. Z.; Anisimov, A. P. *Carbohydr Res* **2002,** *337,* 775–777.

[103] Coderch, N.; Pique, N.; Lindner, B.; Abitiu, N.; Merino, S.; Izquierdo, L.; Jimenez, N.; Tomas, J. M.; Holst, O.; Regue, M. *J Bacteriol* **2004,** *186,* 978–988.

[104] Molinaro, A.; De Castro, C.; Lanzetta, R.; Evidente, A.; Parrilli, M.; Holst, O. *J Biol Chem* **2002,** *277,* 10058–10063.

[105] Osborn, M. J.; Gander, J. E.; Parisi, E. *J Biol Chem* **1972,** *247,* 3973–3986.

[106] Ruiz, N.; Kahne, D.; Silhavy, T. J. *Nat Rev Microbiol* **2009,** *7,* 677–683.

[107] Rick, P. D.; Fung, L. W.; Ho, C.; Osborn, M. J. *J Biol Chem* **1977,** *252,* 4904–4912.

[108] Nishijima, M.; Raetz, C. R. *J Biol Chem* **1981,** *256,* 10690–10696.

[109] Raetz, C. R. H.; Guan, Z.; Ingram, B. O.; Six, D. A.; Song, F.; Wang, X.; Zhao, J. *J Lipid Res* **2009,** *50 Suppl,* S103-8.

[110] Anderson, M. S.; Raetz, C. R. *J Biol Chem* **1987,** *262,* 5159–5169.

[111] Odegaard, T. J.; Kaltashov, I. A.; Cotter, R. J.; Steeghs, L.; van der Ley, P.; Khan, S.; Maskell, D. J.; Raetz, C. R. *J Biol Chem* **1997,** *272,* 19688–19696.

[112] Wyckoff, T. J.; Lin, S.; Cotter, R. J.; Dotson, G. D.; Raetz, C. R. *J Biol Chem* **1998,** *273,* 32369–32372.

[113] Anderson, M. S.; Bull, H. G.; Galloway, S. M.; Kelly, T. M.; Mohan, S.; Radika, K.; Raetz, C. R. *J Biol Chem* **1993,** *268,* 19858–19865.

[114] Young, K.; Silver, L. L.; Bramhill, D.; Cameron, P.; Eveland, S. S.; Raetz, C. R.; Hyland, S. A.; Anderson, M. S. *J Biol Chem* **1995,** *270,* 30384–30391.

[115] Kelly, T. M.; Stachula, S. A.; Raetz, C. R.; Anderson, M. S. *J Biol Chem* **1993,** *268,* 19866–19874.

[116] Babinski, K. J.; Ribeiro, A. A.; Raetz, C. R. H. *J Biol Chem* **2002,** *277,* 25937–25946.

[117] Radika, K.; Raetz, C. R. *J Biol Chem* **1988,** *263,* 14859–14867.

[118] Garrett, T. A.; Kadrmas, J. L.; Raetz, C. R. *J Biol Chem* **1997,** *272,* 21855–21864.

[119] Clementz, T.; Raetz, C. R. *J Biol Chem* **1991,** *266,* 9687–9696.

[120] Brozek, K. A.; Hosaka, K.; Robertson, A. D.; Raetz, C. R. *J Biol Chem* **1989,** *264,* 6956–6966.

[121] Brabetz, W.; Muller-Loennies, S.; Brade, H. *J Biol Chem* **2000,** *275,* 34954–34962.

[122] Bode, C. E.; Brabetz, W.; Brade, H. *Eur J Biochem* **1998,** *254,* 404–412.

[123] Belunis, C. J.; Mdluli, K. E.; Raetz, C. R.; Nano, F. E. *J Biol Chem* **1992,** *267,* 18702–18707.

[124] Brabetz, W.; Lindner, B.; Brade, H. *Eur J Biochem* **2000,** *267,* 5458–5465.

[125] Clementz, T.; Bednarski, J. J.; Raetz, C. R. *J Biol Chem* **1996,** *271,* 12095–12102.

[126] Clementz, T.; Zhou, Z.; Raetz, C. R. *J Biol Chem* **1997,** *272,* 10353–10360.

[127] Mohan, S.; Raetz, C. R. *J Bacteriol* **1994,** *176,* 6944–6951.

[128] Onishi, H. R.; Pelak, B. A.; Gerckens, L. S.; Silver, L. L.; Kahan, F. M.; Chen, M. H.; Patchett, A. A.; Galloway, S. M.; Hyland, S. A.; Anderson, M. S.; Raetz, C. R. *Science* **1996,** *274,* 980–982.

[129] Jackman, J. E.; Raetz, C. R.; Fierke, C. A. *Biochemistry* **1999,** *38,* 1902–1911.

[130] Jackman, J. E.; Raetz, C. R.; Fierke, C. A. *Biochemistry* **2001,** *40,* 514–523.

[131] Hernick, M.; Gattis, S. G.; Penner-Hahn, J. E.; Fierke, C. A. *Biochemistry* **2010,** *49,* 2246–2255.

[132] Whittington, D. A.; Rusche, K. M.; Shin, H.; Fierke, C. A.; Christianson, D. W. *Proc Natl Acad Sci U S A* **2003,** *100,* 8146–8150.

[133] Buetow, L.; Dawson, A.; Hunter, W. N. *Acta Crystallogr Sect F Struct Biol Cryst Commun* **2006,** *62,* 1082–1086.

[134] Gennadios, H. A.; Christianson, D. W. *Biochemistry* **2006,** *45,* 15216–15223.

[135] Barb, A. W.; Jiang, L.; Raetz, C. R. H.; Zhou, P. *Proc Natl Acad Sci U S A* **2007,** *104,* 18433–18438.

[136] Coggins, B. E.; Li, X.; McClerren, A. L.; Hindsgaul, O.; Raetz, C. R. H.; Zhou, P. *Nat Struct Biol* **2003,** *10,* 645–651.

[137] Mochalkin, I.; Knafels, J. D.; Lightle, S. *Protein Sci* **2008,** *17,* 450–457.

[138] McClerren, A. L.; Zhou, P.; Guan, Z.; Raetz, C. R. H.; Rudolph, J. *Biochemistry* **2005,** *44,* 1106–1113.

[139] Hernick, M.; Gennadios, H. A.; Whittington, D. A.; Rusche, K. M.; Christianson, D. W.; Fierke, C. A. *J Biol Chem* **2005,** *280,* 16969–16978.

[140] Robinet, J. J.; Gauld, J. W. *J Phys Chem B* **2008,** *112,* 3462–3469.

[141] Clements, J. M.; Coignard, F.; Johnson, I.; Chandler, S.; Palan, S.; Waller, A.; Wijkmans, J.; Hunter, M. G. *Antimicrob Agents Chemother* **2002,** *46,* 1793–1799.

[142] Jackman, J. E.; Fierke, C. A.; Tumey, L. N.; Pirrung, M.; Uchiyama, T.; Tahir, S. H.; Hindsgaul, O.; Raetz, C. R. *J Biol Chem* **2000,** *275,* 11002–11009.

[143] Chen, M. H.; Steiner, M. G.; de Laszlo, S. E.; Patchett, A. A.; Anderson, M. S.; Hyland, S. A.; Onishi, H. R.; Silver, L. L.; Raetz, C. R. *Bioorg Med Chem Lett* **1999,** *9,* 313–318.

[144] McClerren, A. L.; Endsley, S.; Bowman, J. L.; Andersen, N. H.; Guan, Z.; Rudolph, J.; Raetz, C. R. H. *Biochemistry* **2005,** *44,* 16574–16583.

[145] Cuny, G. D. *Expert Opin Ther Pat* **2009,** *19,* 893–899.

[146] Barb, A. W.; McClerren, A. L.; Snehelatha, K.; Reynolds, C. M.; Zhou, P.; Raetz, C. R. H. *Biochemistry* **2007,** *46,* 3793–3802.

[147] Breazeale, S. D.; Ribeiro, A. A.; Raetz, C. R. H. *J Biol Chem* **2002,** *277,* 2886–2896.

[148] Loutet, S. A.; Bartholdson, S. J.; Govan, J. R. W.; Campopiano, D. J.; Valvano, M. A. *Microbiology* **2009,** *155,* 2029–2039.

[149] Hung, R.-J.; Chien, H.-S.; Lin, R.-Z.; Lin, C.-T.; Vatsyayan, J.; Peng, H.-L.; Chang, H.-Y. *J Biol Chem* **2007,** *282,* 17738–17748.

[150] Breazeale, S. D.; Ribeiro, A. A.; Raetz, C. R. H. *J Biol Chem* **2003,** *278,* 24731–24739.

[151] Breazeale, S. D.; Ribeiro, A. A.; McClerren, A. L.; Raetz, C. R. H. *J Biol Chem* **2005,** *280,* 14154–14167.

[152] Yan, A.; Guan, Z.; Raetz, C. R. H. *J Biol Chem* **2007,** *282,* 36077–36089.

[153] Trent, M. S.; Ribeiro, A. A.; Lin, S.; Cotter, R. J.; Raetz, C. R. *J Biol Chem* **2001,** *276,* 43122–43131.

[154] Gunn, J. S.; Lim, K. B.; Krueger, J.; Kim, K.; Guo, L.; Hackett, M.; Miller, S. I. *Mol Microbiol* **1998,** *27,* 1171–1182.

[155] John, R. A. *Biochim Biophys Acta* **1995,** *1248,* 81–96.

[156] Noland, B. W.; Newman, J. M.; Hendle, J.; Badger, J.; Christopher, J. A.; Tresser, J.; Buchanan, M. D.; Wright, T. A.; Rutter, M. E.; Sanderson, W. E.; Muller-Dieckmann, H. J.; Gajiwala, K. S.; Buchanan, S. G. *Structure* **2002,** *10,* 1569–1580.

[157] Feldman, M. F.; Marolda, C. L.; Monteiro, M. A.; Perry, M. B.; Parodi, A. J.; Valvano, M. A. *J Biol Chem* **1999,** *274,* 35129–35138.

[158] Liu, D.; Cole, R. A.; Reeves, P. R. *J Bacteriol* **1996,** *178,* 2102–2107.

[159] Doerrler, W. T. *Mol Microbiol* **2006,** *60,* 542–552.

[160] Bos, M. P.; Robert, V.; Tommassen, J. *Annu Rev Microbiol* **2007,** *61,* 191–214.

[161] Doerrler, W. T.; Reedy, M. C.; Raetz, C. R. *J Biol Chem* **2001,** *276,* 11461–11464.

[162] Eckford, P. D. W.; Sharom, F. J. *J Biol Chem* **2008,** *283,* 12840–12850.

[163] Zhou, Z.; White, K. A.; Polissi, A.; Georgopoulos, C.; Raetz, C. R. *J Biol Chem* **1998,** *273,* 12466–12475.

[164] Eckford, P.; Sharom, F. *Biochem J* **2010,** .

[165] Sperandeo, P.; Cescutti, R.; Villa, R.; Di Benedetto, C.; Candia, D.; Deho, G.; Polissi, A. *J Bacteriol* **2007,** *189,* 244–253.

[166] Sperandeo, P.; Lau, F. K.; Carpentieri, A.; De Castro, C.; Molinaro, A.; Deho, G.; Silhavy, T. J.; Polissi, A. *J Bacteriol* **2008,** *190,* 4460–4469.

[167] Ruiz, N.; Gronenberg, L. S.; Kahne, D.; Silhavy, T. J. *Proc Natl Acad Sci U S A* **2008,** *105,* 5537–5542.

[168] Narita, S.-i.; Tokuda, H. *FEBS Lett* **2009,** *583,* 2160–2164.

[169] Gronenberg, L. S.; Kahne, D. *J Am Chem Soc* **2010,** *132,* 2518–2519.

[170] Tran, A.; Dong, C.; Whitfield, C. *J Biol Chem* **2010,** .

[171] Tran, A. X.; Trent, M. S.; Whitfield, C. *J Biol Chem* **2008,** *283,* 20342–20349.

[172] Braun, M.; Silhavy, T. J. *Mol Microbiol* **2002,** *45,* 1289–1302.

[173] Bos, M. P.; Tefsen, B.; Geurtsen, J.; Tommassen, J. *Proc Natl Acad Sci U S A* **2004,** *101,* 9417–9422.

[174] Wu, T.; McCandlish, A. C.; Gronenberg, L. S.; Chng, S.-S.; Silhavy, T. J.; Kahne, D. *Proc Natl Acad Sci U S A* **2006,** *103,* 11754–11759.

[175] Chng, S.-S.; Ruiz, N.; Chimalakonda, G.; Silhavy, T. J.; Kahne, D. *Proc Natl Acad Sci U S A* **2010,** *107,* 5363–5368.

[176] Tokuda, H. *Biosci Biotechnol Biochem* **2009,** *73,* 465–473.

[177] Tefsen, B.; Geurtsen, J.; Beckers, F.; Tommassen, J.; de Cock, H. *J Biol Chem* **2005,** *280,* 4504–4509.

[178] Suits, M. D. L.; Sperandeo, P.; Deho, G.; Polissi, A.; Jia, Z. *J Mol Biol* **2008,** *380,* 476–488.

[179] Stenberg, F.; Chovanec, P.; Maslen, S. L.; Robinson, C. V.; Ilag, L. L.; von Heijne, G.; Daley, D. O. *J Biol Chem* **2005,** *280,* 34409–34419.

[180] Cohen, M. L. *Science* **1992,** *257,* 1050–1055.

[181] Vaara, M. *Science* **1996,** *274,* 939–940.

[182] Tomasz, A. *N Engl J Med* **1994,** *330,* 1247–1251.

[183] Loutet, S. A.; Flannagan, R. S.; Kooi, C.; Sokol, P. A.; Valvano, M. A. *J Bacteriol* **2006,** *188,* 2073–2080.

[184] Andrews, J. M. *JAC* **2009,** *64,*.

[185] Mahenthiralingam, E.; Campbell, M. E.; Henry, D. A.; Speert, D. P. *J Clin Microbiol* **1996,** *34,* 2914–2920.

[186] Revets, H.; Vandamme, P.; Van Zeebroeck, A.; De Boeck, K.; Struelens, M. J.; Verhaegen, J.; Ursi, J. P.; Verschraegen, G.; Franckx, H.; Malfroot, A.; Dab, I.; Lauwers, S. *Acta Clin Belg* **1996,** *51,* 222–230.

[187] Millar-Jones, L.; Ryley, H. C.; Paull, A.; Goodchild, M. C. *Respir Med* **1998,** *92,* 178–183.

[188] Speert, D. P.; Bond, M.; Woodman, R. C.; Curnutte, J. T. *J Infect Dis* **1994,** *170,* 1524–1531.

[189] Hobson, R.; Gould, I.; Govan, J. *Eur J Clin Microbiol Infect Dis* **1995,** *14,* 908–911.

[190] Flannagan, R. S.; Aubert, D.; Kooi, C.; Sokol, P. A.; Valvano, M. A. *Infect Immun* **2007,** *75,* 1679–1689.

[191] Shimomura, H.; Matsuura, M.; Saito, S.; Hirai, Y.; Isshiki, Y.; Kawahara, K. *Infect Immun* **2003,** *71,* 5225–5230.

[192] Raetz, C. R. H. Future of CHIR-090 like molecules., 2010.

[193] Rose, H.; Baldwin, A.; Dowson, C. G.; Mahenthiralingam, E. *J Antimicrob Chemother* **2009,** *63,* 502–510.

[194] LiPuma, J. J.; Rathinavelu, S.; Foster, B. K.; Keoleian, J. C.; Makidon, P. E.; Kalikin, L. M.; Baker, J. R. J. *Antimicrob Agents Chemother* **2009,** *53,* 249–255.

[195] Noda, M.; Matoba, Y.; Kumagai, T.; Sugiyama, M. *J Biol Chem* **2004,** *279,* 46153–46161.

[196] Shoji, J.; Hinoo, H.; Masunaga, R.; Hattori, T.; Wakisaka, Y.; Kondo, E. *J Antibiot (Tokyo)* **1984,** *37,* 1198–1203.

[197] Bodewits, K.; Raetz, C. R. H.; Govan, J. R.; Campopiano, D. J. *Antimicrob Agents Chemother* **2010,** *54,* 3531–3533.

[198] Rastogi, N.; Labrousse, V.; Goh, K. S. *Curr Microbiol* **1996,** *33,* 167–175.

[199] Davies, J.; Doring, G.; Hoiby, N.; Livermore, D.; MacGowan, A.; Pitt, T.; Rainey, P. *Antibiotic resitance in cystic fibrosis - an emerging crisis?;* 254 Royal Society of Medicine Press Ltd: 1 Wimpole Street, London W1G 0AE, UK, 2003.

[200] Vargues, T. *Antimicrobial Peptides - Structure, Function and Resistance,* Thesis, The University of Edinburgh, 2009.

[201] Soper, T. S.; Manning, J. M. *J Biol Chem* **1981,** *256,* 4263–4268.

[202] Malashkevich, V. N.; Strop, P.; Keller, J. W.; Jansonius, J. N.; Toney, M. D. *J Mol Biol* **1999,** *294,* 193–200.

[203] Fenn, T. D.; Stamper, G. F.; Morollo, A. A.; Ringe, D. *Biochemistry* **2003,** *42,* 5775–5783.

[204] Lowther, J.; Yard, B. A.; Johnson, K. A.; Carter, L. G.; Bhat, V. T.; Raman, M. C. C.; Clarke, D. J.; Ramakers, B.; McMahon, S. A.; Naismith, J. H.; Campopiano, D. J. *Mol Biosyst* **2010,** *6,* 1682–1693.

[205] Eliot, A. C.; Kirsch, J. F. *Annu Rev Biochem* **2004,** *73,* 383–415.

[206] Olson, G. T.; Fu, M.; Lau, S.; Rinehart, K. L.; Silverman, R. B. *J Am Chem Soc* **1998,** *120,* 2256-2267.

[207] David, S. *J Antimicrob Chemother* **2001,** *47,* 203–206.

[208] Adams, B.; Axelsson, B. S.; Beresford, K. J. M.; Church, N. J.; Spencer, P. A.; Whyte, S. M.; Young, D. W. *Pure and Applied Chemistry* **2000,** *72,* 373-384.

[209] Kishore, G. M. *J Biol Chem* **1984,** *259,* 10669–10674.

[210] Ganesh, V.; Bodewits, K.; Bartholdson, S. J.; Natale, D.; Campopiano, D. J.; Mareque-Rivas, J. C. *Angew Chem Int Ed Engl* **2009,** *48,* 356–360.

[211] Yi, E. C.; Hackett, M. *Analyst* **2000,** *125,* 651–656.

[212] Bartholdson, S. J. *Putative virulence factors and novel antimicrobial targets of the Burkholderia cepacia complex,* Thesis, School of Chemistry, University of Edinburgh, 2009.

# Appendix A

# Supplementary data

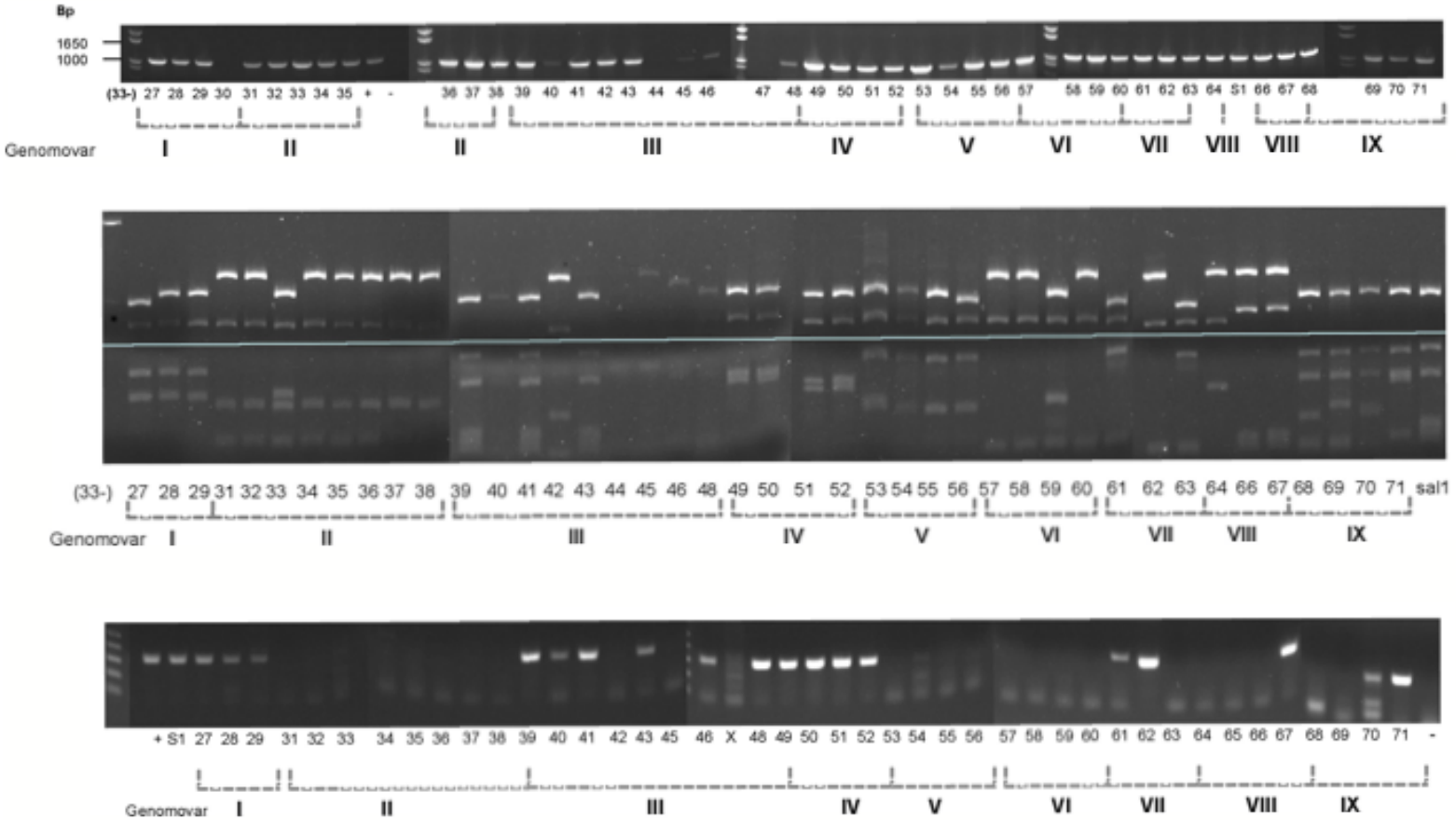


Figure A.1: Top= RecA PCR results of the Bcc reference panel recovered from -80 degrees storage; Centre= RFLP analysis of RecA PCR products; Bottom= $LpxC_2$ check of the Bcc reference panel. Positive control (+) is genomic DNA of *B. cenocepacia* K56-2, S1=Sal1, x= a *recA*negative strain. The numbering in all three analysis corresponds with the storage numbers of the Bcc strains in the -80 degrees freezer.

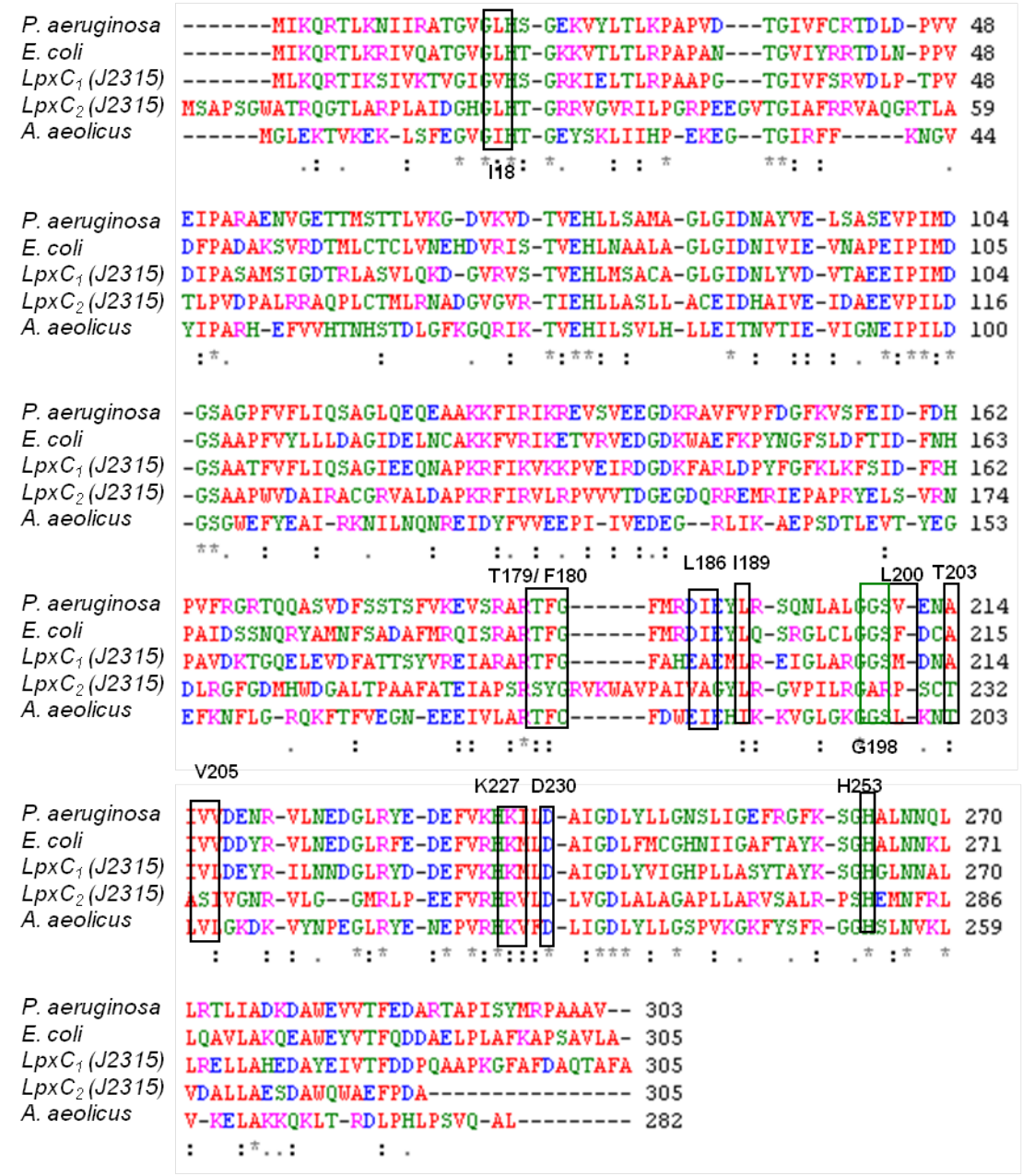


Figure A.2: LpxC alignment of *E. coli*, *P. aeruginosa*, *A. aeolicus*, and *B. cenocepacia* J2315 ($LpxC_1$ and $LpxC_2$). The amino acids important for CHIR-090 binding are indicated.

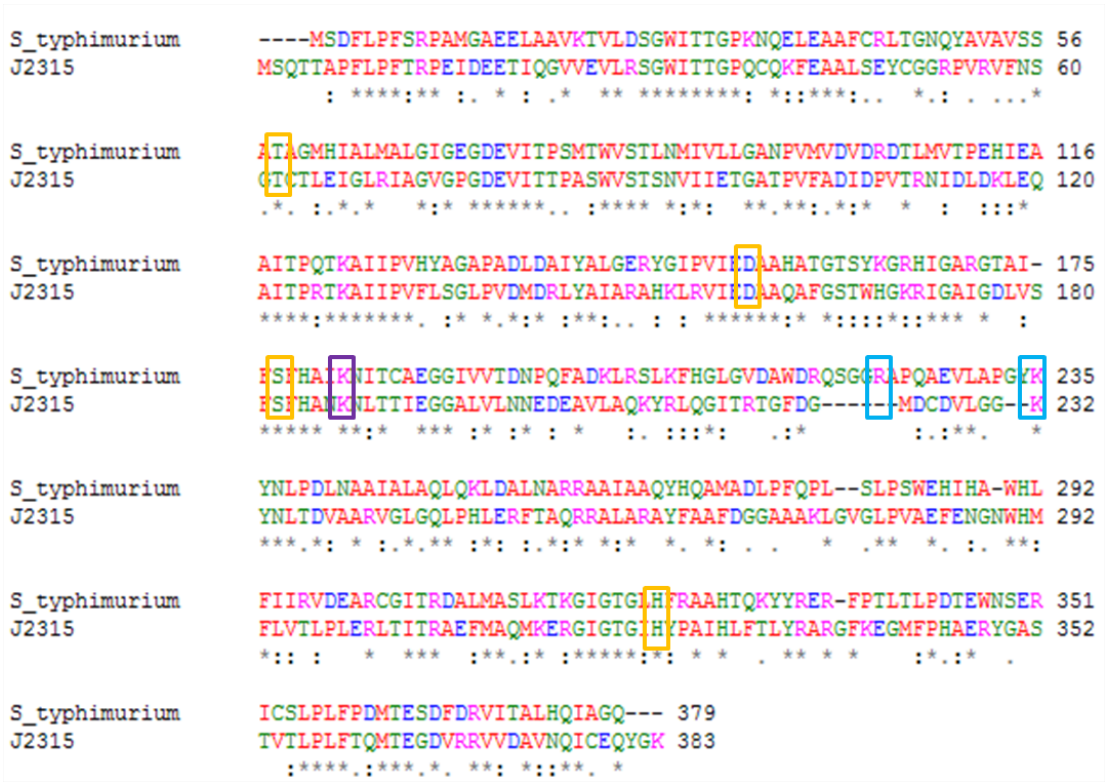


Figure A.3: Alignment of *B. cenocepacia* J2315 ArnB and *S. typhimurium* ArnB. The amino acids involved in stabilisation of the PMP-cycloserine adduct (orange), (amino donor) substrate binding (blue), and the lysine residue (purple, K188) forming a bond with PLP, are indicated.

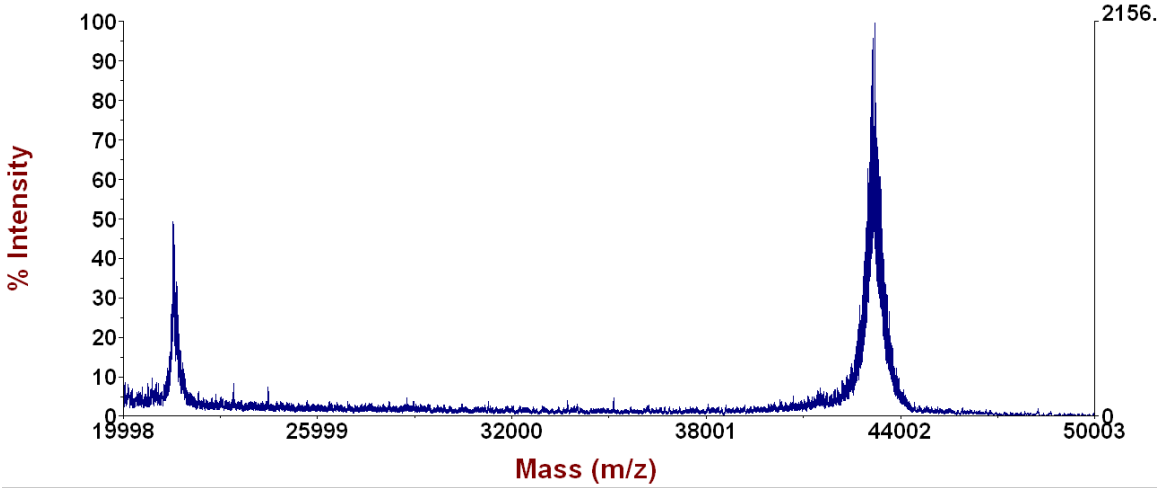


Figure A.4: ArnB-His6 MALDI-TOF mass spectometry analysis.

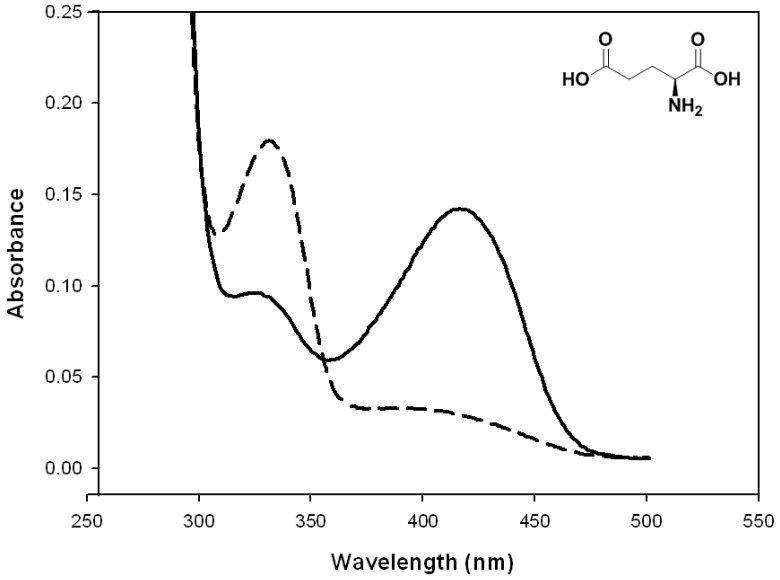


Figure A.5: E-PMP ArnB-His6 post-dialysis (=E-PLP) against an access of PLP overnight (solid line) and ArnB-His6 (post dialysis) reacted with 500 $\mu$M L-glutamate for 1 minute (dashed line)

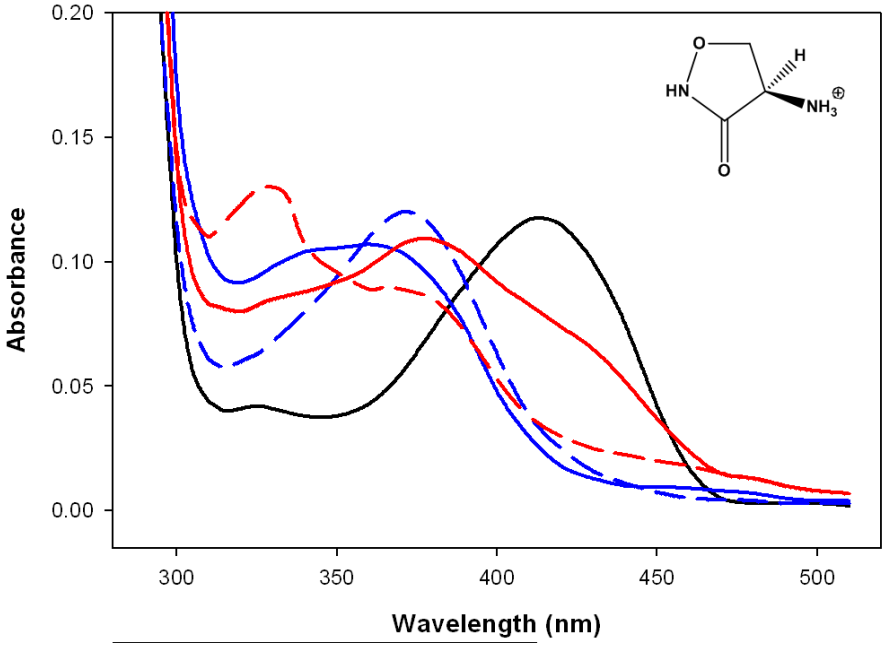


Figure A.6: Absorbance spectra for ArnB-His6 in the E-PLP form (black), 10 minutes after addition of 1 mM DCS (blue-dashed), 3 hours after the addition of 1 mM DCS (blue-solid), DCS-ArnB-His6 post-dialysis against an access of PLP overnight (red-solid) and DCS-ArnB-His6 (post-dialysis) reacted with 500 $\mu$M L-glutamate for 1 minute (red-dashed)

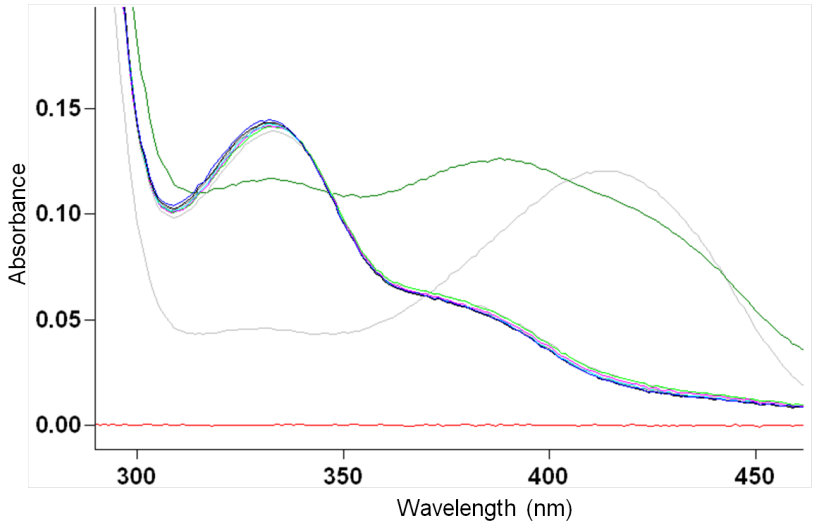


Figure A.7: Absorbance spectra for ArnB-His6 in the E-PLP form (grey). LCS-ArnB-His6 post-dialysis against an access of PLP overnight (green), LCS-ArnB-His6 (post dialysis) reacted with 500 $\mu$M L-glutamate for 1 minute (blue), and base-line (red).

LptA *B. cencoepacia* J2315 (229 a.a., MW = 24.3 kD/ 20.4 kD (-signal sequence)

MNEPFPRQISGGAARAVRAALAATLVALPLVGLAPLAHAEKADQNKPI
NVEADNLTYDDLKQVTVATGNVVITKGTIIIKGDRVEVRQDPEGYQYA
TSFGSGKKHATFRQKREGLDEYIDGDAERIDYDGKQDLTTLTTAATV
RRLQGTSTVADTVHGSVITYDGQRDFYTAKGGKDVAAPGNPNGRVR
AMLSPKNGGPAPLNGAPAKLSPSTTIQGAPGQLEHHHHHHH

Figure A.8: Recombinant LptA *B. cenocepacia* sequence. The signal peptide (blue) and the C-terminal His6 tag (red) are indicated.

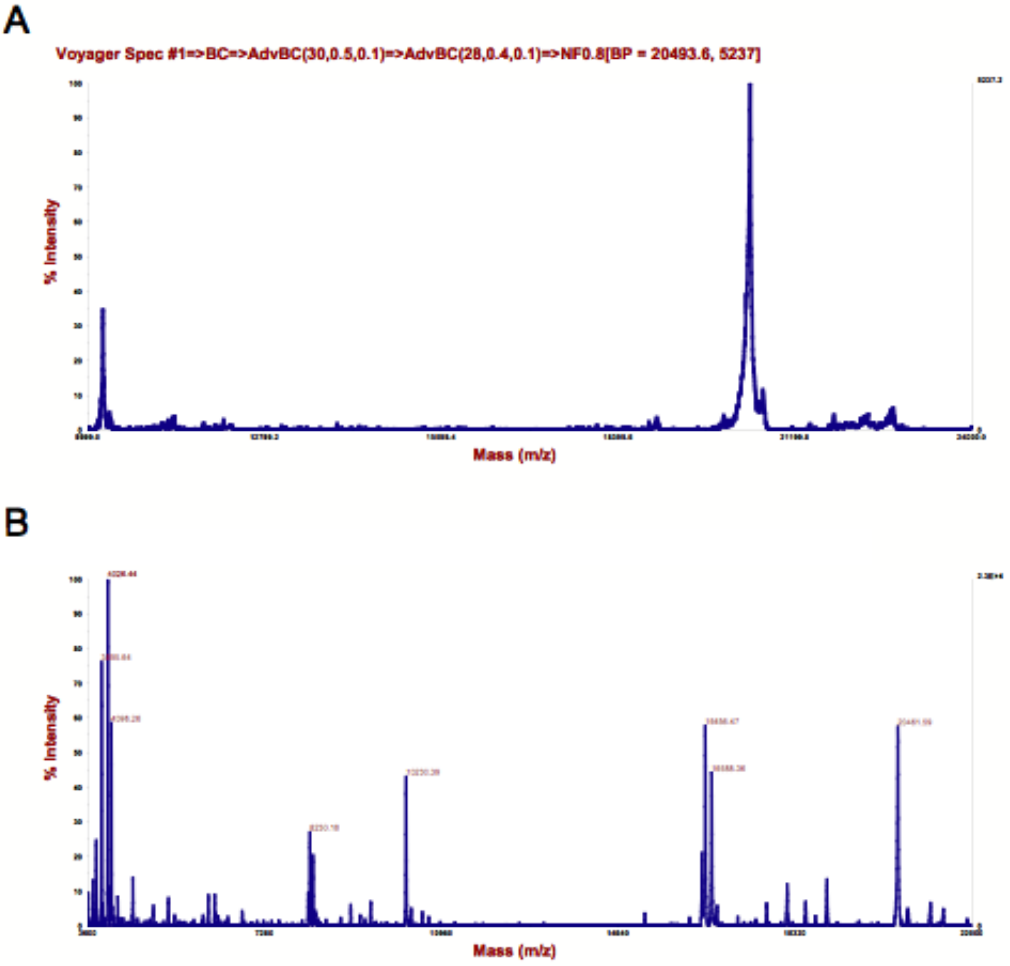


Figure A.9: LptA-His6 MALDI-TOF mass spectometry analysis, 0 hours (A)- and 3 hours (B) after purification.

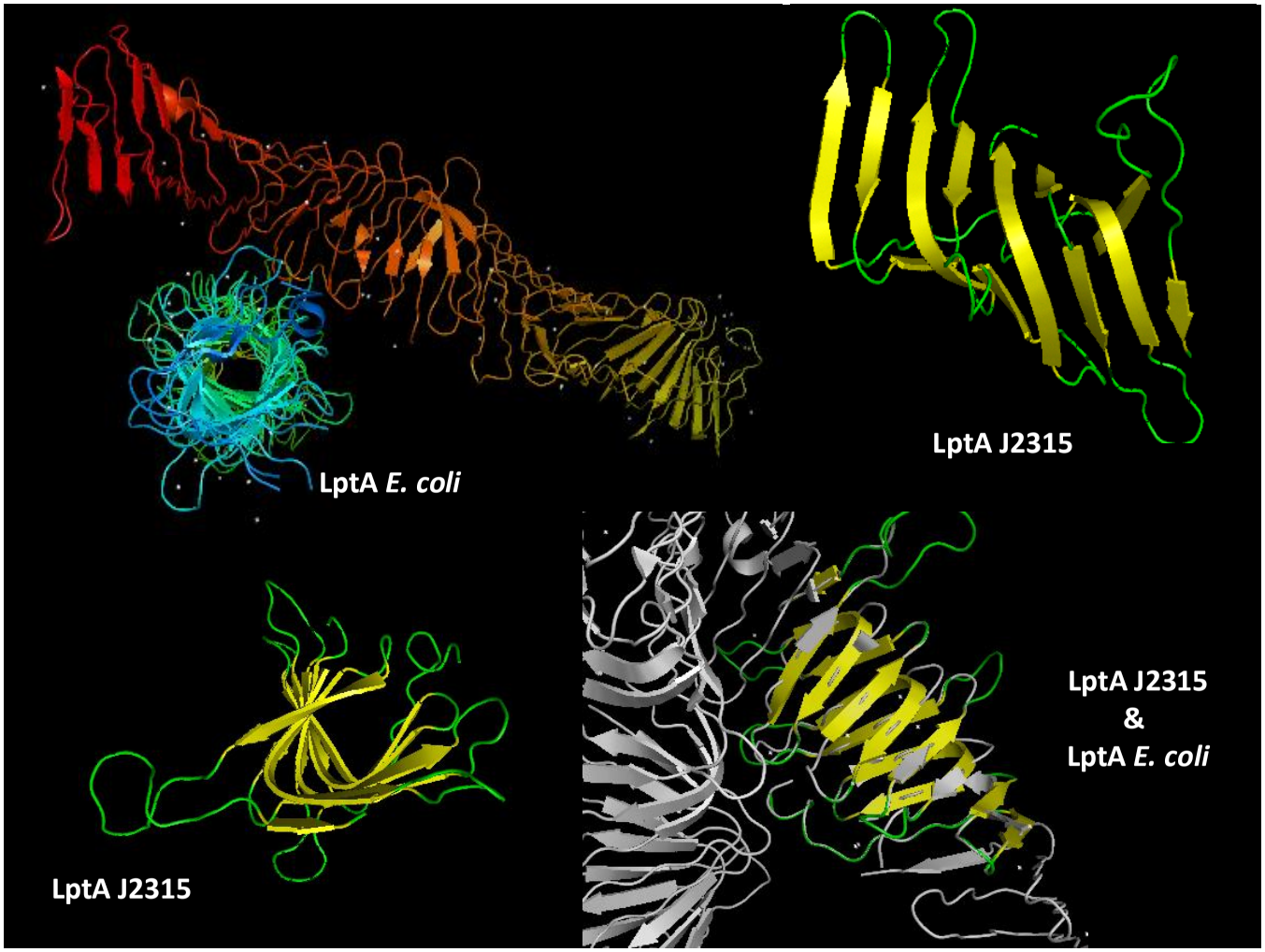


Figure A.10: Structural model of *B. cenocepacia* J2315 LptA which was generated by Swissmodel and *E. coli* LptA as a template.

```
lptB_J2315      MNALPNRQPAGTTSSLVVRNLKKRYGSRTVVKDVSLDVKSGEVVGLLGPNGAGKTTSFYM 60
lptB_E.coli     ------------MATLTAKNLAKAYKGRRVVEDVSLTVNSGEIVGLLGPNGAGKTTTFYM 48
                           ::*..:** * * .* **:**** *:***:*************:***

lptB_J2315      IVGLVPTDAGEITLNGSSISLLPIHKRASLGLSYLPQEASVFRKLTVEENIRAVLELQHD 120
lptB_E.coli     VVGIVPRDAGNIIIDDDDISLLPLHARARRGIGYLPQEASIFRRLSVYDNLMAVLQIRDD 108
                :**:** ***:* ::...*****:* **  *:.*******:**:*:* :*: ***:::.*

lptB_J2315      EDGKRLSKDAISSRTEALLDELQIGHLRENPALSLSGGERRRVEIARALATNPSFILLDE 180
lptB_E.coli     -----LSAEQREDRANELMEEFHIEHLRDSMGQSLSGGERRRVEIARALAANPKFILLDE 163
                     ** :  ..*:: *::*::* ***:. . ****************:**.******

lptB_J2315      PFAGVDPIAVLEIQKIVKFLKQRNIGVLITDHNVRETLGICDHAYIISDGSVLAAGAPSE 240
lptB_E.coli     PFAGVDPISVIDIKRIIEHLRDSGLGVLITDHNVRETLAVCERAYIVSQGHLIAHGTPTE 223
                ********:*::*::*::.*:: .:*************.:*::***:*:* ::* *:*:*

lptB_J2315      IIENESVRRVYLGEHFRMK 259
lptB_E.coli     ILQDEHVKRVYLGEDFRL- 241
                *:::* *:******.**:
```

LptB *B. cenocepacia* J2315 (259 a.a. MW=28227 Da)

Walker A Motif

MNALPNRQPAGTTSSLVVRNLKKRYGSRTVVKDVSLDVKSGEVVGLLGPNGAGKTTSFYMIVGL

VPTDAGEITLNGSSISLLPIHKRASLGLSYLPQEASVFRKLTVEENIRAVLELQHDEDGKRLSKDAISS

ABC transporters family signature

RTEALLDELQIGHLRENPASLSGGERRRVEIARALLATNPSFILLDEPFAGVDPIAVLEIQKIVKFLKQ

RNIGVLITDHNVRETLGICDHAYIISDGSVLAAGAPSEIIENESVRRVYLGEHFRMK

Figure A.11: Alignment of *B. cenocepacia* J2315 LptB and *E. coli* LptB. The amino acids forming the Walker A motif (ATP-binding site) and the "ABC transporters family signature" are indicated.

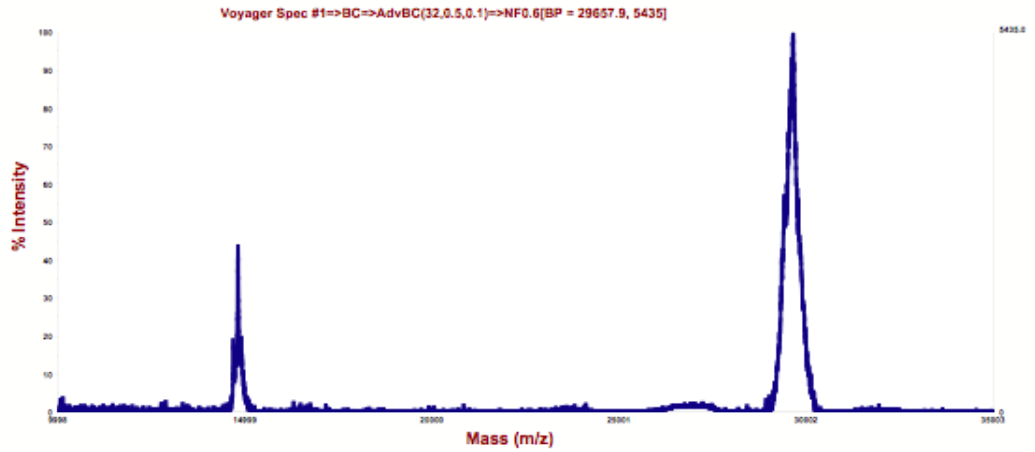


Figure A.12: LptB-His6 MALDI-TOF mass spectometry analysis.

# Appendix A

# Publications